ISCTE IUL
Instituto Universitário de Lisboa

Water Dynamics, Coherent Domains and the Origin of Life

Francisco Cano Marchal

Thesis specially presented for the fulfillment of the degree of

Doctor in Complexity Science

Supervisor:

Maria do Rosário Domingos Laureano, Ph.D. , Assistant Professor, ISCTE – IUL (Portugal)

Co-supervisor:

Eugen Aurelian Preoteasa, Professor (ret.), Horia Hulubei National Institute for Physics and Nuclear Engineering (Romania)

ISCTE IUL

Instituto Universitário de Lisboa

Water Dynamics, Coherence Domains and the Origin of Life

Francisco Cano Marchal

Thesis specially presented for the fulfillment of the degree of

Doctor in Complexity Science

Jury:

Jorge Loucã, Ph.D., Full Professor, ISCTE – IUL (Presidente)

Carlos Correia Ramos, Ph.D., Associate Professor, Universidade de Évora

Ricardo José Mendes Severino, Ph.D., Assistant Professor, Universidade do Minho

Juan Antonio Acebrón Torres, Ph.D., Assistant Professor, ISCTE - IUL

Maria do Rosário Domingos Laureano, Ph.D. , Assistant Professor, ISCTE – IUL

Abstract

The aim of this thesis is to deploy and develop quantum physics to account for the role of fast electronic dynamics on water's characteristics, in particular, for water under confinement, and to explore some of its implications in the context of the origin of life. There are unexplained observations of proton synchronization in water-filled carbon nanotubes, that point at a qualitatively different behavior of water to that predicted by existing theories. A novel study of water as a complex system is proposed and advanced, that combines quantum electrodynamics and quantum chemistry approaches and simulation methods. Several water scales and representations are explored, that aim at the development of a QED-QC multi-scale simulation framework potentially well-adapted for simulation in a biological environment. A multi-scale ontology for water is proposed, with representations at the micro, meso and macroscopic scale, that encode certain properties of the water system. In particular, a polaron model is used at the macroscopic scale, to obtain the size of the polarons that accounts for the observed kinetic energy difference of nanotube water, based on the relationship between radius and number of polarons for kinetic energy value. At the mesoscopic scale, the system is captured through the exciton wave function, using Quantum exciton Hamiltonian, to obtain water quantum dynamics and synchronization. It is argued that the nanotube water molecular dispositions promote quantum electronic synchronization and thus possibly proton synchronization. At the microscopic scale, water is represented as a point charges nuclei, and electron density in 3D space, system. The electron density plots are obtained using linear response, with softening of the potential for the protons. Also, exact Shrödinger equation in the grid is solved using Discrete Variable Representation, in this case for the electron density in 1D, and the time-evolution of the electron density is derived. We show that water molecule's electronic interaction with a common electromagnetic degree of freedom and synchronization provides a mechanism for proton synchronization. The question of water collective behavior possible role for life is tackled in a model for the origin of life based on our findings. The significance of this study is that it offers a plausible explanation of the observed nanotube water behavior, and several avenues of development of QED-QC study of water, contributing to the development of a QED-QC simulation framework in which to simulate water in biology with potential future applications for biology and medicine.

O objetivo desta tese é desenvolver a física quântica para dar conta do papel da dinâmica eletrônica rápida nas características da água, em particular, para a água sob confinamento, e explorar algumas de suas implicações no contexto da origem da água. vida. Existem observações inexplicáveis de sincronização de prótons em nanotubos de carbono cheios de água, que apontam para um comportamento qualitativamente diferente da água ao previsto pelas teorias existentes. Um novo estudo da água como um sistema complexo é proposto e avançado, que combina abordagens de eletrodinâmica quântica e química quântica e métodos de simulação. Várias escalas de água e representações são exploradas, que visam ao desenvolvimento de uma estrutura de simulação multi-escala QED-QC potencialmente bem adaptada para simulação em um ambiente biológico. Uma ontologia multi-escala para a água é proposta, com representações nas escalas micro, meso e macroscópica, que codificam certas propriedades do sistema hídrico. Em particular, um modelo de polaron é

usado na escala macroscópica, para obter o tamanho dos polarons que é responsável pela diferença de energia cinética observada da água do nanotubo, com base na relação entre o raio e o número de polarons para o valor da energia cinética. Na escala mesoscópica, o sistema é capturado por meio da função de onda de exciton, usando o Hamiltoniano do exciton quântico, para obter a dinâmica e a sincronização quântica da água. Argumenta-se que as disposições moleculares da água do nanotubo promovem a sincronização eletrônica quântica e, portanto, possivelmente a sincronização de prótons. Na escala microscópica, a água é representada como um núcleo de carga pontual e densidade eletrônica no espaço 3D, sistema. Os gráficos de densidade de elétrons são obtidos usando resposta linear, com amolecimento do potencial para os prótons. Além disso, a equação exata de Shrödinger na grade é resolvida usando Representação de Variável Discreta, neste caso para a densidade de elétrons em 1D, e a evolução temporal da densidade de elétrons é derivada. Mostramos que a interação eletrônica da molécula de água com um grau eletromagnético comum de liberdade e sincronização fornece um mecanismo para a sincronização de prótons. A questão do possível papel do comportamento coletivo da água para a vida é abordada em um modelo para a origem da vida baseado em nossas descobertas. A significância deste estudo é que ele oferece uma explicação plausível do comportamento da água do nanotubo observado, e várias vias de desenvolvimento do estudo QED-QC da água, contribuindo para o desenvolvimento de uma estrutura de simulação QED-QC na qual simular a água na biologia com potenciais aplicações futuras para biologia e medicina.

Contents

List of Figures

List of Tables

List of Acronyms

BOA - Bohr Oppenheimer Approximation

CD - Coherent Domain

DFT - Density Functional Theory

DVR - Discrete Variable Representation

ED - Exciton Dynamics

H - Hydrogen

JC - Jaynes-Cummings

KS - Kohn-Sham

LJ - Lennard-Jones

MD - Molecular Dynamics

ME - Master Equation

MI - Mutual Information

O - Oxygen

PES - Potential Energy Surface

QC - Quantum Chemistry

QED - Quantum Electrodynamics

QP - Quantum Physics

SAE - Single-Active Electron

TDDFT - Time-Dependent Density Functional Theory

1 Introduction

Water, despite its simple structure, continues to be a challenge for Science. It is the main component in living beings and considered to be essential for life as we know it. The main functions we know of water for biology are presented in Section 1.1.2, as well as some aspects which are still not well understood, such as the nature of the hydrophobic attraction and collective behavior. The nature of the H-bond itself is still to be fully elucidated [101], as the theories of H-bonding are merely phenomenological, a device to classify and organize the observations. The focus of this Thesis has been on understanding the behavior of water under confinement, which challenges the widespread view of water as formed of electrostatically interacting independent molecules and its extrapolation to the study of the origin of life. It is a very complex substance, and thus presented within the context of Complexity Studies, which to our knowledge has not very much been done.

Formulated already 25 years ago is the theory of QED Coherence in Matter [101]. This theory supports that water ground state is a collective dynamical state, with dipole oscillations in phase with a macroscopic electromagnetic potential, within regions of size 60 nm, called the coherence domains (CDs). Applied to the study of water, this theory goes into detail to explain some of water's thermodynamical properties. However, it has not proliferated into mainstream science and remains rather unknown. Some applications of this theory to biology have been proposed and are presented in Section 1.1.4. We have strived to make the ideas presented in the theory of CDs applicable for heterogeneous settings, by proposing simulation tools that allow for a microscopic detailed representation of water in contrast to the initial macroscopic formulations, where the application of the concepts to specific settings was not straightforward.

Therefore, in this Thesis, water is approached as a complex system and studied within Quantum Chemistry (QC) and Quantum Electrodynamics (QED), to characterize, in particular, its collective dynamics. QC and QED tools have been combined into a multi-scale, interdisciplinary setting, in order to build a model of a water-filled nanotube and compare it with a number of observations that challenge the current understanding of water behavior. The possible implications of water electrodynamical effects have been explored in a clay (Halloysite) nanotube model about the origin of life.

The study is situated within the methodological framework of QED-QC, which has been recently explored and formulated. The current availability of tools is limited and only a few first applications to simple models have been made, due to difficulties in terms of computational complexity and its novelty.

The detailed characterization of water light-matter dynamics and the development of tools for simulation is a new area of research that we propose to be important in order to better understand water. QED-QC for the study of water, QED-QC framework has served to address a critical unsolved problem in the study of confined water. It has the potential to better understand water in less extreme situations, as water is known to be a difficult and puzzling substance. The inclusion of these observations into the understanding of water dynamics could help render it a little less perplexing. Finally, water being central to life, understanding water collective effects and its light-matter dynamics can have important implications for biology,

and potential applications to medicine.

1.1 State of the Art

Diagram 1 summarizes the main areas addressed in this Thesis. Along with the presentation of the State of the Art, some commentaries are made about the content, as we consider that it facilitates its framing.

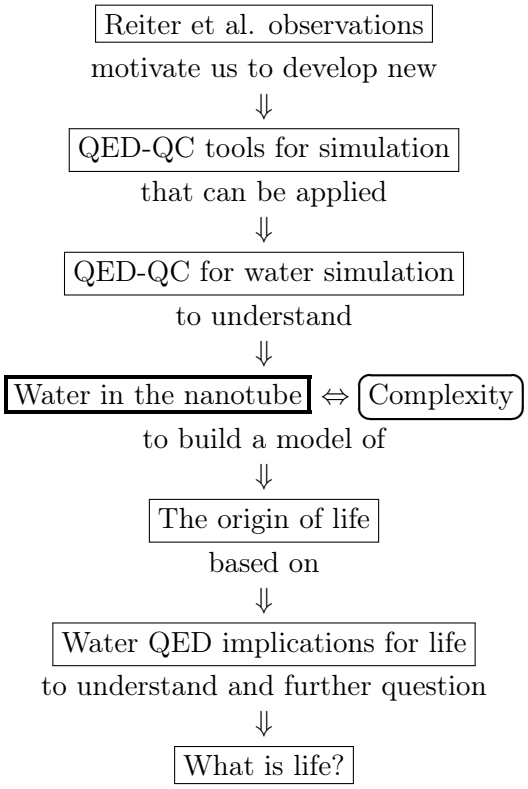

Figure 1: Main areas of study and development and relations.

1.1.1 What is Life?

What is life is one of the most intriguing and challenging questions that we address in science. Numerous definitions of life exist, and usually consist of a set of observable characteristics that we require of a system to call it living. As Luisi puts it [79]:

> the concept of life is too vague and general and loaded with a number of historical, traditional, religious values

Spitzer et al. [117] argue that this lack of agreement on fundamental concepts, and not only the complex evolutionary nature of life, has led to a slow advance of origin of life research. The following table collects several definitions, most of them adapted from [8], which can give us an idea of their variety.

Author	Definition

E. Del Giudice (2010)	The protagonists of the biological process (...) [are] mesoscopic collectives characterized by millions of molecules acting in unison in wide regions of the space for long intervals.
F. Varela (1996)	A physical system can be said to be living if it is able to transform external energy/matter into an internal process of self-maintenance and self-generation. This common sense, macroscopic definition, finds its equivalent at the cellular level in the notion of autopoiesis. This can be generalised to describe the general pattern for minimal life, including artificial life. In real life, the autopoietic network of reactions is under the control of nucleic acids and the corresponding proteins.
T. Ganti (1996)	At the cellular level the living systems are proliferating, program-controlled fluid chemical automatons, the fluid organisation of which are chemoton organisation. And life itself at the cellular level is nothing else but the operation of these systems.
S. Fox (1996)	Life consists of proteinaceous bodies formed of one or more cells containing membranes that permit it to communicate with its environment via transfer of information by electrical impulse or chemical substance, and is capable of morphological evolution by self-organisation of precursors, and displays attributes of metabolism, growth, and reproduction. This definition embraces both protolife and modern life.
E. H. Mercer (1981)	The sole distinguishing feature, and therefore the defining characteristic of a living system is that it is the transient material support of an organization with the property of survival.
M. Eigen (1981)	The most conspicuous attribute of biological organization is its complexity... The problem of the origin of life can be reduced to the question: Is there a mechanism of which complexity can be generated in a regular, reproducible way?
L. Orgel (1973)	Living beings are CITROENS (Complex Information-Transforming Reproducing Objects that Evolve by Natural Selection).
P. Fong (1973)	Life is made of three basic elements: matter, energy and information... Any element in life that is not matter and energy can be reduced to information.
J. Monod (1970)	Living beings are teleonomic machines, self-constructing machines and self-reproducing machines. There are, in other words, three fundamental characteristics common to all living beings: teleonomy, autonomous morphogenesis and invariant reproduction.
J. Bernal (1967)	Life is a partial, continuous, progressive, multiform and conditionally interactive, self-realisation of the potentialities of atomic electron states.

Levels of Life	Examples
Ecological	Sunlight based autotrophs, heterotrophs, predators. Life in liquid water, using carbon dioxide. Multicellular organisms. Compartmentalization by cell membranes and cell walls
Biochemical	Lipid bilayers. Ribisco enzyme. ATP as energy molecule. Triplet code for transcription. DNA and RNA and conserved sequences in genome. Citric acid cycle. L-amino acids; A,T,C,G, and U nucleotide bases.
Chemical	Carbon and water. Matter.

Table 2: A categorization of structures that comprise terrestrial life.

N. Horowitz (1959)	I suggest that these three properties mutability, self-duplication and heterocatalysis comprise a necessary and sufficient definition of living matter.
R. D. Hotchikiss (1956)	Life is the repetitive production of ordered heterogeneity.

Table 1: Definitions of life.

Note that some of the common requirements to consider that a system is alive are: homeostasis or self-regulation, organization, metabolism, growth, adaptation, response to stimuli, information processing, reproduction (adapted from Wikipedia, definition of life).

In this Thesis, we will focus on the first two elements of the concise characterization of life by Spitzer [117], which identifies the following fundamental aspects: metabolism, information processing and reproduction. We may also pay attention to Francisco Varela's definition of life in terms of autopoiesis, a concept that has become widespread and has influenced strongly biology but also other scientific fields, and which has become fairly important in the field of Complex Systems.

In his popular book, *What is life?* [113], Schrdinger argued that the fact that advances in physics and chemistry available at that time did not allow an explanation of life, did not mean that an explanation of life in physical and chemical terms was not possible. This challenge, and the questions that arise, have inspired many of the authors and theories that we will present in the sections to follow.

We have talked about life and assumed we are talking about life as we know it, on the Earth. There may exist different forms of life on other planets, this option has not been ruled out either confirmed by Science. Table 2, adapted from [87], is a categorisation of the structures of life, to show the different levels at which life might be different on other planets. These speculations are important to design methods for life detection on other planets. For example, it is usual speculation that the presence of ammonia and silicon, could constitute a different chemical baseline for life, replacing carbon and liquid water.

Finally, some attempts have been made to characterize the *living state of matter* [15, 16]. This is the point of view adopted in this Thesis because, with the focus on how matter behaves in the living, starting from water itself. Put otherwise, how life can be seen indeed as a very particular state of matter. Other significantly

different approaches exist that try to characterize life independently of the strata in which it takes place as, for example, in artificial life. We may benefit from the insights obtained by considering life abstractly. However, we will always come back to maybe the most basic constituent of living beings, which is matter, and to its characteristics. Table 2 is a reminder that other kinds of life would, in principle, be possible. Of course, we are focusing on life as is accessible to us and the particular form of life that we know exists on Earth. We will study the information processing aspects of life abstractly. But again, as we shall see, information processing in the living uses what we could call biological hardware, through which information processing takes place. These are material, physical, elements that constrain and, in a sense, determine, how this information is processed (see [91]). Two main information processing devices are biochemical components and also, the important although often neglected, electromagnetic fields. The electromagnetic field, and its importance in the understanding of water and therefore of life, is a central theme in this Thesis.

The main building blocks for life are nucleic acids, with 20 aminoacids, proteins (formed of 4 nucleotide bases), polysaccharides (aggregations of monosaccharides or simple sugars), lipids and fatty acids. These are the main constituents of biomass [**?**] and constitute the hardware of life [87]. Apart from these components, living beings are made of 50%-80% in mass of water, and water molecules are approximately 99% of the number of molecules.

Life is usually regarded as constituted by biochemical processes among the different constituents of living beings and with focus on biochemical networks of interaction [89]. We have seen also that one characteristic of living beings is that they process information. Information processing in the living has especially being developed from the point of view of the biochemical networks processes and, on the other hand, in a more explicit way in the study of electric processes in neurons and the brain, which is out of the scope of this Thesis. However, it has been argued that traditional views of biochemical explanations of the cell face some challenges, like the existence of dynamical ordered schemes of biochemical reactions, the emergence of self-organization at the different levels of the biological architecture, the existence of a well-defined interval of temperature where life becomes possible, the selection of the biomolecules among all possible molecule species, and their universal presence in all living species [59, 10, 100]. The efforts of molecular biology to understand cellular dynamics by reducing them exclusively to the movement (usually Brownian) of molecules considered as classical particle-like objects may eventually come up against important challenges.

The concept of organic code is based on the belief that in biology the information is stored in certain structures, which are then deciphered or decoded by other biological agents. The study of how information is coded and interpreted in living beings have been called semantic biology [8]. The genetic code is a well-known example of biological code, and its study and understanding have experienced an immense outburst in the last few decades. However, to understand intra and intercellular recognition processes, the study based only on nucleic acids and proteins is not sufficient. Processes such as cell adhesion or routing remain unexplained [52]. The existence of other biological codes beyond the genetic code is now commonly accepted, such as the sugar code [53, 116, 94] for polysaccharides, or the histonic code [119], in the case of histones, which are a kind of basic proteins. The 'alphabet' of

nucleotides has 'characters', one for each nucleotide base: cytosine (C), thymine (T), adenine (A) and guanine (G). It is the basis for storing genetic information, starting downstream flow to effector molecules by transcription, and ensuring replication.

1.1.2 Water Role's for Life

The reason why water is the solvent suitable for life is succinctly put by Bell as follows.

1. Life most probably needs a solvent.
2. That solvent needs to perform an active, diverse, and flexible role.
3. Water is so far the only common liquid we know that is capable of this.

Summarizing by saying that water is biophilic.

In particular, as stated in [129] about water, (1) it provides an environment for the stability of macromolecular structure by maintaining some chemical bonds; on the other hand, it allows for the dissolution of some other chemical bonds to ensure chemical interchange and energy transformations, maintaining critical concentrations of substances; (2) it allows for the formation of boundary surfaces, such as vesicles or other kinds of interfaces, necessary for creating a protected micro-environments with distinct physicochemical properties and has surface tension; it favours the polymerisation and structural organisation of organic molecules; (3) its liquid phase is stable in as wide a range of temperatures and pressures as possible in order to function as a buffer against environmental fluctuations, as well as to favour a broad spectrum of biochemical reactions; (4) its polarity, the ability to make covalent bonds, confers a polymer-like structure on water; (5) it has dielectric properties, that is, it behaves as an electrical insulator that can be polarized by an applied electric field.

The nature of the hydrophobic attraction in water is still not well understood. This force drives the folding of protein chains, the binding of some proteins to substrates, and aggregation of proteins into functional units, and is key to life [6].

The properties of water are often characterized in terms of Hydrogen-bonding. A Hydrogen bond (or H-bond) is a primarily electrostatic force of attraction between a Hydrogen (H) atom which is covalently bound to a more electronegative atom (or group) –in the case of water, an Oxygen (O), which is the hydrogen bond donor–, and another electronegative atom bearing a lone pair of electrons –the H-bond acceptor. We suggest that this mainly electrostatic picture has its limitations, that some properties and observations can not be explained by a simple electrostatic model, and that collective effects, in particular collective electronic dynamics and synchronization, are important in order to understand water and life. In the following section, the collective behaviour of water, in particular, water coherence, is presented. The theory of QED Coherence in Matter was originally developed by Preparata [101] and applied to water. The implications of this theory for life was explored and developed by several authors.

1.1.3 (History of) Electromagnetism in Biology

Two separate types of experimental evidence regarding electromagnetism and living beings suggest some sort of electromagnetic organization in the living [75]. On one

hand, there are measurable electrical features related to biostructures, which are linked to biological functions, such as growth, development, repair, etc. On the other hand, living beings have shown to be sensitive to external electromagnetic fields, often responding to surprisingly low intensities.

These discoveries are not new. The first accounts for electromagnetic effects in the organism date back to the early nineteenth century, with the observation made by Galvani in the late 1700s that serious injuries, such as amputations, generated an electrical current in the vicinity of the affected area, which is now known as the injury current. Observation of the reverse effects was also made: electromagnetic fields had an impact on biological processes. Lund [80] explained these phenomena by relating the applied fields with the endogenous biological fields, such as the injury current. Both fields could add to or oppose each other. He focused on currents and their measurement and observed that these currents were caused by the bioelectric polarity of ions flows in the organisms. Becker [9] then theorized that the electromagnetic potential and its polarity is used by the organism to signal the injury and eventually to trigger the healing process. He gave an anatomical description of possible physiological systems responsible for these effects, and linked acupuncture and Chinese Medicine meridians, observing that in the acupuncture points the local current measured was maximum. Burr [19, 18] reported links between various pathologies and the electric surface potentials of the impacted organs, and generalized these findings into the concept of a characteristic electric template for wellness. These two authors' ideas have the common ingredient of considering the electromagnetic field as a sort of information field in the living. For a detailed review of the historical development of these ideas, please refer to [75]. Since then, more refined approaches have emerged, exploiting advances in the understanding of electromagnetic phenomena, in particular, of the collective quantum electromagnetic effects that take place in matter.

For example, in 1968, Herlbert Frhlich, a physicist with expertise in condensed matter physics, published an article [49] suggesting that living systems, under certain conditions, undergo a phase transition, reaching a steady-state, far from thermodynamic equilibrium, characterized by long-range correlations. This phenomenon would be similar to the Bose-Einstein condensation, which is the spontaneous proliferation of order in a gas (a large fraction of the molecules occupy the lowest energy quantum state) when it is cooled to temperatures close to absolute zero. However, the existence of a Frhlich condensate would be possible at the relatively high temperature of living beings.

From a more general approach, but consistent with Frhlich's proposal, Preparata, Del Giudice and colleagues, use Quantum Field Theory (QFT) to explain the collective behaviour of matter in the living [37**?** , 34, 36, 60]. Preparata's theory of QED Coherence in Matter theory [101] is applied first to water in living beings. They go one step further and they claim that not only electromagnetic fields are important to understand life, but also that, in the light of the latest physical discoveries, the concept of matter must be upgraded, and a matter field and its properties must be incorporated into physical theories to understand some features of life. QFT provides powerful tools to approach some, otherwise difficult to explain, biological phenomena (see Table 1). We will develop these ideas in the next section.

1. Life and vibration

Terahertz collective dynamics of DNA as affected by hydration and counterions [96]

1.1.4 Water Quantum Coherence and Life

Del Giudice uses QFT to account for long-range order in living systems [11, 37, 34, 10]. The argument is the following. Water molecules, which as we have presented constitute 99% of the total number of molecules in living beings, are capable of oscillating between different quantum states (and different energy levels). Let us assume that molecules can be in two quantum states: a ground state and an excited state. Energy is needed to excite one molecule from the ground to the excited state and, after some time, it will spontaneously relax into the ground state releasing some energy. We can assume that no external electromagnetic field is applied. But according to QFT, a quantum system is never at rest (this has been called *horror quietis* or *fear of resting*); therefore interaction with the vacuum is always assumed. The vacuum is defined as the minimum energy state of a physical system, that is, the energy to sustain the mere existence of the system, including the quantum fluctuations that prevent the system from being still. Due to these quantum fluctuations of the vacuum, an electromagnetic field should always be assumed to be present, coming from the interaction between matter and the vacuum. When water molecules overcome some density threshold, vacuum fluctuations excite with certainty one molecule; note that particles are in big number and close to each other so the electromagnetic wave, which can also be treated as a photon travelling among the molecules, will very likely intercept one of them. This excited atom will eventually relax to its ground state, releasing some energy, which again is treated as the release of a virtual photon (a quantized or discrete amount of energy). This photon will be absorbed with certainty by another molecule, also due to the density of molecules, and will then be in the excited state. So forth and so on, molecules will start to oscillate between ground and excited state, and as they do so, an electromagnetic field will be generated, stimulating other molecules to oscillate as well and at the same frequency. In some time, the whole of molecules and the field will be oscillating in unison, in what is called a *coherent state*. The region of molecules which are in a coherent state is called the *coherent domain* (CD).

Although water is ubiquitous and the main component in living organisms, its properties are not well understood. It presents an important number of perplexing characteristics, which have been called the *water anomalies* [10]. The role of water in biology is an active research field. As we have already mentioned QFT, and in particular QED, is a useful framework to explain some physical properties of water, as well as some aspects of living systems that are closely linked to water characteristics. Table 3 summarizes some of these aspects and references.

Aspect	Description	Suggested Explanation	Refs.
Water Exclusion Zone (EZ)	Colloid particles and different solutes are excluded from aqueous zones closely adjoining to hydrophilic surfaces on the order of tens and hundreds of microns, a potential difference between EZ and bulk water of over 150 mV, lower density, higher viscosity		[34, 38, 131, 130]
Water thermodynamic properties	Measured thermodynamical properties of water	Theoretical calculations from QED theory are in agreement with experiments	[4, 11]
Water infrared (IR) spectrum	The IR spectrum of liquid water is composed of two bands, one centred around 1650cm^{-1} having a Gaussian line shape and another much wider-ranging from 3000 to 3800cm^{-1}	This fact supports a two-phase characterization of water. The value of the energy gap of the coherent water calculated from CD model is in good agreement with the value derived from the IR spectra	[32, 33]
Erythrocytes rouleaux formation	Two erythrocytes too distant for short-range interactions to act (about three cell radii) begin to move towards each other at a rate several times higher than in the Brownian case and contradicting electrostatic laws	Demands some sort of long-range interaction: Frhlich resonance interaction ie. resonance creating an attractive force	[38, 50, 101]
Belousov-Zhabotinsky (BZ) phenomenon	BZ reaction in lamellar lipid structures layout demands the presence of liquid water over a threshold (70% of the weight of the lipid)	Water may be providing the conditions for self-organization (in this layout)	[82]
Sensitivity to environment	Living systems can react to very small changes in the environment: changes in Earth's electromagnetic field, moon eclipse events, among other	Water is an 'amplifier' of electromagnetic signals	[34]
Biomolecules present in living systems	Only certain biomolecules participate in living organisms	These molecules have a vibration spectrum within a particular frequency range.	

Molecular bio-recognition	Bio-molecules have very specific targets which vary in time, and can locate themselves in the right place at the right time	Biomolecules may recognize each other by resonance. For example, it has been shown that the proteins and their targets have the same characteristic frequency in common	[27, 28, 29]

Table 3: Examples of some physical and biological aspects and possible explanations in the frame of water QED.

It is suggested [82?] that Del Giudice's model of water CDs acts, in fact, as a dissipative system in the sense of Prigogine. Just as they absorbed energy from the vacuum oscillations, water molecules would be capable of absorbing high entropy electromagnetic energy waves from the environment, that are independent and noisy, and transforming them into low entropy energy (collective and coherent) waves, energy which would not be released thermally, but stored through the collective oscillations, serving as an energy reservoir. This energy could eventually be released when activating, through electromagnetic resonance, molecules capable of vibrating at a similar frequency as the CD. Therefore, this would explain the time-specific affinities of biomolecules for a certain active process. Although some empirical results support this assertion, further investigation needs to be done.

Biologist Mae-Wan Ho, inspired by the colorful view of a worm in the polarized microscope, integrated and extended some of the presented results and theories into what she called a theory of the organism [63]. She observed that the cyclic nature of biological processes was key to the understanding of life. Using thermodynamics of open systems and the concept of quantum coherence, she envisioned organism as macroscopically quantum coherent beings capable of almost dissipationless cyclic transformation of energy between complementary processes. She coined the term quantum jazz to express how beautifully coordinated are –as much as they are free– the different components in living beings, this being possible thanks to coherence. Again, this is an exciting route to explore, and further enquiry is needed. This Thesis has the goal of presenting some possible tools and data to support, or challenge, these ideas.

Several attempts have been made to extend QFT beyond the limits of the organism into the entire ecosystem [36, 14]. This may be reasonable, as according to QFT a system and its environment are so intimately related. After all, if life is coherent, this could be true at different scales. Vitiello has shown that coherent structures indeed give raise to self-similarity [126, 128, 127, 128]. To what extent this is the case in life and eco-systems still needs to be explored and investigated.

In this review, we have focused on QED and the work of Frhlich and Preparata and Del Giudice's group approach to quantum coherence. Other authors have contributed to the study of coherence in living beings (Table 4).

Author	Science	Main approach	Contributions
E. Schrdinger	Physics	Quantum Mechanics, Philosophy	Neguentropy in Life, suggested Quantum Coherence needed

G. Preparata	Physics	Quantum Field Theory	Quantum Coherence in Matter. QED and thermodynamics of water
G. Ling	Biology	Biological Theoretical Modeling	The Association- Induction Hypothesis
F. Popp	Physics	Physics	Biophotons theory and observations
H. Frhlich	Physics	Statistical Physics, Quantum Field Theory	CDs in Water
A. S. Davidov	Physics	Quantum Physics	Davidov Soliton
E. del Giudice	Physics	Quantum Field Theory	CDs theory extension
G. Pollack	Experimental Physics	Nuclear magnetic resonance (NMR) and other	Exclusion zones experimental validation
G. Vitiello	Physics	Condensed Matter Physics, Defects Theory	Self-similarity and coherence
I. Cosic	Physics, Biology	Spectroscopy, Theoretical Modeling	Resonant Recognition Model (RRM)
M. W. Ho	Biology, Physics	Theoretical biophysics	Theory of the Organism, Macroscopic Quantum Coherence Theories

Table 4: Some authors studying coherence in water and their theories and fields.

It has been shown that Davidov's approach is equivalent to Frhlich's formulation [125], and we have already commented that Frhlich theory is a special case of the more general QFT approach. These theories could be understood qualitatively using Ling's biological model of active-state and rest-state. Popp has focused on biophoton emission, which is closely related to coherence in matter [99]. Resonant recognition has been further developed and tested experimentally by Irena Cosic and colleagues [27, 28, 29]. In his paper [65], Jaeken has reviewed these subjects.

1.1.5 Reiter et al. Observations

Confined water has been probed using experimental techniques, such as Deep Inelastic Neutron Scattering (DINS) or X-Ray Compton Scattering. In DINS, the behaviour of a beam of neutrons incident to the system in study is analyzed, in particular, how they are scattered, that is, how they deviate from their original trajectory, in order to determine the momentum distributions of the atoms that are being probed [78, 3]. In X-Ray Compton Scattering, it is the scattering of photons (of an X-Ray beam) due to the interaction with free electrons or loosely bound valence electrons that is analyzed, to characterize the electron momentum distribution, in this case.

Differences in nanoconfined water to bulk water and ice have been reported [71, 106, 105, 104, 17, 97]. In particular, Reiter et al. [106, 105, 104] have presented X-ray Compton Scattering measurements of electron momentum distribution

in water confined in single-walled carbon nanotubes (SWCNTs) and double-walled carbon nanotubes (DWCNTs) of size 14 Å and 16 Å, respectively, and DINS proton momentum distribution measurements. Carbon nanotubes are cylindrical large molecules consisting of a hexagonal arrangement of carbon atoms, which are formed by rolling up a sheet of graphene for SWCNT or multiple sheets of graphene for multiple-walled carbon nanotubes (MWCNTs). These authors show that the proton is delocalized over distances of the order of 0.2-0.3 Å, with proton more delocalized in SWNT than in DWCNT, and therefore electrons also more delocalized in SWCNT than in DWCNT. The proton momentum distribution shows temperature dependence, as well as the size of confinement. There is a large change in the momentum width (kinetic energy) going from 230 K to 300 K. There is a lack of variation of the momentum distribution between 4 K and 230 K, which would be ordinarily expected up to room temperature. In the case of DWCNT, the width and shape of the proton momentum distribution change continually with temperature T up to room temperature, in a non-monotonic way. The kinetic energy below 230 K was approximately 30% less than that of ice or bulk water at room temperature. The electron momentum distribution and temperature dependence and shape are consistent with the changes in the proton momentum distribution. These authors claim that the magnitude of temperature and size dependence are so large that they cannot be due to independent changes within single molecules, but must require the coherent or synchronized motion of multiple protons. The study beyond electrostatic models of weakly interacting molecules is suggested. An explanation has been offered by suggesting a flat bottom double-well potential for the proton [104, 72], whose origin is not specified, and which, on the other hand, is questioned in [92]. They present kinetic energy values for different nanotube sizes [92].

For comparison, the behaviour of water confined in Nafion nanopores is presented. Nafion is a type of polymer, in particular, a sulfonated tetrafluoroethylene based fluoropolymer-copolymer. Using DINS measurements, it has been reported [56] proton mean kinetic energy differences. In the case of pore size 82 Å only a few meV higher of difference is reported, about 6 % higher compared with to non-confined water, and sensibly higher (27%) for 24 Å. The layers of water near the surface are strongly perturbed, with proton appearing to move coherently between two sites separated by 0.3 Å. The perturbation penetrates the entire pore in the smaller pore and is confined to the surface in the larger pore.

() [13] reducing temperature below 200 K, part of this water behaves as a quasi-free rotor, that is, the orientational energy of such molecules becomes comparable to the rotational energy of water in the gas phase. -> again a modification of the H-bond structure in nanoconfined water, consistent with the variation of the potential over the proton, considering the chains and rings collective potentials also determining/influencing the H-bond structure, as is to expect, since the H-bond interaction derives from usually considered (1) electrostatic interaction and (2) partial covalent character, and thus in our proposal includes these and extends to include the interaction with photons in the QED-QC framework. the observation of abnormal hydrogen bonding supports the attempt to characterize water QED-QC dynamics.

1.2 Overview of the Thesis Approach and Structure

1.2.1 QED-QC Framework

Water has traditionally been studied within Chemistry, and also since the XXth century with Quantum Chemistry tools. These studies focus on electrons and nuclei and their interaction through Coulomb forces. The electromagnetic Coulomb interaction is a simplified expression of the presence of photons in the system that neglects their transversal degrees of freedom. In this picture, the electromagnetic part is simplified and the focus is on the matter part. On the other hand, QED has focused on the electromagnetic part, with a detailed description of the photons. It is the low energy limit of QED, non-relativistic QED, that applies to the study of molecular systems and their interaction with light. In particular, the models in Quantum Optics and Photonics focus on the electromagnetic part, and the atoms and molecules are simplified. There are also linear response treatments based on the macroscopic electromagnetic fields effects on the systems. Therefore the study is placed between these two main approaches, with the attempt to include, both, detailed representation of the matter part, and including the transversal part of the photons. The importance of these transverse electromagnetic degrees of freedom in the case of water has been proposed [101], and its implication for the understanding of water behavior. It offers a radically different view on water, where collective electrodynamical effects are key. In this Thesis, the recent QED-QC emerging framework is presented [47, 111], where the focus is being on the inclusion and development of light-matter descriptions and tools. To this point, it has not been much applied, mainly due to its novelty and computational complexity, and to our knowledge, not used for water. The importance of including both the matter (electron and nuclei) and the light (photons) parts into the description and characterization of water had been advanced, not only for light-matter experimental settings but even for water in its usual state. The interaction of photons with the electrons, and its effects on the nuclei, could be providing the complex and unexpected behaviour of water in confinement. In particular, a formal density functional reformulation of QED [108, 109, 124] has been proposed, the extension of quantum chemical approximations [45] as well as a generalized Green function methods [31]. A few calculations have been done applying these methods for simple systems [46, 47]. In our case, the exploration within the macroscopic, mesoscopic and microscopic scale tools for water has been conducted, to put together methods that can allow for water multi-scale characterisation. Furthermore, complexity science has been, of course, central to the study of this complex substance.

1.2.2 On Multi-Scale and Thesis Approach

Following the proposal of coherent domains (CDs) theory, and with nanoconfined water observations insight, this Thesis is explored a number of ways in which the widespread tools and practices in water science, can be used, combined and extended, to account for Reiter's water observations. A hands-on and practical approach is proposed, a multi-scale simulation method, where each of the tools is used to characterize the water system at the scale in which they have been developed, and are combined to encompass also the predicted coherent dynamics. Each of the scales and each of the Chapter makes use of different tools and models, that although re-

lated to the quest, come from different disciplines. That has brought about a strong multidisciplinary character to this Thesis, including Condensed Matter Physics (Ch. 3) QED/Quantum Optics (Chs. 4 and 6), QC (Chs. 6 and 5), Synchronization in Dynamical Systems Theory (Ch. 4) and Biology (8).

The initial intent to put these two apparently very different approaches to better understand water was confirmed as a good exploration when we came across the QED-QC framework, about halfway in the process of this Thesis. Computer simulation of water within the QED-QC framework is promising in advancing the understanding of water and life itself. Facing such a challenge, an exploration of the available simulation tools both in QED and QC has been made, to assess in which ways they could be combined to model water, and answer specific questions related to its behaviour under nanoconfinement. Several traits were followed simultaneously, a few abandoned on the way, and finally, three options are presented in this Thesis.

The initial exploration of water confronted us with many theories and tools and specific assumptions and simplifications. To make sense of these, and in the style of Complexity Sciences, the notion of scale was used. For this reason, the Thesis is presented separated by scales. At some point, the notion of scales vanishes and loses its central place, just to work within the theoretical framework in question. At other points, the theory is just at the background of the simulation tools used across scales. In this way, this work is placed within complexity science multi-scale modelling approaches, and at the same time is an exploration in Quantum Physics (QP) and QC. The tension between the two approaches made the work interesting and at time complex. A variety of Quantum Representations available for the water system are explored, which themselves already contain an incredible complexity even for the simplest systems.

The following scales are considered in this Thesis.

Macroscale: bulk properties, properties of a considerable volume of molecules, for example, of the order of 10^{23}. The behaviour is generally captured through statistical tools. So, bulk water and the CD. The water system is characterized by a few macroscopic variables, such as density.

Mesoscale: scale between the Macro and the Microscale. The study at the level of the molecule or ring, where they are characterized by an abstract state, and the dynamics are "coarsened" with respect to the microscopic scale, in that the dynamics are characterized by a few parameters and the Hamiltonian. In particular, the excitation energies and the intermolecular coupling and the frequency of the photons. The water system is characterized by the state of each of the molecules or, in the case of this Thesis, the dimer and the rings.

Microscale: scale where the molecules are considered as composed of atoms, which contain a nucleus composed of neutrons and protons, and clouds of electrons that characterize the probability of finding electrons in the regions surrounding the nuclei and in the bonds. The water system is characterized by the position of the nuclei and the electron density in space, which can be captured as the value in a grid in 3D space, or a vector for 1D.

An effort has been made to present also the theoretical aspects, although the majority of the development has been done through simulation. Some analytical results have been presented, that complement the understanding of the system, and that was also a tool when the situation allowed. A hands-on approach was favoured, and

the theoretical details explored to the extent they were needed. Nevertheless, a first step was advanced into putting together the different bits into a unified framework. This open-ended exploration was not without sacrifice, maybe of definiteness of some of the results at this stage of exploration. However, we hope that this document, along with the presented code, serves to reflect a good level of commitment and dedication to the process, along with the excitement in this very novel and exciting field. The fact that the exploration was across fields, which in itself was a very natural choice, brought, however, some extra difficulties when dealing with the presentation of the theoretical aspects. The focus has been on putting together the simulation settings and obtaining the first results. The exploitation of the settings will be done successively for future publications.

The following schema (Fig. 2) shows some of the scales at which we have been working and some of the fields explored. The final model of water in the Halloysite nanotube for the study of the origin of life has unified the different contributions. It has served as the core exploration and theme. It also includes some of the assumptions made.

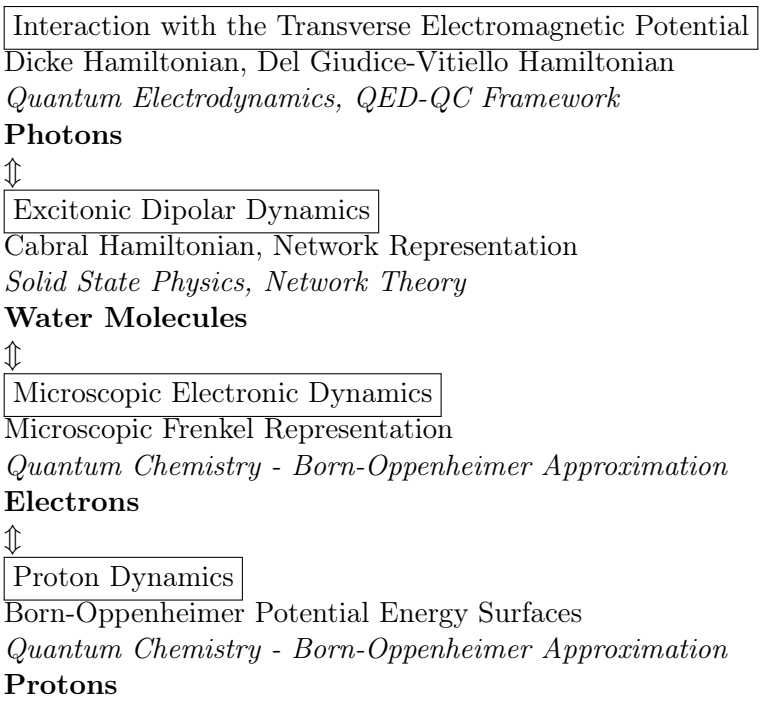

Figure 2: Levels of Representation

1.2.3 On Complexity: Emergence

In 1999 economist Jeffrey Goldstein provided a current definition of *emergence* in the journal entitled Emergence. He initially defined emergence as: "the arising of novel and coherent structures, patterns and properties during the process of self-organization in complex systems".

In 2002 systems scientist Peter Corning described the qualities of Goldstein's definition in more detail. He claims that common characteristics are: (1) radical

novelty (features not previously observed in systems); (2) coherence or correlation (meaning integrated wholes that maintain themselves over some period of time); (3) a global or macro "level" (i.e., there is some property of "wholeness"); (4) it is the product of a dynamical process (it evolves); and (5) it is "ostensive" (it can be perceived).

In this Thesis, the emergent property is time-periodicity for the electron dynamics and synchronization. It has been taken as an expression of QED coherence in matter at the representations, quantum or classical, used. The following classification is used for emergence.

(1) Ontological: emergence implies a new level of theory, that is, the emergent property of the system cannot be explained within the original theoretical setting.

This is the case of Chapter 7, where the system of water molecules, which are represented as nuclei in 3D space and a given electron density cannot, a priori, give rise to the emergent property of synchronized electronic dynamics. It is known, however, that this is the behaviour of the system when the same system, a group of water molecules, in a different representation, that is electric dipoles, gives rise to the emergent property of QED coherence in matter. Therefore, within the QC framework, which has the strength and advantage of specificity and resolution, the emergent property is a sort of foreign element. Therefore, this property is ascribed to the system rather artificially, through an external electromagnetic field, and the consequences for the system in that representation. Thus, top-down causation is studied and its implications at, what we have called, the micro-level, to compare with empirical data. The original theory, QED coherence in matter, allows comparison with bulk properties but does not allow, at present, for the resolution we are needing for our data. The emergence of oscillations does not derive from the theory, but from a different theoretical framework, and is externally imposed to the system, as Time-Dependent Density Functional theory (TDDFT) allows us to obtain the quantities we are interested in.

We are imposing the "higher level" dynamics into the system. And we aimed to be able to study the specific implications at the level of the "parts". To our concern, and at our level of representation, there is an emergent property that we use to explain properties that had not been successfully explained by the "atomistic" models, but that its causality is not contained within the original framework.

(2) Epistemological / methodological: the emergence can be characterized within the same theoretical framework through the use of a "wholistic" property or variable. This is the case of Chapters 4.

The emergent property is in Chapter 4 characterized through two measures of synchronization, and the emergence of this collective or wholistic property of the water system is within the theoretical framework, causality is within the theory and does not need to be imposed externally. Moreover, the study of emergence within this framework has computational advantages to dealing with a microscopic representation, which is more costly.

Chapter 6 is somewhere in between (1) and (2), depending on how we consider the emergent property to be defined in the water system. The causality of electronic oscillations is contained in the theoretical framework, but in this case, it is a model of a single unit, therefore the collective property is observed for this unit as a property

of the unit. Chapter 4.3.6 provides additional support that allows to understand that the observed property at the level of the unit is, indeed, a collective property of the water system.

Finally, for Chapter 3, it can be argued that there is no emergence and it is simply an order of magnitude estimation. The representation is, and can only be collective, but the question is not whether the property of interest, in this case, the number of polarons and their size, can or cannot be logically deduced in the water system. The system is being granted with this property without questioning: we assume there are several polarons of a certain size. Then we ask the question, how many polarons and what would their size be in that case.

In Chapter 8 the emergent property is life. We argue that the study using water dynamics could potentially provide a theoretical framework of the type (2) that could potentially allow understanding causality in the event of the origin of life, within this same framework.

1.2.4 Summary of Main Results and Thesis Structure

The following scheme summarizes, for each article in progress, what representations have been used to model water behaviour, separating them into macro, meso and microscopic scales. Also, it is indicated whether a multi-scale method has been used or not.

Scale	[23]	[22]	[21]
Macroscopic	CDs (implicit)	CDs (implicit)	CDs (implicit)
Mesoscopic	water rings, photons	water molecules, photons	water molecules, photons
Microscopic	electron density in 3D		electron density in 1D
Multi-scale?	Yes.	No.	Yes.

The following scheme presents the articles methods and main results, concerning the Thesis Chapters.

Article	Results	Method
[23]	Ring dynamics (analytical) Induced electron density and proton potential plots Proton potential energy surface (PES) *compare with Reiter observations*	Schrdinger Equation - analytical (Ch. 4) TDDFT-LCAO (Ch. 5) Multi-scale simulation (Ch. 7)
[22]	Parameter space and time evolution synchronization plots *effects of intermolecular coupling*	Schrdinger Equation - simulation (Ch. 4)

Continued on next page

Article	Results	Method
[21]	Proton PES in SAE	Single Active Electron approximation, Discrete Variable Representation (DVR)
	proton synchronization (in progress)	Classical synchronization theory

The Thesis is structured as follows.

In Chapter 2 the theoretical background is presented. Chapter 3 presents a classical picture of Condensed Matter Physics which is applied to the case of water. Chapter 4 explores a Exciton model of water and the dynamics are studied, in particular, quantum synchronization. Chapter 5 is the application of Time-Dependent Density Functional theory simulation to a water ring. In Chapter 6 the single active electron approximation is proposed to characterize water H-bond dynamics in dimer, using the Shin-Metiu model. Chapter 7 combines the approaches of Chapter 4 and 5 into a multi-scale simulation setting for water in the nanotube. Finally, Chapter 8 approaches QED-QC dynamics possible implications for biology in a model of the origin of life.

2 Theoretical Background

?The general theory of quantum mechanics is now almost complete. The underlying physical laws necessary for the mathematical theory of a large part of physics and the whole of chemistry are thus completely known, and the difficulty is only that the exact application of these laws leads to equations much too complicated to be solvable.?

P.A.M. Dirac 1929

2.1 Quantum Physics

2.1.1 A Quantum System

First, let us consider a classical dynamical system of N point-like particles, for example, a protein made up of its atoms. If we specify the position and momenta (mass times velocity) of each of the particles, then we have completely characterized the system. To specify the position and momenta of each particle, we need, in fact, three values for each of them: one for each of the coordinates of 3D space. So the object $(p_{1x}, p_{1y}, p_{1z}, q_{1x}, ...)$ gives a complete description of the system. This object is called a real vector of dimension $6N$, since it is constituted by an ordered collection of $6N$ real numbers. We call the space of all possible real vectors of dimension $6N$, $\mathbb{R}^{6N}$, where $\mathbb{R}$ stands for a real number. So, the space of all possible states for the system is the space of states, in this case, $\mathbb{R}^{6N}$.

Let us see this with an example. We can imagine the system is composed of only two particles which can only move in one dimension in space. The space of states is then $\mathbb{R}^4$. Each state of the system is then specified by a vector $\vec{v} = (p_1, q_1, p_2, q_2)$. We can express this as:

$$\vec{v} = \begin{pmatrix} p_1 \\ q_1 \\ p_2 \\ q_2 \end{pmatrix} = p_1 \begin{pmatrix} 1 \\ 0 \\ 0 \\ 0 \end{pmatrix} + q_1 \begin{pmatrix} 0 \\ 1 \\ 0 \\ 0 \end{pmatrix} + p_2 \begin{pmatrix} 0 \\ 0 \\ 1 \\ 0 \end{pmatrix} + q_2 \begin{pmatrix} 0 \\ 0 \\ 0 \\ 1 \end{pmatrix}$$

and the vectors

$$\vec{e_1} = \begin{pmatrix} 1 \\ 0 \\ 0 \\ 0 \end{pmatrix}, \vec{e_2} = \begin{pmatrix} 0 \\ 1 \\ 0 \\ 0 \end{pmatrix}, \vec{e_3} = \begin{pmatrix} 0 \\ 0 \\ 1 \\ 0 \end{pmatrix}, \vec{e_4} = \begin{pmatrix} 0 \\ 0 \\ 0 \\ 1 \end{pmatrix}$$

are the canonical basis vectors for $\mathbb{R}^4$. This means that we can specify any vector $\vec{v}$ of the Euclidean space $\mathbb{R}^4$ as a linear combination of these four basis vectors, and that they are orthogonal (in 3D space this means perpendicular) to each other and have modulus one[1]. A linear combination is an expression of the form $\vec{v} =$

[1] We call it an orthonormal basis if they are orthogonal to each other and have norm equal to one. In general, two vectors are orthogonal if their inner product is zero. The inner product of two vectors (a_1, a_2, a_3, a_4) and (b_1, b_2, b_3, b_4) is just $a_1b_1 + a_2b_2 + a_3b_2 + a_4b_4$.

$p_1\vec{e}_1 + q_1\vec{e}_2 + p_2\vec{e}_3 + q_2\vec{e}_4$, where we only sum the basis vectors pre-multiplied by a real number if needed, called a scalar or coefficient. [2]

In Quantum Physics (QP) the situation is slightly different. To describe the state of a system, it is not a vector in Euclidean space that we need to specify. It is also a vector, but in a complex vector space, which is called a Hilbert space. The principal[3] difference is that now the coefficients are not real numbers but complex numbers. A complex number has the form $a + bi$, where i is the imaginary unit defined as $i^2 = -1$. This may seem a bit awkward at this point, but it will prove very useful and the way to characterize the state of quantum systems to be able to understand the results of the experiments.

For example, let us consider the case of a qubit, the quantum equivalent to a classical coin, a two-state quantum system, that can be called a two-level system (TLS). The system has two possible values, head and tails. We can assign $+1/2$ to head and $-1/2$ to tail. So our space of states is {head, tails} so {$+1/2$,$-1/2$}. This example follows reference [121].

Just as in the above example we can define the basis as

$$\vec{e}_1 = \begin{pmatrix} 1 \\ 0 \end{pmatrix}, \quad \vec{e}_2 = \begin{pmatrix} 0 \\ 1 \end{pmatrix}$$

or using the Quantum Mechanics notation, as

$$|1/2\rangle = \begin{pmatrix} 1 \\ 0 \end{pmatrix}, \quad |-1/2\rangle = \begin{pmatrix} 0 \\ 1 \end{pmatrix}$$

These two vectors *span* the space of states. It means that we can express any state in the space as a linear combination of these two vectors. However, as we have anticipated, in the case of QP we will allow the coefficients to be complex. Therefore, any state of the system is, in general, given as

$$|\psi\rangle = \alpha\,|+1/2\rangle + \beta\,|-1/2\rangle$$

where α and β are allowed to be complex numbers. We will require, though, for it to be normalized (or of length one), so the norm of $|\psi\rangle$, given by $\alpha^*\alpha + \beta^*\beta$, has to be equal to one. We say, then, that our space is $\mathbb{C}^2$, where $\mathbb{C}$ stands for a complex number.

So we see that our quantum mechanical coin is slightly different to a classical coin, in the sense that it can be in a state that is a combination of head and tails. What does this mean physically?

Let us imagine now that we have an apparatus that can read the state of the system, and has a display that shows $+1/2$ if the system is in the head state and $-1/2$ if the system is in the tail state. What would be the result of measurement if the system is in state $\alpha\,|+1/2\rangle + \beta\,|-1/2\rangle$? The answer is that it will be either $+1/2$ or $-1/2$, and it will be $+1$ with a probability of $\alpha^*\alpha$ and $-1/2$ with probability $\beta^*\beta$, where α^* is the complex conjugate of α. Note that if $\alpha = \alpha_R + i\alpha_C$ then its conjugate is $\alpha^* = \alpha_R - i\alpha_C$. The numbers $\alpha^*\alpha$ and $\beta^*\beta$ are always real numbers, because

[2] For example, in real 3D space, we would have three basis vectors, each one responsible for each of the directions in space.

[3] There are probably other but this one is our main point.

	$\|0\rangle$	$\|1\rangle$	$\|2\rangle$
$\|+1/2\rangle$	$\|+1/2, 0\rangle$	$\|+1/2, 1\rangle$	$\|+1/2, 2\rangle$
$\|-1/2\rangle$	$\|-1/2, 0\rangle$	$\|-1/2, 1\rangle$	$\|-1/2, 2\rangle$

Table 7: Possible combination of basis vectors of systems A and B.

$(\alpha_R + i\alpha_C)(\alpha_R - i\alpha_C) = \alpha_R^2 + \alpha_C^2 i^2 + \alpha_C\alpha_R i - \alpha_R\alpha_C i = \alpha_R^2 + \alpha_C^2$. This means that if we have a very large number of identical systems, all in state $|\psi\rangle$, and we conduct a measurement in each of them with the apparatus, a fraction corresponding to $\alpha^*\alpha$ will result in the apparatus giving $+1/2$ and a fraction of $\beta^*\beta$ giving $-1/2$. Because we required the state vector $|\psi\rangle$ to be normalized, we have that the probability for the apparatus to display $+1/2$ plus the probability for it to display $-1/2$, so $\alpha^*\alpha + \beta^*\beta$, is equal to one. This makes sense as our apparatus will display for sure one of the two alternative values, $+1/2$ or $-1/2$. Here we see why a Hilbert Space proves useful to define the state of the system.

2.1.2 Composite Quantum Systems

A qubit is an example of a quantum system. But combining more than one system is something that is usually done in QP, as when we do so interesting, non-trivial effects take place, which often escapes (even further) our intuitive notion of physical reality.

We can consider another example of a quantum system, a quantum harmonic oscillator. As its name indicates, this is the quantum equivalent of the classical harmonic oscillator. This is a very important and well-known example of a quantum system, but here we will say very little about it. We only need to know that it is characterized by an integer number that can go from 0 to infinity, and which defines the state of the system.

For simplicity, we will consider a truncated harmonic oscillator, with states over a finite number of possibilities, namely 0, 1 and 2 for example. Therefore, the basis would be $\{|n\rangle\}, n \in \{0, 1, 2\}$ for the harmonic oscillator, and as we have seen, $\{|s\rangle\}, s \in \{-1/2, +1/2\}$ for the qubit. As we have introduced, these basis states span the Hilbert space of states for each system. We can call $\mathcal{H}_A$ the Hilbert space for the Two-Level System (TLS) or qubit and $\mathcal{H}_B$ that of the Harmonic Oscillator (HO).

We may guess that the space of states of the composite system consisting of a TLS and a HO has to include all the possible combinations of the two states. Table 7 contains all combinations, where we have represented the state where A is in $|s\rangle$ and B is in $|n\rangle$ by $|s, n\rangle$.

We can expect that the space of states has to contain at least these elements. But, are these the only possible states for the composite system?

If we remember, we could have the qubit in a superposition of states such as $|\psi\rangle_A = \alpha_1 |+1/2\rangle + \alpha_2 |-1/2\rangle$. Let's imagine that B is also in a superposition state $|\psi\rangle_B = \beta_1 |0\rangle + \beta_2 |1\rangle + \beta_3 |2\rangle$. What is the state of the composite system? Then, it may seem natural for it to be in a superposition of the combined states of Table 7. We can express such a state in general as

$$|\psi\rangle = \sum_{s,n} \psi(s,n)\,|s,n\rangle$$

where $s \in \{-1/2, 1/2\}$ and $n \in \{0, 1, 2\}$. We call the values $\psi(s,n)$ for each pair (s,n) the wave function of state $|\psi\rangle$, which can be a complex-valued function. What are the values for this example? The answer is that we can obtain them by doing *tensor multiplication* or *tensor product* of states $|\psi\rangle_A$ and $|\psi\rangle_B$, which is expressed as

$$|\psi\rangle_A \otimes |\psi\rangle_B$$

The tensor product of both vectors is defined by

$$\begin{aligned}
&(\alpha_1\,|+1/2\rangle + \alpha_2\,|-1/2\rangle) \otimes (\beta_1\,|0\rangle + \beta_2\,|1\rangle + \beta_3\,|2\rangle)\\
=&\alpha_1\beta_1\,|-1/2\rangle \otimes |0\rangle + \alpha_1\beta_2\,|-1/2\rangle \otimes |1\rangle + \alpha_1\beta_3\,|-1/2\rangle \otimes |2\rangle\\
+&\alpha_2\beta_1\,|+1/2\rangle \otimes |0\rangle + \alpha_2\beta_2\,|+1/2\rangle \otimes |1\rangle + \alpha_2\beta_3\,|+1/2\rangle \otimes |2\rangle\\
=&\alpha_1\beta_1\,|-1/2, 0\rangle + \alpha_1\beta_2\,|-1/2, 1\rangle + \alpha_1\beta_3\,|-1/2, 2\rangle\\
+&\alpha_2\beta_1\,|+1/2, 0\rangle + \alpha_2\beta_2\,|+1/2, 1\rangle + \alpha_2\beta_3\,|+1/2, 2\rangle
\end{aligned}$$

We say that the Hilbert space of the composite system is $\mathcal{H}_\mathcal{A} \otimes \mathcal{H}_\mathcal{B}$ or simply $\mathcal{H}_{\mathcal{AB}}$; it is the space spanned by the vectors in Table 7. We can express any vector as a (complex) linear combination of the vectors in Table 7. The case of $|\psi\rangle_A \otimes |\psi\rangle_B$ is a particular case of vector which is called the *product state*. In general, not all vectors in $\mathcal{H}_{\mathcal{AB}}$ can be expressed as the tensor product of a state of A by a state of B. States that can not be expressed as a product state are called *entangled states*.

2.1.3 Open Quantum Systems

Very often, in QP, we consider the systems of study to be closed. This means that we act as if in the world we study there were nothing more than the system itself and therefore the only thing we take into account. This is an abstraction to help us construct theory, but real systems are never completely isolated.

As many of the theoretical results apply to closed systems, we want to use a formalism that will let us use the results also in the case of open systems. What we do is to construct a new system, which we can accurately enough be considered as a closed system, which includes our system of interest and any (or the main) elements or systems with which it is interacting, usually called the *environment*. We call the space of states of the system $\mathcal{H}_S$ and the space of states of the environment $\mathcal{H}_E$.

So now our 'world' consists of the system and its environment. As we have seen in the previous section, the space of states of the system plus its environment is $\mathcal{H}_S \otimes \mathcal{H}_E$, that we can call $\mathcal{H}_{SE}$. The dimensionality of the composite system is $dim(\mathcal{H}_{SE}) = dim(\mathcal{H}_S) \cdot dim(\mathcal{H}_E)$. This means that, for example, if we are modelling a system that has 2 possible states and an environment with say 3 possible states, our composite system representations will have dimension 6 instead of dimension 2 of our system of interest. So it means we need more computational power to keep track of the system and its environment. Often, as will be the case in this Thesis, we want our environment to be 'rich' so we need a fairly big dimension to represent

it, which implies costly computations if we keep exact track of the environment as well as the system.

More importantly, we often just do not have complete knowledge of the environment, so we would like to account for its effect on the system without having to consider a very accurate description of the environment itself. We want to consider environmental effects 'on average'.

A way to do it is to use the density matrix formalism. A density matrix is a matrix that describes a quantum system as a statistical ensemble of several quantum states. It can also describe incomplete knowledge about the system. For example, if we know that a system is in state $|\psi\rangle$ with probability 0.5 and in state $|\phi\rangle$ with probability 0.5, then the density matrix is $\rho = 0.5\,|\psi\rangle\langle\psi| + 0.5\,|\phi\rangle\langle\phi|$. This is a mixed state. Up until now, we had considered only pure states, which could be represented with a state vector $|\psi\rangle$. The average value (over the ensemble of states) of an operator A acting on the system state, now represented with a density matrix ρ instead of our state vector $|\psi\rangle$, is

$$\langle A|A\rangle = Tr(\rho A)$$

Note that ρ and A can be represented as a matrix once we have selected a basis. We can calculate this matrix using $M_{ij} = \langle i|\,M\,|j\rangle$, where $\langle i|$ and $|j\rangle$ are basis vectors. $Tr()$ is the trace operator, this is, the sum of the diagonal elements.

Similarly, in the case of the open system, we wanted an average 'over the environment'. This can be done using partial trace, $Tr_B(\rho) = \sum_j \langle j|\,\rho\,|j\rangle$, where, $\{|j\rangle\}$ is a basis of $\mathcal{H}_\mathcal{B}$, so

$$\rho_S = Tr_B(\rho)$$

In pure states the density matrix corresponds to $\rho = |\psi\rangle\langle\psi|$ and we say the system is *coherent*. It corresponds to a matrix in which off-diagonal elements are non-zero. When off-diagonal elements are zero, in general density matrix cannot be written as $|\psi\rangle\langle\psi|$, we say the system is in a *mixed state*, or *decohered*.

2.1.4 Non-unitary Time-Evolution: The Quantum Markovian or Lindblad Master Equation

Formally, the Lindblad Master Equation is defined as follows [1]. Let A be a Banach space. A Banach space is a vector space X over any scalar field K, equipped with a norm $\|\|_X$ and which is complete for the distance function induced by this norm, that is to say, for every Cauchy sequence $\{x_n\}$ in X, there exists an element x in X such that

$$\lim_{n\to\infty} x_n = x,$$

which is equivalent to

$$\lim_{n\to\infty} \|x_n - x\|_X = 0,$$

The general form of the Markovian master equation satisfying the complete positivity condition is outlined. The quantum dynamical semigroup is a one-parameter family of linear maps $\{\Lambda_t, t \geq 0\}$ that satisfy

a) Λ_t is a dynamical map,

b) $\Lambda_t \Lambda_s = \Lambda_{t+s}$, called the semigroup condition or Markov property,

c) $Tr[(\Lambda_t \rho)A]$ is a continous function of t for any density matrix ρ and a linear and bonded operator A.

As a result, there exist a densely defined linear map L, called the infinitesimal generator (or, shortly, the generator) of the semigroup, defined by

$$\frac{d}{dt}\rho_t = L\rho_t \tag{1}$$

where $\rho_t = \Lambda_t \rho$, for $\rho \in D(L)$, being $D(L)$ the domain of L.

The equation (1) is called the quantum Markovian master equation in the Schrdinger picture.

In principle, we can derive the Markovian master equation from the Hamiltonian for the total system using the Markov approximation. However, in practice, it is usually not possible to do that and a phenomenological prescription is needed.

2.2 Quantum Chemistry

The main problem in QC is to find a solution of a non-relativistic time-independent Schdinger equation [122]

$$H\,|\Psi\rangle = E\,|\Psi\rangle \tag{2}$$

where H is the Hamiltonian operator for a system of M nuclei and N electrons.

The coordinates of the system are $\mathbf{R}_i, i = 1, \ldots, M$ for the nuclei and $\mathbf{r}_j, j = 1, \ldots, N$ for the electrons.

The Hamiltonian (in atomic units) is then

$$H = -\sum_{i=1}^{N} \frac{1}{2}\nabla_i^2 - \sum_{A=1}^{M} \frac{1}{2M_A}\nabla_A^2 - \sum_{i=1}^{N}\sum_{A=1}^{M} \frac{Z_A}{r_{iA}} + \sum_{i=1}^{N}\sum_{j>i}^{N} \frac{1}{r_{ij}} + \sum_{i=1}^{M}\sum_{B>A}^{M} \frac{Z_A Z_B}{R_{AB}}$$

where M_A is the ratio of the mass of the nucleus A to the mass of an electron, and Z_A is the atomic number of nucleus A. That is, QC deals with the application of QP to the system composed of M positively charged nuclei and N electrons in 3D space.

We can write this Hamiltonian in a more succinct notation (in SI) as

$$H = K_{ion}(\boldsymbol{R}) + K_e(\boldsymbol{r}) + V_{e-ion}(\mathbf{R}, \mathbf{r}) + V_{e-e}(\mathbf{r}) + V_{ion-ion}(\mathbf{R})$$

Here $\mathbf{R}$ is the vector of nuclear coordinates for each nuclei $(\boldsymbol{R}_1, \boldsymbol{R}_2, ..., \boldsymbol{R}_M)$. We can call a fixed set of nuclear positions a nuclear configuration. Idem for the electrons, $\mathbf{r} = (\boldsymbol{r}_1, \boldsymbol{r}_2, ..., \boldsymbol{r}_N)$. We use lower case for the electronic momentum $\mathbf{p}$ and capital $\mathbf{P}$ for the nuclei, so the kinetic energy operators are

$$K_{ion} = \sum_{A}^{M} \frac{\mathbf{P}_A^2}{2M_A} \quad \text{and} \quad K_e = \sum_{i}^{N} \frac{\mathbf{p}_i^2}{2m_e}.$$

Due to the mass difference between the nuclei and the electrons, we can consider the electrons to be fast and the protons to be slow. Therefore, we fix the positions for the nuclei and solve the Schrdinger equation for the electrons, being

$$H_{elec}(\mathbf{r},\mathbf{R}) = \sum_{i}^{N} \frac{\mathbf{p}_i^2}{2m_e} + V_{e-ion}(\mathbf{R},\mathbf{r}) + V_{e-e}(\mathbf{r})$$

the Hamiltonian.

We then solve the Schrdinger equation for a fixed position of the nuclei, let us say $\mathbf{R}$, which will give the electronic eigenstates for this particular nuclear configuration $\mathbf{R}$. We then write the electronic Schrdinger equation as

$$H_{elec}\,\phi_{\mathbf{R}}(\mathbf{r}) = E_{elec}(\mathbf{R})\,\phi_{\mathbf{R}}(\mathbf{r}) \tag{3}$$

where the eigenvector has a $\boldsymbol{R}$ subscript to indicate that they are valid for the given nuclear configuration $\boldsymbol{R}$. For a different configuration $\boldsymbol{R'}$, the eigenvectors and eigenvalues of the electronic Schrdinger equation (3) will be, in general, different.

From the Schrdinger equation (3), we get a set of eigenstates $\phi_{\boldsymbol{R}}^{(i)}$ and eigenvalues $\boldsymbol{E}_e^{(i)}$. The set of eigenstates $\phi_{\boldsymbol{R}}^{(i)}$ forms a basis of the electronic space. Therefore, we can write a general electronic wave function of a molecule as the linear combination of these basis elements

$$\Psi(\boldsymbol{R},\boldsymbol{r}) = \sum_i a_i\,\phi_{\boldsymbol{R}}^{(i)}(\boldsymbol{r})$$

The coefficients a_i are, in fact, the nuclear wave functions, so

$$\Psi(\boldsymbol{R},\boldsymbol{r}) = \sum_i \eta^{(i)}(\mathbf{R})\phi_{\boldsymbol{R}}^{(i)}(\boldsymbol{r}) \tag{4}$$

The expression (4) is called the Born-Huang expansion. Note that the system's wave function is written as products of electronic and nuclear wave functions. The Born-Oppenheimer approximation (BOA) consists of considering only the first term. The wave function can be written then as

$$\Psi(\boldsymbol{R},\boldsymbol{r}) = \eta(\mathbf{R})\,\phi_{\boldsymbol{R}}(\boldsymbol{r})$$

which is the well-known separation of the total wave function into electronic and nuclear wave functions.

In practice, the BOA consists of solving the electronic Schrdinger equation (3) for a fixed nuclear configuration. We then obtain a set of energies, and we write $\epsilon(\mathbf{R})$ for each specific nuclear configuration $\mathbf{R}$. We say that the energy depends parametrically on the nuclear coordinates. It is customary to add the constant nuclear repulsion to the electronic energy

$$E_{tot}(\mathbf{R}) = E_{elec}(\mathbf{R}) + V_{ion-ion}(\mathbf{R})$$

Solving the electronic Hamiltonian (3), obtaining the expression of the (electronic) wave function $\phi_{\boldsymbol{R}}$ and the energies $E_{\mathbf{R}}$ and $E_{tot}(\mathbf{R})$, is called the electronic

problem. Then the nuclear wave function can be calculated, once the electronic problem has been solved, replacing the electronic degrees of freedom by their average values, which is again justified due to the difference in time-scales or velocities between electrons and nuclei. The nuclear Hamiltonian for the motion of the nuclei is

$$\begin{aligned} H &= \sum_{A}^{M} \frac{\mathbf{P}_A^2}{2M_A} + V_{ion-ion}(\mathbf{R}) + \langle \sum_{i}^{N} \frac{\mathbf{p}_i^2}{2m_e} + V_{e-ion}(\mathbf{R},\mathbf{r}) + V_{e-e}(\mathbf{r}) \rangle \\ &= \sum_{A}^{M} \frac{\mathbf{P}_A^2}{2M_A} + V_{ion-ion}(\mathbf{R}) + E_{elec}(\mathbf{R}) = \sum_{A}^{M} \frac{\mathbf{P}_A^2}{2M_A} + E_{tot}(\mathbf{R}) \end{aligned}$$

The total energy $E_{tot}(\mathbf{R})$ is the potential energy surface (PES) for the nuclear coordinates $\mathbf{R}$. Thus, in the BOA, they move on PES obtained by solving the electronic problem. The solutions to the nuclear Schrdinger equation

$$H_{nucl}\,\eta(\mathbf{R}) = E\,\eta(\mathbf{R})$$

describe the vibration, rotation and translation of a molecule. The energy E is the Born-Oppenheimer approximation to the total energy (eigenvalue for the equation 2), and includes electronic, vibrational, rotational and translational energy. This way, we now have all the elements to write the total wave function for the system.

Several methods are used to obtain approximate solutions to the electronic problem, such as HF or Density Functional Theory (DFT). In the former, the electronic wave function is constructed as an antisymmetrised product of single electron wave functions. In the latter, the properties of the system are obtained as a functional of only one variable that contains all the information of the system, the electron density.

Molecular dynamics (MD) simulation consists of solving the electronic problem and obtaining the PES for the nuclei for a given nuclear configuration and then evolving the system of nuclei classically in that potential using the Newton equation of motion, for a given timestep. Then, solving the electronic problem for the new configuration, and so on and so forth.

2.3 Condensed Matter Physics

Condensed matter physics is a very vast subject dealing with the macroscopic and microscopic physical properties of matter [2]. It is concerned with the "condensed" phases, that is, phases that appear whenever the number of constituents in a system is extremely large and the interactions between the constituents are strong. It is the case of solids and liquids, which arise from the electromagnetic forces between atoms. The laws of QP, electromagnetism and statistical mechanics are used to characterize condensed phases. Theoretical understanding of condensed matter physics is related to the notion of emergence. The collection of particles behave in ways dramatically different from their constituents, allowing particular methods that simplify their study.

Only some results on crystalline solids have been used in condensed matter physics for the case of the ice shield, that is formed in the case of water in the

nanotube, and the concept of quasiparticles, in particular, excitons, polarons and polaritons, and related theory. Quasiparticles excitations are emergent phenomena that occur when a microscopically complicated system, for example, a solid, behaves as if it contained different weakly interacting particles in the vacuum, and modern condensed matter theory asserts that a solid crystal is a gas of weakly interacting quasiparticles. The following quasiparticles are defined.

- Electron: a quasiparticle consisting of a real electron and the cloud of effective charge of opposite sign due to exchange an correlation effects arising interaction with all other electrons in the system. The electron is a fermion with a spin 1?2. The Fermi energy (highest occupied state) is of the order of 5 eV, so it can be treated like a nonrelativistic particle. The mass of the quasiparticle can be substantially different from that of the free electron.
- Hole: a quasiparticle, like an electron, but of opposite charge; it corresponds to the absence of electron for a single particle state which lies below the Fermi energy level. The notion of a hole is particularly convenient when the reference state consists of a quasiparticle state that is fully occupied and are separated by an energy gap from the unoccupied state.
- Exciton: bound state of electron and hole, with binding energy 10 eV
- Phonon: This is a collective excitation, corresponding to the coherent motion of all the atoms in the solid. It is quantized lattice vibration with a typical energy scale $\hbar\omega \sim 0.1$ eV.
- Polaron: a quasiparticle, like an electron, whose motion in polar crystals distorts the lattice of positive and negative ions around it.
- Polariton: a hybrid light-matter quasiparticle arising from the strong coupling of excitons and photons.

Even for QC systems, of a single molecule or a few molecules, the task of solving the Schrdinger equation for modest multi-electron atoms is an insurmountable task without the use of approximations. In the case of condensed matter, where the number of nuclei and electrons are $N_N \sim N_e \sim 10^{23}$, it is hugely so. Translational invariance of crystalline solids is often exploited to simplify the problem, so the Hamiltonian

$$H_{elec} = T_e + V_{e-ion} + V_{e-e}$$

satisfies the property

$$V_{e-ion}(\mathbf{r} + \mathbf{r}_n) = V_{e-ion}(\mathbf{r})$$

where

$$\mathbf{r}_n = n_1\mathbf{a}_1 + n_2\mathbf{a}_2 + n_3\mathbf{a}_3$$

that is, the potential obeys the translation symmetry of the lattice. There exists a set of basis vectors $(\mathbf{a}_1, \mathbf{a}_2, \mathbf{a}_3)$ such that the atomic structure remains invariant under translations through any vector $\mathbf{r}_n$, with $(n_1, n_2, n_3) \in \mathbb{Z}$.

2.4 Quantum Electrodynamics

QED is the fundamental theory describing how single quanta of light (photons) and matter (atoms) interact.

2.4.1 Classical Electrodynamics and Plane Waves

Maxwell equations are [85, 62, 64] are a set of coupled partial differential equations that, together with the Lorentz force law, form the foundation of classical electromagnetism, classical optics, and electric circuits.

$$\begin{aligned} \nabla \boldsymbol{E} &= 4\pi\rho \\ \nabla \boldsymbol{B} &= 0 \\ \nabla \times \boldsymbol{E} &= \frac{1}{c}\frac{\partial \boldsymbol{B}}{\partial t} \\ \nabla \times \boldsymbol{B} &= \frac{4\pi}{c}\boldsymbol{j} + \frac{1}{c}\frac{\partial \boldsymbol{E}}{\partial t} \end{aligned}$$

In free space, we have $\rho = 0$ and $\boldsymbol{j} = 0$, and therefore

$$\begin{aligned} \nabla \boldsymbol{E} &= 0 \\ \nabla \boldsymbol{B} &= 0 \\ \nabla \times \boldsymbol{E} &= \frac{1}{c}\frac{\partial \boldsymbol{B}}{\partial t} \\ \nabla \times \boldsymbol{B} &= \frac{1}{c}\frac{\partial \boldsymbol{E}}{\partial t} \end{aligned}$$

The wave equations, which follow, are

$$\begin{aligned} \nabla^2 \boldsymbol{E} - \frac{1}{c}\frac{\partial^2}{\partial t^2}\boldsymbol{E} = 0 \\ \nabla^2 \boldsymbol{B} - \frac{1}{c}\frac{\partial^2}{\partial t^2}\boldsymbol{B} = 0 \end{aligned}$$

Maxwell vector equations show that $\boldsymbol{B}$ and $\boldsymbol{E}$ are constraint in a double sense: they are constrained in space and also they are related to each other. It is useful to express these fields $\mathbf{E}$ and $\mathbf{B}$ in terms of a vector potential $\mathbf{A}$ and a scalar potential ϕ, with

$$\begin{aligned} \mathbf{E} &= -\nabla\phi - \frac{1}{c}\cdot\mathbf{A} \\ \mathbf{B} &= \nabla \times \mathbf{A} \end{aligned}$$

Considering a pure radiation field, that is, light waves, we normalize the scalar potential ϕ to be zero. The vector potential $\mathbf{A}$ will then satisfy the equations [62]

$$\begin{aligned} \nabla^2 \mathbf{A} - \frac{1}{c^2}\mathbf{A} &= 0 \\ \nabla \cdot \mathrm{A} &= 0 \end{aligned}$$

The potential $\mathbf{A}$ is a function in all points in time and space. To describe $\mathbf{A}$ in terms of canonical variables, we would then need an infinite number of such variables. It is possible, however, to choose an enumerable set. For this, we assume that the radiation field is enclosed in a certain volume, such as a volume L^3, so it has to satisfy some boundary condition at the surface of this volume. We impose $\mathbf{A}$ to be periodic on the surface, and L is considered to be large compared to the system. The behavior of the system will not depend on L. It is usual to use $L = 1$. Given this condition for $\mathbf{A}$, the solutions have the form

$$\mathbf{A} = \sum_{\lambda} q_\lambda(t)\mathbf{A}_\lambda(\mathbf{r})$$

where $q_\lambda(t)$ only depends on time and $\mathbf{A}_\lambda(\mathbf{r})$ only depends on space. The $\mathbf{A}_\lambda$ will then satisfy the wave equation

$$\begin{aligned} \nabla^2 \mathbf{A}_\lambda + \frac{\nu_\lambda^2}{c^2}\mathbf{A}_\lambda &= 0 \\ \mathrm{div}\mathbf{A}_\lambda &= 0 \\ \mathbf{A}_\lambda \text{ periodic in } L & \end{aligned} \tag{5}$$

The q_λ satisfy the equation for the harmonic oscillator

$$\ddot{q}_\lambda + \nu_\lambda^2 q_\lambda = 0$$

The solutions to (5) represent an infinite set of orthogonal waves normalised as

$$\int (\mathbf{A}_\lambda \mathbf{A}_\mu) = 4\pi c^2 \delta_{\lambda,\mu}$$

It is useful to represent the field by complex exponential functions. The potential is real and, therefore, can be represented by a series

$$\mathbf{A} = \sum_{\lambda} (q_\lambda(t)\mathbf{A}_\lambda + q_\lambda^*(t)\mathbf{A}_\lambda^*)$$

where the amplitude $q_\lambda(t)$ is now complex.

The solutions to (5) can be expressed as

$$\begin{aligned} \mathbf{A}_\lambda &= \mathbf{e}_\lambda \sqrt{4\pi c^2}\exp\{i(\mathbf{k}_\lambda \mathbf{r})\},\ |\mathbf{k}_\lambda| = \nu/c \\ q_\lambda &= |q_\lambda| \exp\{-i\nu_\lambda t\} \end{aligned}$$

where $q_\lambda \mathbf{A}_\lambda$ represents a wave travelling in the direction of $\mathbf{k}_\lambda$ and $\mathbf{e}_\lambda$ is the direction of polarisation.

2.4.2 Quantisation of the Electromagnetic Field

The electromagnetic field is expressed in terms of the resonant modes of the particular volume V in consideration, bounded by a close surface S. Let $\mathbf{E}_a(x)$ be the eigenfunctions and $k_z^2 = \omega_a^2/C^2$ the eigenvalues of the boundary-value problem

$$\nabla \times \nabla \times E - k^2 E = 0 \quad \text{in } V \qquad \text{and} \qquad n \times E = 0 \quad \text{on } S$$

where $\mathbf{n}$ is the unit vector normal to the surface S. The $\mathbf{E}_a(x)$ functions are normalized

$$\int_v (\mathbf{E}_a \cdot \mathbf{E}_b)\, dV = \delta_{a,b}$$

The electric and magnetic fields can be expanded in the forms

$$E(\mathbf{x}, t) = -\sqrt{4\pi} \sum_a p_a(t) \cdot \mathbf{E}_a(x)$$

and

$$E(\mathbf{x}, t) = \sqrt{4\pi} \sum_a \omega_a q_a(t) \cdot \mathbf{H}_a(x)$$

The Hamiltonian reads then

$$H = \int \frac{E^2 + H^2}{8\pi} dV = \frac{1}{2} \sum_a \left(p_a^2 + \omega_a^2 q_a^2\right)$$

and the Maxwell equations

$$\nabla \times \mathbf{E} = \frac{1}{c} \frac{\partial \mathbf{H}}{\partial t} \nabla \times \mathbf{H} = \frac{1}{c} \frac{\partial \mathbf{E}}{\partial t}$$

reduce to the Hamiltonian equations of motion

$$\dot{q}_a = \frac{\partial H}{\partial p_a} = p_a \quad \text{and} \quad \dot{p}_a = -\frac{\partial H}{\partial q_a} = -\omega_a^2 q_a.$$

To quantize the field, the canonical conjugate coordinates and momenta satisfy the commutation relations

$$[q_a, q_b] = [p_a, p_b] = 0 \quad \text{and} \quad [q_a, p_b] = i\hbar\delta_{a,b}$$

The operators C_a^* and C_a which create or annihilate a photon in the a-th volume mode are respectively

$$C_a^* = \frac{p_a + i\omega_a q_a}{\sqrt{2\hbar\omega_a}} \quad \text{and} \quad C_a = \frac{p_a - i\omega_a q_a}{\sqrt{2\hbar\omega_a}},$$

with the commutation relations verifying

$$[C_a, C_b^*] = \delta_{a,b}.$$

Denote by $\phi(n_1, n_2, \dots)$ the state vector of the field for which there are n_1 quanta in mode 1, n_2 in mode 2, etc. The C_a^* and C_a operators have the properties

$$C_a\,\phi(\dots, n_a, \dots) = \sqrt{n_a}\,\phi(\dots, n_a - 1, \dots)$$
$$C_a^*\,\phi(\dots, n_a, \dots) = \sqrt{n_a + 1}\,\phi(\dots, n_a + 1, \dots)$$

from which the commutation relations are easily verified. To obtain the matrix elements in the n_a representation

$$\langle n_a|\, C_a\, |n_a'\rangle = \langle n_a'|\, C_a^*\, |n_a\rangle = \sqrt{n_a + 1}\,\delta(n_a', n_a + 1)$$

Finally, the Hamiltonian with zero-point energy removed is

$$H = \sum_a \hbar\omega_a C_a^* C_a = \sum_a \hbar\omega_a n_a$$

2.4.3 Quantum Optics

In classical theory, the radiation emitted by an atom is determined by the (time-rate of variation) of the electric dipole moment [12]. By the correspondence principle, this connection has to subsist in QP. The dipole moment in QP is

$$p = e\int \mathbf{r}\,|\Psi_n|^2 dv = e\int \mathbf{r}\,\Psi_n^*\Psi_n\,dv,$$

where $\mathbf{r}$ stands for the radius vector from the nucleus to the point of integration, also called field point. The integral represents the position of the centroid of the electronic cloud. It can be proved easily that this integral vanishes for all states of an atom, the derivatives of the dipole moment vanishes, and then also the emitted radiation. In summary, a stationary state does not radiate.

In a more sense, for the transition between stationary states of a system induced by the coupling to another system with a dense distribution of stationary states, we obtain a transition probability, given by

$$P_{mn} = \frac{2\pi}{\hbar}\left|H'_{mn}\right|^2\rho(\epsilon),$$

where H'_{mn} is the matrix element of the coupling energy corresponding to the two states. The motion of a free electron is described by the Schrdinger equation

$$-\frac{\hbar^2}{2m}\nabla^2\Psi = i\hbar\frac{\partial\Psi}{\partial t}.$$

The probability of finding an electron at position $\mathbf{r}$ and time t, that is, the density probability is

$$P(\mathbf{r}, t) = |\Psi(\mathbf{r}, t)|^2,$$

and $\Psi(\mathbf{r}, t)$ is a solution to the Schrdinger equation. Therefore, we have

$$\Psi_1(\mathbf{r}, t) = \Psi(\mathbf{r}, t)e^{i\chi},$$

where χ is an arbitrary constant phase. The probability density $P(\mathbf{r},t)$ is unaffected by the choice of χ, which is completely arbitrary. Two functions differing only by a constant phase factor represent the the same physical state.

If the phase of the wave function is allowed to vary locally,

$$\Psi_1(\mathbf{r},t) \rightarrow \Psi(\mathbf{r},t)e^{i\chi(\mathbf{r},t)},$$

the probability $P(\mathbf{r},t)$ remains unaffected but the Schrdinger equation is no longer satisfied. In order to satisfy local gauge (phase) invariance, the Schrdinger equation has to be modified by adding new terms, as

$$\left[\frac{-\hbar^2}{2m}\left(\nabla - i\frac{e}{\hbar}\mathbf{A}(\mathbf{r},t)\right)^2 + e\Phi(\mathbf{r},t)\right]\Psi = i\hbar\frac{\partial\Psi}{\partial t},$$

and we have

$$\mathbf{A}(\mathbf{r},t) \rightarrow \mathbf{A}(\mathbf{r},t) + \frac{\hbar}{e}\nabla\chi(\mathbf{r},t)\Phi(\mathbf{r},t) \rightarrow \Phi(\mathbf{r},t) - \frac{\hbar}{e}\frac{\partial\chi(\mathbf{r},t)}{\partial t},$$

where $\mathbf{A}(\mathbf{r},t)$ and $\Phi(\mathbf{r},t)$ are the vector and scalar potentials of the external field, respectively. Both $\mathbf{A}(\mathbf{r},t)$ and $U(\mathbf{r},t)$ are gauge-dependent potential, while the electric and magnetic fields

$$\mathbf{E} = -\nabla\Phi - \frac{\partial\mathbf{A}}{\partial t}\mathbf{B} = \nabla\mathbf{A}$$

are gauge-independent.

An electron of charge e and mass m interacting with an external electromagnetic field is described by the minimal coupling Hamiltonian,

$$H = \frac{1}{2m}[\mathbf{p} - e\mathbf{A}(\mathbf{r},t)]^2 + e\Psi(\mathbf{r},t)$$

where $\mathbf{p} = -i\hbar\nabla$ is the canonical momentum operator. The electrons are described by the wave function $\psi(\mathbf{r},t)$ and the external field is described by the vector and scalar potentials $\mathbf{A}$ and Φ. If the entire atom is immersed in a plane electromagnetic wave

$$\mathbf{A}(\mathbf{r}_0+\mathbf{r},t) = \mathbf{A}(t)e^{i\,\mathbf{k}\cdot(\mathbf{r}_0+\mathbf{r})} \approx A(t)e^{i\,\mathbf{k}\cdot\mathbf{r}_0}$$

where $\mathbf{r}_0$ is the location of the electron. The dipole approximation, $\mathbf{A}(\mathbf{r},t) \approx \mathbf{A}(\mathbf{r}_0,t)$, and the minimal coupling Hamitonian becomes then

$$H = \frac{1}{2m}\left[\mathbf{p} - e\mathbf{A}(\mathbf{r}_0,t)\right]^2 + e\Phi(\mathbf{r},t) + V(\mathbf{r}),$$

where $V(\mathbf{r})$ is the atomic binding potential.

In the radiation gauge, we have

$$\Phi(r,t) = 0 \quad \text{and} \quad \nabla\cdot\mathbf{A}(r,t) = 0$$

The minimal coupling Hamiltonian becomes

$$H = \frac{\mathbf{p}^2}{2m} + V(r) + e\,\mathbf{r}\,\frac{\partial\mathbf{A}(r_0,t)}{\partial t},$$

and, in the dipole approximation, it

$$H = \frac{1}{2m}\left[\mathbf{p} - e\mathbf{A}(\mathbf{r}_0, t)\right]^2 + e\Psi(\mathbf{r}, t) + V(\mathbf{r})$$

Also, the wave function with a local phase is given by

$$\Psi(\mathbf{r}, t) = \Psi(r, t)e^{\frac{ie}{\hbar}\mathbf{A}(\mathbf{r}_0,t)\cdot\mathbf{r}}$$

and then we can write

$$i\hbar\left[\frac{ie}{\hbar}\,\mathbf{r}\cdot\frac{\partial\mathbf{A}(\mathbf{r}_0,t)}{\partial t}\,\Psi(\mathbf{r},t) + \frac{\partial\Psi(\mathbf{r},t)}{\partial t}\right] e^{\frac{ie}{\hbar}\,\mathbf{A}\cdot\mathbf{r}} = \left[\frac{\mathbf{p}^2}{2m} + V(\mathbf{r})\right] e^{\frac{ie}{\hbar}\,\mathbf{A}\cdot\mathbf{r}}$$

In terms of the gauge-independent field $\mathbf{E}$, the Hamiltonian for $\Psi(\mathbf{r}, t)$ is

$$H = \frac{\mathbf{p}^2}{2m} + V(r) + e\,\mathbf{r}\cdot\frac{\partial\mathbf{A}(\mathbf{r}_0,t)}{\partial t} = \frac{\mathbf{p}^2}{2m} + V(\mathbf{r}) - e\,\mathbf{r}\cdot\mathbf{E}(\mathbf{r}_0,t) = H_0 + H_1$$

in terms of the gauge-independent field $\mathbf{E}$, and where

$$H_0 = \frac{\mathbf{p}^2}{2m} + V(r) \quad \text{and} \quad H_1 = -e\mathbf{r}\cdot\mathbf{E}(\mathbf{r}_0,t).$$

Considering now the interaction of a single-mode radiation field of frequency ν, and two-level atom with the ground and excited states $|a\rangle$ and $|b\rangle$, respectively. The unperturbed part of the Hamiltonian $\tilde{H}_0$ has the eigenvalues $\hbar\omega_a$ and $\hbar\omega_b$ for the atom and the wave function can be written in the form

$$|\Psi(t)\rangle = c_a(t)\,|a\rangle + c_b(t)\,|b\rangle\,.$$

The corresponding Schrdinger equation is

$$i\hbar\frac{\partial\Psi(t)}{\partial t} = \left(\tilde{H}_0 + \tilde{H}_1\right),$$

where

$$\tilde{H}_0 = (|a\rangle\langle a| + |b\rangle\langle b|)\,\tilde{H}_0\,(|a\rangle\langle a| + |b\rangle\langle b|) = \hbar\omega_a\,|a\rangle\langle a| + \hbar\omega_b\,|b\rangle\langle b|$$

and

$$\begin{aligned}\tilde{H}_1 &= -e\,\boldsymbol{r}\cdot\boldsymbol{E}(t) = -e\,(|a\rangle\langle a| + |b\rangle\langle b|)\,\boldsymbol{r}\,(|a\rangle\langle a| + |b\rangle\langle b|)\,\boldsymbol{E}(t)\\ &= -\left(\boldsymbol{p}_{ab}\,|a\rangle\langle b| + \boldsymbol{p}_{ba}\,|b\rangle\langle a|\right)\boldsymbol{E}(t)\end{aligned}$$

In the dipole approximation, we have

$$\tilde{H}_0 = \hbar\omega_a\,|a\rangle\langle a| + \hbar\omega_b\,|b\rangle\langle b| \quad \text{and} \quad \tilde{H}_1 = -\left(\boldsymbol{p}_{ab}\,|a\rangle\langle b| + \boldsymbol{p}_{ba}\,|b\rangle\langle a|\right)\boldsymbol{E}(t)$$

with $\boldsymbol{p}_{ab} = \boldsymbol{p}_{ba} = e\,|a\rangle\,\boldsymbol{r}\,\langle b|$.

For a single mode field $\boldsymbol{E}(t) = E_0 cos\nu t$, the equations of motion for the probability amplitude are

$$\frac{dc_a}{dt} = -i\omega_a c_a + i\Omega_R cos(\nu t)e^{-i\phi}c_b, \quad \frac{dc_b}{dt} = -i\omega_b c_b + i\Omega_R cos(\nu t)e^{i\phi}c_a,$$

where $\Omega_R = \frac{|\boldsymbol{p}_{ab}|E_0}{\hbar}$ is the Rabi frequency, which is proportional to the amplitude of the classical field and ϕ is the phase of the dipole matrix element $\boldsymbol{p}_{ab} = |\boldsymbol{p}_{ab}|^{i\phi}$. From now on we note c_a as $\tilde{c}_a$ and the same for c_b and define the slowly varying amplitudes

$$c_a = \tilde{c}_a e^{i\omega_a t} \quad \text{and} \quad c_b = \tilde{c}_b e^{i\omega_b t}$$

Then we have

$$\frac{dc_a}{dt} = -i\frac{\omega_R}{2}e^{-i\phi}[e]c_a + i\Omega_R cos(\nu t)e^{-i\phi}c_b$$
$$\frac{dc_b}{dt} = -i\omega_b c_b + i\Omega_R cos(\nu t)e^{i\phi}c_a$$

The Dicke model has also been called the Dicke-Preparata model in honor to G. Preparata [115]. It is presented including the expression for the coupling constant condition for superradiance.

The linear coupling between the dipole moment per unit volume and the electric field can be modelled by the resonant photon creation and annihilation terms [115]

$$\mu\sqrt{\frac{2\pi\hbar\omega_0}{\Omega}}\sum_{i=1}^{N}\left(b\sigma_i^+ + b^\dagger\sigma_i^-\right),$$

where $2\sigma_i^\pm = \sigma_i^x \pm i\sigma_i^y$ and μ is the excitation matrix element of the electric dipole operator of a single molecule. The Dicke-Preparata model is

$$H_{DP} = \varepsilon\frac{1}{2}\sum_{i=1}^{N}\sigma_i^z + \hbar\omega_0 b^\dagger b + \mu\sqrt{\frac{2\pi\hbar\omega_0}{\Omega}}\left(bS^+ + b^\dagger S^-\right)$$

and

$$S^\pm = \frac{1}{2}\sum_{i=1}^{N}(\sigma_i^x \pm i\sigma_i^y) = \frac{1}{2}\sum_{i=1}^{N}2\sigma_i^\pm.$$

It may be written in terms of the oscillator coordinate Q and momentum P using

$$b = \frac{P - i\omega_0 Q}{\sqrt{2\hbar\omega_0}}, \qquad b^\dagger = \frac{P + i\omega_0 Q}{\sqrt{2\hbar\omega_0}}$$

It yields

$$H'_{DP} = \frac{P^2 + \omega_0^2 Q^2}{2} + \mathbf{h}\cdot\mathbf{S},$$

where the vector $\mathbf{h}$ is given by

$$\mathbf{h} = \mu\sqrt{\frac{4\pi}{\Omega}}\left(P\mathbf{i} + \omega_0 Q\mathbf{j}\right) + \varepsilon\mathbf{k}.$$

1. Interaction with the Electromagnetic Field - the Dicke-Preparata Hamiltonian

The Dicke Hamiltonian [39, 69] accounts for the fact that in spontaneous radiation processes, molecules are interacting with a common radiation field. It has been applied to the case of water [61, 115]. We represent the ground and excited states of each of N two-level atoms denoted by $|0\rangle_i$ and $|1\rangle_i$, for $i = 1, \ldots, N$, which are associated with the eigenvalues $+1/2$ and $-1/2$ of the operator

$$\sigma_{3i} = \frac{1}{2}\left(|1\rangle_i \langle 1|_i - |0\rangle_i \langle 0|_i\right)$$

The operators $\sigma_i^+ = |1\rangle_{ii} \langle 0|$ and $\sigma^- = (\sigma_i^+)^\dagger$ generate the transition between the two levels, induced by the action of the electric field. The N-atoms system is described by the collective operators $\sigma^+ = \sum_{i=1}^N \sigma_i^+$ and $\sigma^- = \sum_{i=1}^N \sigma_i^-$, which obey the $SU(2)$ algebra

$$\begin{aligned}
\left[\sigma_3, \sigma^+\right] &= \sigma^+ \\
\left[\sigma_3, \sigma^-\right] &= -\sigma^- \\
\left[\sigma^-, \sigma^+\right] &= -2\sigma_3
\end{aligned}$$

With the $\mathbb{C}^2$ representation for the operators,

$$\begin{aligned}
|0\rangle &= \begin{pmatrix} 0 \\ 1 \end{pmatrix}, \\
|1\rangle &= \begin{pmatrix} 1 \\ 0 \end{pmatrix}
\end{aligned}$$

the operators σ^+ and σ^- are

$$\sigma^+ = |1\rangle \langle 0| = \begin{pmatrix} 1 \\ 0 \end{pmatrix} \begin{pmatrix} 0 & 1 \end{pmatrix} = \begin{pmatrix} 0 & 1 \\ 0 & 0 \end{pmatrix}$$

and

$$\sigma^- = |0\rangle \langle 1| = \begin{pmatrix} 0 \\ 1 \end{pmatrix} \begin{pmatrix} 1 & 0 \end{pmatrix} = \begin{pmatrix} 0 & 0 \\ 1 & 0 \end{pmatrix},$$

respectively. Finally, σ_3 is

$$\begin{aligned}
\sigma_3 &= \frac{1}{2}\left[|1\rangle \langle 1| - |0\rangle \langle 0|\right] = \frac{1}{2}\left[\begin{pmatrix} 1 \\ 0 \end{pmatrix} \begin{pmatrix} 1 & 0 \end{pmatrix} - \begin{pmatrix} 0 \\ 1 \end{pmatrix} \begin{pmatrix} 0 & 1 \end{pmatrix}\right] \\
&= \frac{1}{2}\left[\begin{pmatrix} 1 & 0 \\ 0 & 0 \end{pmatrix} - \begin{pmatrix} 0 & 0 \\ 0 & 1 \end{pmatrix}\right] = \begin{pmatrix} 1 & 0 \\ 0 & -1 \end{pmatrix}
\end{aligned}$$

The interaction Hamiltonian is

$$H = g(b^{\dagger}\sigma^{-} + b\sigma^{+}),$$

where g is the coupling constant, $b^{\dagger}$ and b are the creation and annihilation operators of the electromagnetic field, and σ^{+} and σ^{-} are the collective raising and lowering operators defined as

$$\sigma^{+} = \sum_{i=1}^{N} \sigma_i^{+}, \quad \sigma^{-} = \sum_{i=1}^{N} \sigma_i^{-}$$

with operators $\sigma_i^{+} = |1\rangle_i \langle 0|_i$ and $\sigma^{-} = (\sigma_i^{+})^{\dagger}$ generating the transition between the ground and excited states. The system state is represented as the normalized superposition $|l\rangle$ defined as

$$\begin{aligned} |l\rangle = \frac{1}{\sqrt{\binom{N}{l}}} (&|1\rangle_1 |1\rangle_2 \dots |1\rangle_l |0\rangle_{l+1} \dots |0\rangle_N \\ &+ |0\rangle_1 |1\rangle_2 \dots |1\rangle_{l+1} |0\rangle_{l+2} \dots |0\rangle_N \\ &+ \dots \\ &+ |0\rangle_1 \dots |0\rangle_{N-l} |1\rangle_{N-l+1} \dots |1\rangle_N) \end{aligned}$$

The operators $\sigma^{+} = \sum_i \sigma_i^{+}$ and $\sigma^{-} = \sum_i \sigma_i^{-}$ acting on $|l\rangle$ result in

$$\begin{aligned} \sigma^{+} |l\rangle &= \sqrt{l+1}\sqrt{N-l}\, |l+1\rangle \\ \sigma^{-} |l\rangle &= \sqrt{N-(l-1)}\sqrt{l}\, |l-1\rangle \end{aligned}$$

It was shown in 1973 that the Dicke model in the thermodynamic limit exhibits a second-order phase transition from a normal to a steady-state superradiant phase. Taking into account the counter-rotating terms, it was pointed out by Carmichael et al. [24] that the critical coupling strength is given by

$$\lambda_c = \sqrt{\frac{\omega\omega_0}{4tanh\beta\frac{\hbar\omega_0}{2}}}$$

with $\beta = 1/k_b T$.

The critical coupling strength increases with temperatures while for low temperatures, the slope of the curve diverges as it approaches the zero-temperature limit $\lambda_c = \sqrt{\omega\omega_0}/2$.

The gain or loss in the photon energy due to Doppler effect is equal to the loss or gain in the kinetic energy of a radiating element [39], that is,

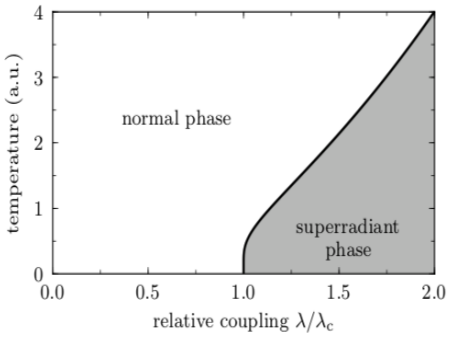

Figure 3: Dicke superradiance coupling condition.

$$\frac{\Delta\omega}{\omega} = \frac{\hbar(\mathbf{S} - \frac{1}{2}\mathbf{k}) \cdot \mathbf{k}}{Mck},$$

where M is the molecular mass, and $\mathbf{k}$ defined the direction of coherence. For energy states where $|m| \ll \frac{n}{2}$, the expression becomes

$$\frac{\Delta\omega}{w} = \frac{\mathbf{v} \cdot \mathbf{k}}{ck}$$

where $\mathbf{v}$ is the total momentum of the gas divided by the total mass.

2.5 QED Coherence in Matter

We assume there are N atoms per unit volume which are collectively described by the complex dipole wave field $\phi(\mathbf{x}, t)$. The system is assumed to be spatially homogeneous and in a thermal bath kept at a non-vanishing temperature T. Under such conditions the system is invariant under dipole rotations and, since the density is assumed to be spatially uniform, the only relevant variables are the angular ones. We use natural units $\hbar = c = 1$ and denote with $d\Sigma = sin\theta\, d\theta\, d\phi$ the element of solid angle and with (r, θ, ϕ) the polar coordinates of $\mathbf{r}$. The dipole wave field $\phi(\mathbf{x}, t)$ integrated over the sphere of unit radius $\mathbf{r}$ gives

$$\int d\Sigma |\phi(\mathbf{x}, t)|^2 = N$$

In terms of a rescaled field defined as $\chi(\mathbf{x}, t)$ we obtain

$$\int d\Sigma |\chi(\mathbf{x}, t)|^2 = 1. \tag{6}$$

In full generality under the assumed conditions, the field $\chi(\mathbf{x}, t)$ may be expanded in the unit sphere in terms of spherical harmonics

$$\chi(\mathbf{x}, t)) = \sum_{l,m} \alpha_{l,m}(t) Y_l^m(\theta, \phi).$$

Restricted to the case $l = 0$ and $l = 1$ it reduces to the expansion into four levels, which are $(l, m) = (0, 0)$ and $(1, m)$, with $m = 0, \pm 1$. The populations of these levels are given by $N|\alpha_{l,m}(t)|^2$ and at thermal equilibrium, in the absence of interaction, they are given by the Boltzmann distribution. Thermal equilibrium and dipole rotation invariance imply that there is no preferred direction in the dipole orientation, which means that $|\alpha_{1,m}(t)|$ have in average the same value, for any m. We then can write

$$\alpha_{0,0}(t) \equiv a_0(t) \equiv A_0(t)e^{i\delta_0(t)}$$
$$\alpha_{1,m}(t) \equiv a_{1,m}(t)e^{i\omega_0 t} \equiv A_1(t)e^{i\delta_{1,m}(t)e^{-i\omega_0 t}}$$

The amplitudes $A_0(t)$ and $A_1(t)$, and the phases $\delta_0(t)$ and $\delta_{1,m}(t)$, are real and $\omega_0 \equiv 1/I$, with I the moment of inertia of the atom, which gives a relevant scale for the system, $\omega \equiv k \equiv 2\pi/\lambda$. By denoting with $\mathbf{L}^2$ the squared angular momentum operator, the eigenvalue of $\frac{\mathbf{L}^2}{2I}$ on the state $(1, m)$ is

$$\frac{l(l+1)}{2I} = \frac{1}{I} = \omega_0$$

The fact that the three levels $(1, m)$, with $m = 0, + - 1$, are in the average equally populated under normal conditions is confirmed by the absence of permanent polarization in the system. In the assumed conditions, the time average of the polarization $P_{\mathbf{n}}$ along any direction $\mathbf{n}$ is equal to zero. Setting the $\mathbf{z}$ axis parallel to $\mathbf{n}$ and putting $\omega t \equiv \delta_{1,0}(t) - \delta_0(t)$ we obtain

$$P_{\mathbf{n}} = \int d\Sigma\, \chi^*(\mathbf{x}, t)\, (\mathbf{x} \cdot \mathbf{n})\, \chi(\mathbf{x}, t) = \frac{2}{\sqrt{3}} A_0(t) A_1(t) cos(\omega - \omega_0)t$$

whose time average is zero. Then we can write

$$\sum_m |\alpha_{1,m}(t)|^2 = 3\,|a_1(t)|^2$$

The normalisation condition (6) gives

$$Q \equiv |\alpha_{0,0}|^2 + \sum_m |\alpha_{1,m}(t)|^2 = |a_0(t)| + 3|a_1(t)|. \tag{7}$$

for all t, and then the conservation law $\dfrac{\partial Q}{\partial t} = 0$ gives

$$\frac{\partial}{\partial t}|a_1(t)|^2 = -\frac{1}{3}\frac{\partial}{\partial t}|a_0(t)|^2 \tag{8}$$

The conservation law expresses the conservation of the total number of atoms. Equation (8) means that due to rotation invariance, the rate of change of the population of each of the levels $(1, m)$, with $m = 0, + - 1$, equally contributes, on average, to the rate of change of the level $(0, 0)$, at each time t. That is because the $(0, 0)$ level is spherically symmetric and the rest are not.

Given the condition in equation (7) we can express the value of $|a_0(t)|$ and $|a_1(t)|$ in terms of a single parameter θ for a given time t

$$|a_0(t)|^2 = cos^2\theta, \;\; |a_1(t)|^2 = cos^2\theta, \quad \text{for} \quad 0 < \theta < \frac{\pi}{2}$$

We can then write the initial conditions at $t = 0$ as

$$|a_0(0)|^2 = cos^2\theta_0, \;\; |a_1(0)|^2 = cos^2\theta_0, \quad \text{for} \quad 0 < \theta < \frac{\pi}{2}$$

The values $\theta_0 = 0$ and $\theta_0 = \pi/2$ are excluded because it is physically unrealistic for the state $(0, 0)$ to be completely filled (zero) or completely empty $(\pi/2)$. For example, $\theta_0 = \pi/3$ describes the equipartition of the field modes of energy $E(k)$ between the four levels $(0, 0)$ and $(1, m)$, $|a_0(0)|^2 \approx |a_{1,m}(0)|^2$, with $m = 0, \pm 1$, as given by the Boltzmann distribution when the temperature T is high enough, $k_B T >> E(k)$. The lower bound for the parameter θ_0 is imposed by the dynamics in a self-consistent way.

Let $u_r(\mathbf{k}, t) = 1/\sqrt{N}\, c_r(\mathbf{k}, t)$, and $c_k(\mathbf{k}, t)$ denote the radiative electromagnetic field operator with polarization r, d the value of the electric dipole moment, $\rho = \frac{N}{V}$ and $\mathbf{e}_r$ the polarization vector of the electromagnetic mode (for which we assume the transversality condition $\mathbf{k} \cdot \mathbf{e}_r = 0$). The field equations for the system are

$$i\frac{\partial \chi(\mathbf{x}, t}{\partial t} = \frac{\mathbf{L}^2}{2I}\chi(\mathbf{x}, t) - i\sum_{\mathbf{k},t} d\sqrt{\rho}\sqrt{\frac{k}{2}}\,(\mathbf{e}_r \cdot \mathbf{x})\left[u_k(\mathbf{k}, t)e^{-ikt} - u_r^\dagger(\mathbf{k}, t)e^{ikt}\right]\chi(\mathbf{x}, t),$$

$$i\frac{\partial u_r(\mathbf{k}, t)}{\partial t} = id\sqrt{\rho}\sqrt{\frac{k}{2}}e^{ikt}\int d\Omega(\mathbf{e}_r \cdot \mathbf{x})|\chi(\mathbf{x}, t)|^2.$$

There is an enhancement by the factor of $\sqrt{N}$ in the coupling $d\sqrt{\rho}$ due to the rescaling of the fields.

2.6 The Quantum Electrodynamics-Quantum Chemistry Framework

In Section 2.2 we introduced the molecular Schrdinger equation and the electronic problem of QC. Even in the absence of electromagnetic fields, QED shows that the interaction between the molecule and the electromagnetic vacuum, or with photons if they are present, have an impact on the state of the system, which is usually neglected. In this paragraph we introduce a framework in which the photon part and interaction is included [12, 44, 47, 112, 110]

(") The Pauli Hamiltonian comprises the standard Schrdinger Hamiltonian and the Pauli (Stern?Gerlach) term $\sigma \cdot B(\mathbf{r})$, which describes the coupling between the electron spin (characterized by a vector of the usual Pauli matrices σ) and the magnetic field $B(\mathbf{r})$.

(") Within the non-relativistic limit for the matter subsystem, the full QED Hamiltonian can be simplified to the Pauli Hamiltonian (for the matter subsystem) describing the evolution of charged particles in spinor representation, which are coupled through the charge-density and charge-current operators to the quantized photon field. For a system of Ne electrons and Nn nuclei, the corresponding Hamiltonian,

known as the Pauli?Fierz Hamiltonian. Matter Hamiltonian for a single molecule in the electric dipole limit, known as the Pauli-Fiez Hamiltonian is [40, 62, 114, 118, 43]

$$H_m(t) = \sum_{i=1}^{N} K_i(\mathbf{p}_i - \frac{q_i}{c}\mathbf{A}(t)) + V(\mathbf{r}_1, \ldots, \mathbf{N})$$

where $K_i(\mathbf{p_i}) = (\mathbf{p}_i^2/2m_i)$ is the kinetic energy of the i-th particle in the molecule, $V(\mathbf{r}_1, \ldots, \mathbf{N})$ is the internal Coulomb energy of the molecule, and $\mathbf{A}$ is the electromagnetic potential.

The photon and photon interaction part can be expressed as [112, 46, 124]

$$H_p + H_{ep} + H_{np} = \frac{1}{2}\sum_{\alpha=1}^{M_p}\left[p_\alpha^2 + \omega_\alpha^2\left(q_\alpha - \frac{\lambda_\alpha}{\omega_\alpha}\cdot\mathbf{R}\right)^2\right]$$

where M_p is a finite but arbitrary large number of photon modes. They are the most relevant modes but in principle run from the fundamental mode of our arbitrarily large but for simplicity finite quantization volume up to a maximum sensible frequency, for example, an ultra-violet cut-off at rest mass energy of the electrons. $\mathbf{R}$ is the total dipole of electrons and nuclei.

$$\mathbf{R} = \sum_{j=1}^{N_e}\mathbf{r}_j - \sum_{j=1}^{N_n} Z_j\mathbf{R}_j$$

The quantized oscillators representing the photonic system consists of the canonical coordinate corresponding to the displacement field

$$q_\alpha = \frac{1}{2\sqrt{\omega_\alpha}}(a_\alpha^\dagger + a_\alpha)$$

and the conjugate momentum

$$p_\alpha = -i\sqrt{\frac{\omega_\alpha}{2}}(a_\alpha^\dagger - a_\alpha^\dagger) \equiv -i\frac{\partial}{\partial q_\alpha}$$

with

$$[q_\alpha, p'_\alpha] = i\delta\alpha\alpha'$$

The fundamental coupling strength $\lambda_\alpha = \lambda_\alpha \mathbf{e}_\alpha$ describes the coupling between the total dipole and the photonic mode α with wavevector $\mathbf{k}_\alpha$ and transverse polarisation vector $\mathbf{e}_\alpha$.

[43]

The self-polarization part in the photonic Hamiltonian naturally arises in the length form to make the Hamiltonian bounded from below, which is a prerequisite to allow for ground states of an interacting light-matter many-body system

[98]

A system with arbitrarily large number of electrons N at coordinates $\{\mathbf{r}_i\}_{i=1}^N\}$, e.g. an atom, an ion, or a molecular cluster, interacting with M quantized radiation modes of momenta $\{p_\alpha\}_{i=1}^M$ and frequencies ω_α. Denoting $H_0 = T + V_{ee} + V_{ext}$ the Hamiltonian of the unperturbed electronic system with kinetic energy T, Coulomb

interaction V_{ee}, and external time-dependent potential $V_{ext} = \sum_{i=1}^{N} v_e xt(\mathbf{r}_i, t)$, due to the nuclear attraction and any classical field applied to the system. Adopting the length gauge in the dipole approximation, the Hamiltonian of the fully interacting electron-photon system takes the form

$$H = H_0 + \frac{1}{2}\sum_{\alpha}\left[p_\alpha^2 + \omega_\alpha^2\left(q_\alpha + \omega_\alpha^2\left(q_\alpha - \frac{\lambda_\alpha}{\omega_\alpha}\cdot\mathbf{R}\right)^2\right)\right]$$

where $\mathbf{R} = \sum_{i=1}^{N} \mathbf{r_i}$ the dipole operator of the electronic system and λ_α the coupling constant of the α photon mode. The photon coordinates are defined in terms of annihilation and creation operators as

$$q_\alpha = -\sqrt{\frac{1}{2\omega_\alpha}}(a_\alpha + a_\alpha).$$

The interaction Hamiltonian consists of two terms: the cross-term that describes the dipole-photon coupling, and the squared term that represents the polarization energy of the electronic system due to Coulomb-like interaction.

Part I
Macroscopic Scale

In this Part, the behavior of water at the macroscopic scale is studied. There is a large number of molecules and, at this level, the focus is on average properties. The water molecules are not characterized individually and the details of behavior at the microscopic scale are not available. That is, nuclei positions, if considered classical, and electron density distributions. Quantum Electrodynamics (QED) Coherence in Matter [101] gives a descriptive explanation of water behavior at the average, macroscopic scale. Condensed Matter Physics deals with quasiparticles, which are collective excitations, and for which the microscopic details are not specified. The approach is inspired in QED Coherence in Matter, which suggests collective effects to be important in water, and results from Condensed Matter Physics are used.

The objective of Chapter 3 is to have a general idea of the order of magnitude of the quantities involved and see if they encourage to look further into the details. An order of magnitude calculation is conducted for water in the nanotube, to study the possibility of kinetic energy differences to be due to polaronic effects. Using a simple classical description, two possible scenarios are considered, one with the electron in the vicinity of each proton, and an alternative with the electron trapped between four protons in the squares formed by the Oxygens in the hexagonal ice shield. The polaron size in each case is calculated.

3 Polaron Kinetic Energy in the Nanotube

3.1 Elements of Theory

The polaron classical picture by Landau is a classical picture to estimate the orders of magnitude for the size and energy of an electron charge density distribution in a lattice, assuming the electron distribution to be localized. This part follows the presentation in the book [25].

At small distances from the electron distribution, considered as a spherical charge distribution of radius R the potential at a point $r < R$ is given by

$$\phi(r) = \frac{e}{2\epsilon R}\left(3 - \frac{r^2}{R^2}\right)$$

The potential energy of the electron, considered distributed as a uniform charge density in a sphere of radius R, is given by

$$U = \int |\nabla\phi(r)|^2 \, dr \approx -\frac{e^2}{\epsilon R}$$

The kinetic energy of the electron is of the order of $\hbar^2 k^2/2m$, where k is the wavenumber of a system confined in a space of the size order R. The uncertainty ΔR has to be smaller than R. According to the uncertainty principle, the minimum error in the estimation of the momentum Δp is given by

$$(\Delta p)_{min} = \frac{2\pi\hbar}{R}$$

Therefore, the momentum cannot be less than $(2\pi\hbar)/R$ and the kinetic energy is given, then by

$$K = \frac{4\pi^2\hbar^2}{2mR^2}$$

This approximation is also valid for the case of the proton, given that it experiences a potential of the same form, by introducing the proton mass instead of the electron mass. On the other hand, the approximation is valid for a polaron size up to about 10 Å.

3.2 Results and Discussion

The possibility of a polaron explaining the kinetic energy difference measured by Reiter [106, 105] is studied. Specifically, water confined in a carbon nanotube of diameter 14 Å and length 10 nm, has a kinetic energy 35 meV lower than regular ice, at 5 K, and it can be studied whether this difference could be potentially due to the existence of polarons in the system.

A simple formula that estimates the minimum kinetic energy in the lattice due to a polaron of size R is used, which is based on a static electron density Coulomb interaction. It is deduced which size of the polaron would correspond to the kinetic energy difference.

It has been shown that water molecules entering the nanotube form a structured, ice-like, layer lining the nanotube surface, for example, polygonal water rings

stacked one-dimensionally along the tube axis [90, 7] or helical [95], with anomalous characteristics, as have already presented in the Introduction.

Hexagonal ice structures are assumed, with about 3 Å separation between molecules and similar reasoning used, as for the electron kinetic energy. In the case of a Coulomb potential, and using the uncertainty relations to derive limits to the energy values, a relationship between radius and number of polarons is obtained, for the given kinetic energy difference

$$R = \hbar\sqrt{\frac{2n\pi}{m_p K}}$$

The total kinetic energy is 35 meV per proton or 420 meV per hexagonal ring. Two scenarios are considered:

(a) The electron get's trapped in the "squares" formed by 4 Oxygens, that is, one of the 6 square sides of the hexagonal prism formed by the oxygens of two stacked rings. In that case, the number of polarons is 3 per ring. The polaron size is, in that case, 0.61 Å.

(b) The electron get's trapped in the vicinity of each proton. The number of polarons is then 12 per ring. The polaron size is, then, 0.86 Å.

A more detailed study is conducted, with the specific setting for the electron in the chain in the Chapters to follow. In this section, it is only shown that the kinetic energy difference could roughly be of the order of magnitude of these quasiparticles in the tube. The electronic state of the electrons has been reported to be very different to general ice structure, with, for instance, proton delocalised and synchronised, so could be expected some exotic electronic dynamics taking place in this configuration as, for example, in polarons.

Another aspect to study is the interaction with the nanotube surface, which is formed of carbon atoms. Other types of quasiparticles can be considered for water in the nanotube, such as the possibility of a surface polaron-polariton, among other options. In Chapter 4, excitons are used to simulate the electronic dynamics of water in the nanotube, as will be presented.

Some of the electronic effects in the nanotube could promote the circulation of electron density. However, the electron density circulation in space is beyond the scope of this Thesis. A toroid flow with longitudinal circulation along the central chain, or circular flow around the central chain, are examples of electronic dynamics that could take place and be explored. The effects of a macroscopic electric field along the nanotube axis on the electron density is, nevertheless, studied in a quasi-static representation, in Chapter 5, as a possibility of a self-induced electromagnetic field to explain the observed lower proton kinetic energy explored in this Chapter.

3.3 Conclusions

A rough picture of water in the nanotube has been drafted to conclude that the proton kinetic energy difference of 35 meV observed by Reiter could be accounted considering a polaron, either in the vicinity of each proton or in the space between 4 protons, on the sides of the hexagonal prism formed by the Oxygens in two stacked rings. The polaron size for each case has been calculated, which is 0.61 and 0.86

Å, respectively. A detailed time-resolved (Ch. 4) and space-resolved (Ch. 6 and 5) representations of collective electronic states are explored in this Thesis.

Part II
Mesoscopic Scale

In this Part, the behavior of water at a lower level of representation is studied. Note that at the macroscopic scale the water system was described by average values. At the lower level, the state of the individual molecules is known, which are represented as electric dipoles.

Solid State Physics and Open Quantum Systems methods are used. Solid State Physics deals with matter when there is spatial periodicity, as is the case in the geometrically ordered water molecules in the nanotube. Open Quantum Systems theory allows to simulate the dynamics of the water system in interaction with its environment and ask questions about each of the molecules. In particular, the interaction of the electric dipoles with the electromagnetic surrounding is considered, and therefore the water system is an open system and the electromagnetic field around it is the environment. It can be said then, that water is an open quantum system.

The methodology used allows studying water molecular excitations dynamics, that are not easily dealt with in three-dimensional (3D) space using standard QC methods. This gives the possibility of simulating the electronic dynamics, and in particular, studying electronic synchronization. QED Coherence in Matter theory predicts collective dipolar behavior and allows to make predictions at the level of the CDs. This Part goes further to characterize each and every water molecule within the system.

The interaction between water and photons surrounding is modelled using a Dicke-type Hamiltonian [39], that accounts for the fact that molecules are interacting with a common radiation field. It has been applied to the case of water [101, 61, 115] to deduce, using analytical methods, the system undergoing synchronized collective oscillations. Instead of the macroscopic approach, where the global behavior is deduced, and deviations from this picture analyzed *a posteriori* [101, 61], a simulation setting based on the individual molecular states is presented. It is studied how water molecules approach a collective state, to understand how the specificities of the setting (eg. water spatial dispositions, specific electromagnetic environment) determine how interrelated water electronic states are.

It means diving into understanding the water system at an intermediate state, where some molecules may behave independently and some are in synchronization. Also, to study which conditions are conducive to higher levels of synchronization, for which two synchronization measures are used, namely Mutual Information (MI) and R Pearson correlation index.

4 Water Exciton Dynamics

4.1 Elements of Theory

4.1.1 Bloch Theorem

Bloch theorem states that solutions to the Schrdinger equation in a periodic potential have the form

$$\Psi(\mathbf{r}) = e^{i\mathbf{k}\cdot\mathbf{r}}u(\mathbf{r},)$$

where $\mathbf{r}$ is the position, Ψ is the wave function, $\mathbf{k}$ is the wave vector and u is a periodic function with the same periodicity as the potential, that is,

$$u_{\mathbf{k}}(\mathbf{x}) = u_{\mathbf{r}}(\mathbf{x} + \mathbf{n}\cdot\mathbf{a}).$$

In other words, the solutions take the form of a plane wave modulated by a periodic function. These are known as Bloch functions or Bloch states, and serve as a basis for the wave functions of electrons in crystals.

4.1.2 Exciton Hamiltonian

A Frenkel exciton is essentially an excited state of a single atom where the excitation can hop from one atom to another due to the coupling between neighbors. The electronic excitation energy transfer between two molecules occurs, according to the scheme [86]

$$|1\rangle_1 + |0\rangle_2 \rightarrow |0\rangle_1 + |1\rangle_2$$

where $|1\rangle_i$, represents each molecule ($i = 1, 2$) in the excited state and $|0\rangle_i$ in its ground state. Often, they correspond to the lowest unoccupied molecular orbital (LUMO) and highest occupied molecular orbital (HOMO) and therefore the two states considered. In our case, we consider also Rydberg excitations where $|0\rangle$ represents ground state and $|1\rangle$ a Rydberg-excited state.

It corresponds to the situation where molecule one is first in an excited state, for example through interaction with an electromagnetic field, and molecule 2 is in the ground state. Then, due to Coulomb interaction between the molecules, a reaction takes place where electrostatic energy is transferred from molecule 1 to molecule 2, and the former is de-excited while the ladder is excited.

Alternatively, the final state can be reached through an electron exchange between molecules 1 and 2. For this to happen the wave functions between both molecules need to overlap.

We consider a system of N molecules arranged in arbitrary geometry, with the center of mass of the i-th molecule located at $\mathbf{x}_i$. The system Hamiltonian is constructed in analogy with the individual molecule case.

For a single molecule, it consists of the electronic and nuclear contributions of the Quantum Chemistry Hamiltonian and the eigenstates are the solutions to the nonrelativistic Schrdinger equation

$$H_j\Psi(\mathbf{r}, \sigma; \mathbf{R}) = \epsilon\Psi(\mathbf{r}, \sigma; \mathbf{R})$$

where $\mathbf{r}$ are the coordinates of the electrons, σ the spin and $\mathbf{R}$ the nuclei coordinates.

In the case of a system composed of several parts or molecules, the total Hamiltonian is

$$H = \sum_i H_i(\mathbf{R_c}) + \frac{1}{2}\sum_{i,j} V_{ij}(\mathbf{R_c}) \tag{9}$$

with $\mathbf{R}_c$ is the center of mass of each molecule and V_{ij}, the interaction between pair of molecules or parts in the system.

Similarly, the H_i part can be separated into electronic and nuclear parts. In this case, *all* nuclei are interacting with the electrons in the system and therefore the electronic spectrum will be different.

To be able to classify the transfer processes with respect to intramolecular electronic excitations, the Hamiltonian is expanded in terms of the adiabatic electronic states $|\phi\rangle_i$ of molecule i. They are defined through the Schrdinger equation

$$H_i^{el}(\mathbf{R})\,\varphi_i(\mathbf{r}_i;\mathbf{R}) = E_i(\mathbf{R})\,\varphi_i(\mathbf{r}_i,\mathbf{R}_i) \tag{10}$$

where $\mathbf{r}_i$ denotes the electronic coordinates of molecule i, and note that $\mathbf{R}$ includes the coordinates of *all* nuclei.

From this point, we can construct a Hartree-Fock basis for a given state $\mathbf{a}$

$$\tilde{\Phi}_{\mathbf{a}}(\mathbf{r}_m,\mathbf{R}) = \prod_{i=1}^{N} \varphi_{i,\mathbf{a}}(\mathbf{r}_i,\mathbf{R})$$

where the set $\mathbf{a}$ is the total configuration of the system, described by the single-molecule electronic states or quantum numbers.

We can then generate an antisymmetric wave function

$$\Phi_{\mathbf{a}}(\mathbf{r}_m,\mathbf{R}) = \frac{1}{\sqrt{N_p!}}\sum_{\mathcal{P}}(-1)^p\,\mathcal{P}\,\left[\tilde{\Phi}_{\mathbf{a}}(\mathbf{r}_m,\mathbf{R})\right]$$

where $\mathcal{P}$ generates a permutation of electron coordinates of the different molecules and p counts the number, N_p, of permutations.

The single-molecule states are assumed to be known, and not subject to a variational procedure. The functions $\Phi_{\mathbf{a}}$ are not orthogonal neither normalised. Expanding a state $|\psi\rangle$ of the system in the Hartree-Fock basis

$$|\psi\rangle = \sum_{\mathbf{a}} c(\mathbf{a})\,|\psi_{\mathbf{a}}\rangle$$

we obtain

$$\sum_{\mathbf{b}} \left(\langle\psi_{\mathbf{a}}|\,H\,|\psi_{\mathbf{b}}\rangle - E\,\langle\psi_{\mathbf{a}}|\psi_{\mathbf{b}}\rangle\right) = 0$$

Let us consider the example of two molecules. For the electronic part V^{el-el} of the intermolecular interaction, we obtain

$$\begin{aligned}\langle\psi_{\mathbf{a}}|\, V_{12}^{el-el}\,|\psi_{\mathbf{b}}\rangle &= \int dr_1 dr_2 \frac{1}{\sqrt{N_p!}} \sum_{\mathcal{P}} (-1)^p\, \mathcal{P}\, \left[\Phi^*_{1,a_1}(\mathbf{r}_1,\mathbf{R})\Phi_{2,a_2}(\mathbf{r}_2,\mathbf{R})\right] \\ &\cdot V_{12}^{el-el} \sum_{\mathcal{P}} (-1)^{p'}\mathcal{P}'\left[\Phi^*_{2,b_2}(\mathbf{r}_2,\mathbf{R})\Phi_{1,b_1}(\mathbf{r}_1,\mathbf{R})\right] \\ &\equiv J_{12}^{el-el}(a_1,a_2;b_2,b_1) - K_{12}^{el-el}(a_1,a_2;b_2,b_1)\end{aligned}$$

The spatial wave function overlap is responsible for the exchange contribution $K_{12}^{el-el}(a_1\, a_2; b_2\, b_1)$, and it decreases exponentially with increasing intermolecular distance. For distances larger than about 1 nanometer, which is the case, we can neglect the exchange contributions to the interaction energy. That means that we can use the Hartree-product $\tilde{\phi}$ instead of ϕ for the electronic wave function. Then, $\langle\varphi_{i,a}|\varphi_{j,b}\rangle = \delta_{i,j}\delta_{a,b}$ and the states $\tilde{\Phi}_{\mathbf{a}}$ form a complete basis. From this point on we drop the tilde an use $\Phi_{\mathbf{a}}$ for the Hartree-Fock product wave function. Equation 9 is then

$$\begin{aligned}H &= \sum_{\mathbf{a},\mathbf{b}} \langle\Phi_{\mathbf{a}}|\, H\,|\Phi_{\mathbf{b}}\rangle\; |\Phi_{\mathbf{a}}\rangle\langle\Phi_{\mathbf{b}}| \\ &= \sum_i \sum_{ab} H_i(a,b)\,|\varphi_{i,a}\rangle\langle\varphi_{i,b}| \\ &+ \frac{1}{2}\sum_{i,j}\sum_{a,b;c,d} J_{ij}(a,b,c,d)\,|\Phi_{i,a}\Phi_{j,b}\rangle\langle\Phi_{j,c}\Phi_{i,d}|\end{aligned}$$

The quantities $H_j(a,b)$ are the matrix elements $\langle\Phi_{i,a}|\, H_i\,|\Phi_{j,b}\rangle$ of the single molecule part of equation 9. These off-diagonal terms are due to nonadiabatic couplings. The diagonal parts are given by the eigenvalues of equation 10.

The matrix elements for the Coulomb interaction, considering only the direct part of the electron-electron coupling

$$\begin{aligned}J_{ij}(a,b;c,d) &\equiv \langle\varphi_{i,a}\,\varphi_{j,b}|\, V_{ij}\,|\varphi_{j,c}\,\varphi_{i,d}\rangle \\ &\int dr_i\, dr_j\, \varphi^*_{a,j}(r_j)\,\varphi^*_{b,i}\, V_{ij}^{el-el}(r_i,R_j)\,\varphi_{i,c}(r_i)\,\varphi_{j,d}(r_j) \\ &+ \delta_{a,d}\,\delta_{b,c}\, V_{j,i}^{nuc-nuc} \\ &+ \delta_{b,c}\int dr_j\,\varphi^*_{a,j}(r_j)\, V_{ji}^{el-nuc}(r_i,R_i^{intra})\,\varphi_{j,d}(r_j) \\ &+ \delta_{b,c}\int dr_i\,\varphi^*_{b,i}(r_i)\, V_{ji}^{nuc-el}(R_i^{intra},r_i)\,\varphi_{i,c}(r_i)\end{aligned}$$

All these terms depend on the intermolecular coordinates also, assuming here that the vibrational degrees of freedom are fixed.

Noting $\varphi_{i,a}$ as $|i,a\rangle$ and from now on using Greek letters for the states, and Latin characters to refer to which molecule, that is $|\nu,i\rangle$, we can write for the case of water, the molecular Hamiltonian [83]

$$H = \sum_{i=1}^{N_f}\sum_{\nu\in i}^{N_e} E_i^{\nu}\,|\nu\rangle_{ii}\langle\nu| + \sum_{i\neq j}^{N_f}\sum_{\nu\in i}^{N_e}\sum_{\mu\in j}^{N_e} J_{ij}^{\nu\mu}\,|\nu\rangle_{ij}\langle\mu| \tag{11}$$

N_f is number of fragments: fragment $i, j \in [1, Nf]$; N_e is number of excited states: excitation level $\nu, \mu \in [1, Ne]$.

The term $J_{ij}^{\nu\mu}$ is the coupling between the states $|\nu\rangle$ in fragment i and state $|\mu\rangle$ in fragment j. It will be coded, in the static case, by an adjacency matrix indicating nearby molecules, and only depends on the molecules states.

We have shown in the previous section how to construct the antisymmetric wave function. We have used both a fermionic algebra and a qubit one, which correspond neither to boson nor fermion statistics and, therefore does not represent physically a quantum particle [**?**], both for electrons and water molecules. The algebraic details and how they are related and the specific mathematical properties of these two options are out of the scope of the study. We will compare the results and leave a formal study for future work.

4.1.3 Exciton Hamiltonian for Water

The simulation is based on an effective Frenkel Exciton Hamiltonian [30, 26, 84, 83], where each molecule is considered as a site or *hole* where an electron is bound. This Hamiltonian has been used to obtain the electronic absorption spectrum of liquid water [84, 83], with good agreement with experimental data. This representation is extended to include interaction with the electromagnetic environment and model water as an open quantum system.

Denoting the single-molecule wave functions as $|\nu\rangle_i$ [4] the molecular exciton Hamiltonian for water is written as [83]

$$H = \sum_{i=1}^{N_f} \sum_{\nu \in i}^{N_e} E_i^{\nu} \, |\nu\rangle_{i\,i} \langle\nu| + \sum_{i \neq j}^{N_f} \sum_{\nu \in i}^{N_e} \sum_{\mu \in j}^{N_e} J_{ij}^{\nu\mu} \, |\nu\rangle_{i\,j} \langle\mu| \tag{12}$$

where N_f is the number of fragments (fragment $i, j \in [1, N_f]$) N_e is the number of excitation levels (level $\nu, \mu \in [1, N_e]$), $J_{ij}^{\nu\mu}$ is the intermolecular coupling between the states $|\nu\rangle$ and $|\mu\rangle$ in fragments i and j, respectively, and E_i^{ν} is the energy of the i-th fragment at the state ν.

4.1.4 Exciton Molecular Hamiltonian Notation for Computational Algebra

A matrix formulation of exciton dynamics is defined, and the number of excitations, fixed to a value of two, corresponding to the ground and excited states.

To simplify the use of symbols, an alternative notation [5] is introduced. The following convention is used for the ground and the excited state (all molecules are assumed to be in the ground state unless stated differently)

[4] From now on using Latin characters to refer to each molecule and Greek letters for each of its states

[5] It is eventually useful to work in Python, and coincides with the functions presented in the code Appendix.

$$\text{ground state is represented by } \begin{pmatrix} 0 \\ 1 \end{pmatrix}$$

$$\text{excited state is represented by } \begin{pmatrix} 1 \\ 0 \end{pmatrix}$$

The function $S(N,i)$ is considered which defines the state where N molecules are in the ground state except for one of them, that on i position. When $S(N,i)$, i is used, it is assumed to run between 1 and N. The space spanned by $S(N,i)$ is often called the single excitation subspace. $S(N,i)$ can be calculated as follows

$$S(N,i) := \begin{pmatrix} 0 \\ 1 \end{pmatrix} \otimes \begin{pmatrix} 0 \\ 1 \end{pmatrix} \otimes \cdots \otimes \begin{pmatrix} 1 \\ 0 \end{pmatrix} \otimes \cdots \otimes \begin{pmatrix} 0 \\ 1 \end{pmatrix}$$

where the excited state term is in the i-th position out of N terms. $S(N,i)$ corresponds to a column vector and $S(N,i)^\dagger$ to a row vector, of dimension $2N$. Therefore, the outer product of $S(N,i)$ and any $S(N,j)^\dagger$ is a $2N \times 2N$ matrix.

Using this notation, the first part of the Hamiltonian is

$$H^M = E^1 \cdot S(N,i) \cdot S(N,i)$$

where the convention to sum over lower case indices is used. E^1 is a number, the energy of the excited state. All molecules are assumed to be equal, so $E^1 = E$. The energy of the ground state is assumed to be zero, $E^0 = 0$. Once N is fixed, N is dropped and write $S(i)$. The first part of the Hamiltonian (12) is then

$$H^M = E \cdot S(i) \cdot S(i)$$

The second part of the Hamiltonian (12) has the J^{01} coupling between ground and first excited transition. It is calculated in section 4.2.1 and depends on the energy E and the distance. A cut-off is introduced, and dipole interaction neglected beyond some distance d_0. An adjacency function $A(N,i,j)$ then captures the geometry of the system. N is also omitted when it is fixed and only write $A(i,j)$ for the coefficients,

$$A(i,j) \in \{0,1\}$$

It reads values from an adjacency matrix with a given structure, $A(i,j) = A_{ij}$. For example, in the case of a ring, it will be a tridiagonal matrix where the diagonal is also zero. This will be the main case of this Chapter.

Only the term J^{01} in Hamiltonian (12) is considered, corresponding to the dipole interaction between the ground-to-excited transition of one molecule and excited-to-ground transition. Often, it will only depend on the pair of molecules being adjacent or not, to be able to write

$$J(i,j) = J^{01} \cdot A(i,j)$$

The second part of the Hamiltonian (12) is then (with IM indicator of "Interaction between Molecules")

$$H^{IM} = J(i,j) \cdot S(i) \cdot S(j)$$

The interaction with the electromagnetic field can be treated as follows. The state of n photons in a truncated Fock space of maximum N photons is noted as $F(N, n)$, where n is the actual number of photons present in the state. When $F(N, n)$ is used, it is assumed that n runs between 1 and N. The number N of molecules and the number n of possible photons in the model formulation coincide and is omitted once it is fixed.

4.1.5 Interaction with the Electromagnetic Field

The interaction between water molecules and the surrounding electromagnetic environment is modelled through the Hamiltonian [101, 61]

$$H^I = g(b^\dagger \sigma^- + b\sigma^+)$$

where g is the coupling constant, $b^\dagger$ and b are the creation and annihilation operators of the electromagnetic field, and σ^+ and σ^- are the collective raising and lowering operators defined as

$$\sigma^+ = \sum_{i=1}^{N} \sigma_i^+$$

and

$$\sigma^- = \sum_{i=1}^{N} \sigma_i^-$$

with operators $\sigma_i^+ = |1\rangle_i \langle 0|_i$ and $\sigma^- = (\sigma_i^+)^\dagger$ generating the transition between ground and excited states. The algebra commutator expressions are $[\sigma_z, \sigma^\pm] = \pm 2\sigma^\pm$ and $[\sigma^-, \sigma^+] = -\sigma_3$.

4.1.6 Quantum Synchronisation Measures

1. R Pearson correlation coefficient

   The R Pearson correlation coefficient is a standard measure of the degree of linear dependence between two variables, also used for the study of quantum synchronization [55]. It is defined as

   $$C_{X,Y} = \frac{E[XY] - E[X]E[X]}{\sqrt{E[X^2] - (E[X])^2}\sqrt{E[Y^2] - (E[Y])^2}}$$

   where $E[\cdot]$ means the average value. $C_{X,Y}$ varies from -1 to 1, with 1 and -1 indicating total positive and negative correlation, respectively, and 0 indicating no correlation.

2. Mutual information

   The *mutual information* (MI) also can be used as a measure of quantum synchronisation. It is defined as

   $$I(A : B) := S(\rho_A) + S(\rho_B) - S(\rho_{AB})$$

   where $S(.)$ is the von Neumann entropy defined by $S(\rho) = -Tr\rho\, log\rho$

The system in study is $S := S_{ring} \otimes S_{emf}$, with S_{ring} including each of the N molecules, $S_{ring} = \otimes_{i=1}^{N} S_i$. To calculate the MI of the system S, first, the electromagnetic field part is traced out. Then, the system is separated into two parts, the first molecule S_1 on one side, and the $N-1$ rest of molecules on the other, that is, $S_A \otimes S_B$, with $S_A = S_1$ and $S_B = \otimes_{i=2}^{N} S_i$.

4.2 Simulation Scheme

For the open quantum simulation QuTip (Python) [66, 67] is used. QuTiP is open-source software for simulating the dynamics of open quantum systems that depends on Python Numpy, Scipy, and Cython numerical packages. In addition, graphical output is provided by Matplotlib.

QuTiP aims to provide user-friendly and efficient numerical simulations of a wide variety of Hamiltonians, including those with arbitrary time-dependence, commonly found in a wide range of physics applications such as quantum optics, trapped ions, superconducting circuits, and quantum nanomechanical resonators.

The Markovian ME presented in the study is thus obtained and simulated with Qutip.

For the bulk molecular dynamics, two TIP3P Langevin molecular simulations are run using GPAW [93, 42] and ASE [74] (Python).

The Molecular Dynamics (MD) simulation has a time-step of 1 fs. Lindblad ME also has a time-step is 1 fs. The positions are used to calculate the interaction coefficients of the ED. The electronic dynamics are simulated. On average, half of the molecules are initially in a ground state, and half are excited, where these states are assigned randomly.

Synchronisation measures R Pearson correlation coefficient and MI are analysed, both for static and bulk (variation of relative positions obtained from MD TIP3P dynamics) scenarios.

Langevin dynamics are simulated in GPAW.

The following boxes show the simulation details for simulation, in Qutip, of the Jaynes-Cummings and Tavis-Cummings Hamiltonians. The parameters of the model are presented in the next section.

Simulation Description Boxes (to integrate)

Qutip (Python) – simulation description box Jaynes-Cummings – Shrdinger Equation

Parameters

Model:
$\lambda = 0.934\,\mathrm{fs}^{-1}\mathrm{\AA}^{-1}$
$\hbar\omega = \hbar\omega_0 = 12.06\,\mathrm{eV}$

Solver:
$\mathrm{t}_i \in \{0, 0.5, 1 \ldots 200\}\,\mathrm{fs}$

Method

Numerical integration of (time-dependent) Schrdinger Equation

$$i\hbar\frac{d}{dt}\left|\Psi\right\rangle = H\left|\Psi\right\rangle$$

defined by its Hamiltonian and initial state vector.

Hamiltonian

Expressed in the basis

$$\left|g\right\rangle = \begin{pmatrix}0\\1\end{pmatrix}, \quad \left|e\right\rangle = \begin{pmatrix}1\\0\end{pmatrix}$$

for the molecular system, and

$$\left|1\right\rangle = \begin{pmatrix}0\\1\end{pmatrix}, \quad \left|0\right\rangle = \begin{pmatrix}1\\0\end{pmatrix}$$

for the electromagnetic field, the Hamiltonian matrix is (17)

$$H = \begin{pmatrix} \hbar\omega_0 & 0 & 0 & \hbar\lambda \\ 0 & \hbar(\omega+\omega_0) & 0 & 0 \\ 0 & 0 & -\hbar\omega_0 & 0 \\ \hbar\lambda & 0 & 0 & \hbar(\omega-\omega_0) \end{pmatrix}$$

where the tensor product is defined in the order $S_{atom} \otimes S_{emf}$.

Initial State

$$\left|\Psi_{initial}\right\rangle = \left|e\right\rangle \otimes \left|0\right\rangle = \begin{pmatrix}1\\0\\0\\0\end{pmatrix}$$

Qutip (Python) – simulation description box Jaynes-Cummings – Von Neumann Equation

Parameters

Model:
$\lambda = 0.934\,\mathrm{fs}^{-1}\mathrm{\AA}^{-1}$
$\hbar\omega = \hbar\omega_0 = 12.06\,\mathrm{eV}$

Solver:
$\mathrm{t}_i \in \{0, 0.5, 1 \ldots 200\}\,\mathrm{fs}$

Method

Numerical integration of Von Neumann equation

$$\dot{\rho} = -\frac{i}{\hbar}[H, \rho]$$

defined by its Hamiltonian and initial density matrix.

Hamiltonian

See **??**.

Initial State

Initially atom *maximum coherence state*

$$\rho_{atom} = \frac{1}{2}\left(|e\rangle\langle e| + |g\rangle\langle g| + |e\rangle\langle g| + |g\rangle\langle e|\right) = \begin{pmatrix} 0.5 & 0.5 \\ 0.5 & 0.5 \end{pmatrix}$$

Initially no photons (pure state)

$$\rho_{emf} = |0\rangle\langle 0|$$

Initial state for combined system

$$\rho_{intial} = \rho_{atom} \otimes \rho_{emf}$$

Qutip (Python) – simulation description box Tavis-Cummings – Von Neumann Equation

Parameters

Model:
$\lambda = 0.934\,\mathrm{fs}^{-1}\mathrm{\AA}^{-1}$
$\hbar\omega = \hbar\omega_0 = 12.06\,\mathrm{eV}$
E_i
J_{ij}

Method

Numerical integration of Von Neumann equation.

Hamiltonian

Molecular energies, including intermolecular interaction, and atom-field interaction

$$H = H_m^{(1)} + H_m^{(2)} + H_i$$

with

$$H_m^{(1)} = \sum_i E_i \left|i\right\rangle \left\langle i\right|$$
$$H_m^{(2)} = \sum_{ij} Jij \left|i\right\rangle \left\langle j\right|$$
$$H_i = g\left(\sigma^+ a + \sigma^- a^\dagger\right)$$

Basis

The basis used is[a]

$$\left|i\right\rangle = \begin{pmatrix}0\\1\end{pmatrix} \otimes \cdots \begin{pmatrix}1\\0\end{pmatrix} \cdots \otimes \begin{pmatrix}0\\1\end{pmatrix}$$

The operators σ^+ and σ^- are

$$\sigma^+ = \sum_i \sigma_i^+, \quad \sigma^- = \sum_i \sigma_i^-$$

with

$$\sigma_i^\pm = \mathbb{1} \otimes \cdots \otimes \mathbb{1} \otimes \sigma^\pm \otimes \mathbb{1} \otimes \cdots \otimes \mathbb{1}$$

and

$$\mathbb{1} = \begin{pmatrix}1 & 0\\0 & 1\end{pmatrix}, \quad \sigma^+ = \begin{pmatrix}0 & 1\\0 & 0\end{pmatrix}, \quad \sigma^- = \begin{pmatrix}0 & 0\\1 & 0\end{pmatrix}$$

[a] The vector $|i\rangle$ is noted S(N,i) elsewhere to refer to the functions used to obtain these states in Qutip.

4.2.1 Numerical Evaluation of Model Parameters

The study is focused in a particular geometrical disposition of water molecules inside the nanotube, which are forming hexagonal rings stacked to each other, creating a cylindrical shield, which is periodic [70].

It has been reported *ab-initio* simulations resulting in stacked-ring structure with square, pentagonal, hexagonal ice [70], as well as octogonal ice [71] and helical ice [95], with nearest-neighbour distances in both ice nanotube and encapsulated liquid water fairly constant, about 2.7 to 2.8 Å [70]. These other possible dispositions are left for future study, and here $N = 6$ is set as the number of ring molecules.

The expression for dipole-dipole interaction is

$$V(r) = -\frac{\mu_1 \mu_2}{4\pi\epsilon_0 r_{12}^3}\kappa$$

where $\kappa = cos\theta_{12} - 3cos\theta_1 cos\theta_2$.

For $\kappa = 1$, the intermolecular distances of 2.7 and 2.8 Å result in intermolecular coupling J with values 0.682 and 0.611, respectively. The calculation of the exact values from the positions of the molecules in space in GPAW have been developed, although they are not fully exploited and only the code is presented.

1. Coupling constant g

   The coupling constant g is given by

   $$g = e\sqrt{\frac{\omega}{2\epsilon_0 \hbar V}}$$

   The dimensionality of g is analyzed by looking at the Hamiltonian

   $$\hat{H} = \frac{1}{2}\hbar\omega_0\hat{\sigma}_3 + \hbar\omega\hat{a}^\dagger\hat{a} + \hbar g\left(\hat{\sigma}^+\hat{a} + \sigma^-\hat{a}^\dagger\right)$$

   describing the interaction of water molecules with the electromagnetic field [58].

   Regarding the dimensionality of $\hbar\omega a^\dagger a$, it must be the same as that of $\hat{H}$ which is that of energy, and then $\hat{a}^\dagger a$ and $\hat{a}$ or $\hat{a}^\dagger$ must be adimensional. The same argument applies to $\frac{1}{2}\hbar\omega\sigma_z$, so σ_z is adimensional. Finally, $\hbar g$ must have dimensions of energy and then g must have dimensions of frequency. Nevertheless, g_0 is sometimes given per unit length, then its dimensionality is $L^{-1}T^{-1}$.

   The expression $V = \lambda^3$ is used for the quantisation volume, with $\lambda \approx 100$ nm corresponding to the excitation energy value of 12.06 eV. For $\omega = 12.06\,\text{eV}$, as proposed in QED Coherence in Matter theory, the value is 6.1×10^{11} Å^{-1} s^{-1} or 0.61 Å^{-1} ps^{-1}. That is, a coupling constant value of approximately 610 ps^{-1}.

   For reference, the CDs predicted size of 0.1 μm is used. A nanotube of length of 10 μm would be consisting of 100 CDs. Considering a separation between rings of 2.7-2.8 Å, the number of rings would be approximately 360 per CD and 36000 in total in the nanotube. That is, 2160 molecules per CD for the external hexagonal ice shield (N=6) and 2590 if also a central chain (N=7) is considered.

The enhanced coupling constant factor enhancement $\sqrt{NM}$ would, then, be $\sqrt{2160} \approx 46.5$ and $\sqrt{2520} \approx 50$ per CD (465 and 500 total in the nanotube) for $N = 6$ and $N = 7$, respectively. Therefore, the coupling constant would have a value of $g \approx 30\,\mathrm{fs}^{-1}$ if the CD is considered and of $g \approx 300\,\mathrm{as}^{-1}$ if the nanotube water is considered. For a 6-molecule ring ($N = 6$), the enhanced coupling constant is $g \approx 1.5\,\mathrm{fs}^{-1}$ and $g \approx 1.5\sqrt{M}\,\mathrm{fs}^{-1}$ for M rings.

4.3 Results and Discussion

4.3.1 Exciton Molecular Hamiltonian for the Water System

The calculation of the Exciton Hamiltonian matrix elements is presented, including an alternative formulation, based on creation and annihilation operators.

1. First Quantisation Matrix Elements Calculation

   As introduced, the Exciton Hamiltonian 4.1.3 for the water system is [83]

$$H = \sum_{i=1}^{N_f} \sum_{\nu \in i}^{N_s} E_i^{\nu} \left|i, \nu\right\rangle \left\langle \nu, i\right| + \sum_{i \neq j}^{N_f} \sum_{\nu \in i}^{N_e} \sum_{\mu \in j}^{N_e} J_{ij}^{\nu\mu} \left|i, \nu\right\rangle \left\langle \mu, j\right|$$

   N_f number of fragments or monomers; fragment $i, j \in [1, Nf]$
   N_e number of excited states; excitation level $\nu, \mu \in [1, Ne]$
   $|i, \nu\rangle$ is the excited state $|\nu\rangle$ in the fragment i with energy E_i^{ν}
   $J_{ij}^{\nu\mu}$ is the coupling between the states $|\nu\rangle$ in fragment i and state $|\mu\rangle$ in fragment j

   Given a state $|\psi\rangle = |k, \eta\rangle$, with $k \leq N_f$ and $\eta \leq N_e$, the objetive is to calculate the energy, $\langle\psi| H |\psi\rangle$

   Let's calculate the Hamiltonian matrix in the single excitation basis $|i, \nu\rangle$

$$\begin{aligned}
&\langle l, \zeta| H |k, \eta\rangle \\
&= \langle l, \zeta| \sum_{i=1}^{N_f} \sum_{\nu \in i}^{N_s} E_i^{\nu} \left|i, \nu\right\rangle \left\langle \nu, i | k, \eta\right\rangle + \langle l, \zeta| \sum_{i \neq j}^{N_f} \sum_{j}^{N_f} \sum_{\nu \in i}^{N_e} \sum_{\mu \in j}^{N_e} J_{ij}^{\nu\mu} \left|i, \nu\right\rangle \left\langle \mu, j | k, \eta\right\rangle \\
&= \langle l, \zeta| E_k^{\eta} |k, \eta\rangle + \langle l, \zeta| \sum_{i \neq k}^{N_f} \sum_{\nu \in i}^{N_e} J_{ik}^{\nu\eta} \left|i, \nu\right\rangle
\end{aligned}$$

   If $l = k$ and $\eta = \zeta$ (diagonal elements)

$$\langle k, \eta| H |k, \eta\rangle = E_k^{\eta}$$

   If $l \neq k$ and $\eta \neq \zeta$ (off-diagonal elements)

$$\langle l, \zeta| H |k, \eta\rangle = J_{kl}^{\eta\zeta}$$

2. Second Quantisation Matrix Elements Calculation

The Exciton Hamiltonian in second quantisation [30] is

$$H = \sum_i \sum_\nu E_{i\nu} a_{i\nu}^+ a_{i\nu} + \sum_{i \neq j} \sum_\nu \sum_\mu J_{ij}^{\nu\mu} a_{i\nu}^+ a_{j\mu}^+ a_{j\mu} a_{i\nu}.$$

The energy for the state $|\psi\rangle = |k, \eta\rangle$ is calculated as

$$\begin{aligned}\langle k,\eta| H |k,\eta\rangle &= \langle k,\eta| \sum_i \sum_\nu E_{i\nu} a_{i\nu}^+ a_{i\nu} |k,\eta\rangle + \langle k,\eta| \sum_{i\neq j} \sum_\nu \sum_\mu J_{ij}^{\nu\mu} a_{i\nu}^+ a_{j\mu}^+ a_{j\mu} a_{i\nu} |k,\eta\rangle \\ &= \langle k,\eta| E_{k,\eta}\, a_{k,\eta}^+ |0\rangle = \langle k,\eta| E_{k,\eta} |k,\eta\rangle = E_{k,\eta} \langle k,\eta|k,\eta\rangle = E_{k,\eta}.\end{aligned}$$

For $|\psi\rangle = |k, \eta; l, \zeta\rangle$ we have

$$\begin{aligned}\langle k,\eta;l,\zeta| H |k,\eta;l,\zeta\rangle &= \langle k,\eta;l,\zeta| \sum_i \sum_\nu E_{i\nu} a_{i\nu}^+ a_{i\nu} |k,\eta;l,\zeta\rangle \\ &\quad + \langle k,\eta;l,\zeta| \sum_{i\neq j} \sum_\nu \sum_\mu J_{ij}^{\nu\mu} a_{i\nu}^+ a_{j\mu}^+ a_{j\mu} a_{i\nu} |k,\eta;l,\zeta\rangle .\end{aligned}$$

The first summand is then developed as

$$\begin{aligned}\langle k,\eta;l,\zeta| \sum_i \sum_\nu E_{i\nu} a_{i\nu}^+ a_{i\nu} |k,\eta;l,\zeta\rangle &= \langle k,\eta;l,\zeta| E_{k,\eta}\, a_{k,\eta}^+ |l,\zeta\rangle \\ &= E_{k,\eta} \langle k,\eta;l,\zeta|k,\eta;l,\zeta\rangle + E_{l,\zeta} \langle k,\eta;l,\zeta|k,\eta;l,\zeta\rangle \\ &= E_{k,\eta} + E_{l,\zeta}\end{aligned}$$

and the second summand

$$\begin{aligned}\langle k,\eta;l,\zeta| \sum_{i\neq j} \sum_\nu \sum_\mu J_{ij}^{\nu\mu} a_{i\nu}^+ a_{j\mu}^+ a_{j\mu} a_{i\nu} |k,\eta;l,\zeta\rangle &= \langle k,\eta;l,\zeta| \sum_{j\neq k} \sum_\mu J_{ij}^{\nu\mu} a_{k\eta}^+ a_{j\mu}^+ a_{j\mu} |l,\zeta\rangle \\ &= \langle k,\eta;l,\zeta| J_{kj}^{\eta\mu} a_{k\eta}^+ a_{l\zeta}^+ |0\rangle \\ &= \langle k,\eta;l,\zeta| J_{kj}^{\eta\mu} a_{k\eta}^+ |l,\zeta\rangle \\ &= J_{kl}^{\eta\zeta} \langle k,\eta;l,\zeta|k,\eta;l,\zeta\rangle \\ &= J_{kl}^{\eta\zeta}.\end{aligned}$$

The Hamiltonian can be expressed in a matrix form choosing a basis. The basis states are $|i, \nu\rangle$ and the creation operator $\sigma_{i,\nu}^+$ creates an excited state ν for the i-th molecule. In second quantisation the state of the system is encoded with the occupation number $N_{i,\nu}$ that is equal to 1 if the system contains a "particle", in this case, a molecule, in the state (i, ν) and equal to zero if it does not.

A general state of the system (in the case of $N_e = 2$) is noted as

$$\left|N_{0,0}, N_{0,1}, N_{1,0} \dots N_{N_f-1,0} N_{N_f-1,1}\right\rangle$$

where $N_f \in [0, N_f - 1]$ to match $N_e \in [0, 1]$ has been used, and because it will eventually be useful where working with Python. For example, the state $|0,1\rangle = |0\rangle \otimes |1\rangle \otimes \ldots \otimes |0\rangle = |010 \ldots 0\rangle$. The vacuum state, in this case, is $|0\rangle = |0\rangle \otimes |0\rangle \otimes \ldots \otimes |0\rangle$, where the dimension is the product $N_f N_e$. It corresponds with an empty system.

The creation and annihilation operators create molecules in a particular state.

$$\sigma^+_{i,\nu} |0\rangle = |i, \nu\rangle$$

The single excitation basis corresponds to only one particle in the system, so the states

$$|100 \ldots 00\rangle, |010 \ldots 00\rangle, \ldots |000 \ldots 01\rangle$$

They are represented as $N_{i,\nu} = 0$ as $|0\rangle$ and $N_{i,\nu} = 1$ as $|1\rangle$, with

$$|0\rangle = \begin{pmatrix} 0 \\ 1 \end{pmatrix}, \ |1\rangle = \begin{pmatrix} 1 \\ 0 \end{pmatrix}.$$

The results of the operations of the creation and annihilation acting on one molecule are

$$\sigma^+ |0\rangle = |1\rangle \qquad \sigma^+ |1\rangle = 0$$

and

$$\sigma^- |0\rangle = 0 \qquad \sigma^- |1\rangle = |0\rangle .$$

For multiple particle states, the σ^+_i operator is defined as

$$\sigma^+_{N_e i+\nu} = a_{i,\nu}$$

that is, $\sigma^+_{i,\nu}$ and $\sigma^-_{i,\nu}$ operate on the i-th element and leave the rest as it is; in fact, we have

$$\sigma^+_i |v\rangle = |i\rangle \quad \sigma^+_k |i; j\rangle = |i; j; k\rangle \quad \sigma^+_k |i; j; k\rangle = 0$$

and

$$\sigma^-_k |i; j; k\rangle = |i; j\rangle \quad \sigma^-_k |i; j\rangle = 0$$

for $k \neq i \neq j$.

4.3.2 Exciton Hamiltonian for Various Molecular Dispositions

1. Water Dimer

   The Exciton Hamiltonian (12) for the water dimer (in the single excitation basis) is

$$H = \sum_{i=1}^{2} \sum_{\nu=0}^{1} E_i^{\nu} \, |\nu\rangle_{i\,i} \langle\nu| + \sum_{i=1}^{2} \sum_{\substack{j=1 \\ j\neq i}}^{2} \sum_{\nu=0}^{1} \sum_{\mu=0}^{1} J_{ij}^{\nu\mu} \, |\nu\rangle_{i\,j} \langle\mu| \tag{13}$$

   where $|\nu\rangle_i$ is the excited state $|\nu\rangle$ in the fragment i with energy E_i^{ν}. The individual energies are identical for each molecule and therefore only depend on the state ν, $E_i^{\nu} = E^{\nu}$. $J_{ij}^{\nu\mu}$ is the intermolecular coupling between the states $|\nu\rangle$ in fragment i and state $|\mu\rangle$ in fragment j. In the case of the water dimer the interaction network is characterized by

$$\mathbf{A} = \begin{pmatrix} 0 & 1 \\ 1 & 0 \end{pmatrix}$$

   the adjacency matrix representing the geometry.

   Therefore, $J_{ij}^{\nu\mu}$ is simply

$$J_{ij}^{\nu\mu} = A_{ij} J^{\nu\mu} = J^{\nu\mu}$$

   where the interaction $J^{\nu\mu}$ only depends on the states of the molecules in interaction, with three possibilities, $J^{00}, J^{01} \equiv J^{10}$ and J^{11}.

   By representing the ground and excited states, in the standard basis vectors of $\mathbb{C}^2$, as

$$|1\rangle = \begin{pmatrix} 1 \\ 0 \end{pmatrix}, \qquad |0\rangle = \begin{pmatrix} 0 \\ 1 \end{pmatrix}$$

   respectively, the basis vectors of the combined system are obtained calculating the tensor product

$$|11\rangle = \begin{pmatrix} 1 \\ 0 \end{pmatrix} \otimes \begin{pmatrix} 1 \\ 0 \end{pmatrix} = \begin{pmatrix} 1 \\ 0 \\ 0 \\ 0 \end{pmatrix} \qquad |10\rangle = \begin{pmatrix} 1 \\ 0 \end{pmatrix} \otimes \begin{pmatrix} 0 \\ 1 \end{pmatrix} = \begin{pmatrix} 0 \\ 1 \\ 0 \\ 0 \end{pmatrix}$$

$$|01\rangle = \begin{pmatrix} 0 \\ 1 \end{pmatrix} \otimes \begin{pmatrix} 1 \\ 0 \end{pmatrix} = \begin{pmatrix} 0 \\ 0 \\ 1 \\ 0 \end{pmatrix} \qquad |00\rangle = \begin{pmatrix} 0 \\ 1 \end{pmatrix} \otimes \begin{pmatrix} 0 \\ 1 \end{pmatrix} = \begin{pmatrix} 0 \\ 0 \\ 0 \\ 1 \end{pmatrix}$$

The system is restricted to at most one excitation, and then the individual energies part for the Hamiltonian (13) is

$$H^M = E^1 \left(|10\rangle \langle 01| + |01\rangle \langle 10| \right)$$

with $E^0 = 0$ as the reference energy, and the interaction energy part for the Hamiltonian (13) is

$$H^{IM} = J^{01} \left(|01\rangle \langle 01| + |10\rangle \langle 10| \right)$$

where only the interaction between ground-to-excited and excited-to-ground transition is taken into a account. The outer product terms are simply

$$|01\rangle \langle 10| = \begin{pmatrix} 0 \\ 0 \\ 1 \\ 0 \end{pmatrix} \begin{pmatrix} 0 & 0 & 1 & 0 \end{pmatrix} = \begin{pmatrix} 0 & 0 & 0 & 0 \\ 0 & 0 & 0 & 0 \\ 0 & 0 & 1 & 0 \\ 0 & 0 & 0 & 0 \end{pmatrix}$$

$$|10\rangle \langle 01| = \begin{pmatrix} 0 \\ 1 \\ 0 \\ 0 \end{pmatrix} \begin{pmatrix} 0 & 1 & 0 & 0 \end{pmatrix} = \begin{pmatrix} 0 & 0 & 0 & 0 \\ 0 & 1 & 0 & 0 \\ 0 & 0 & 0 & 0 \\ 0 & 0 & 0 & 0 \end{pmatrix}$$

$$|01\rangle \langle 01| = \begin{pmatrix} 0 \\ 0 \\ 1 \\ 0 \end{pmatrix} \begin{pmatrix} 0 & 1 & 0 & 0 \end{pmatrix} = \begin{pmatrix} 0 & 0 & 0 & 0 \\ 0 & 0 & 0 & 0 \\ 0 & 1 & 0 & 0 \\ 0 & 0 & 0 & 0 \end{pmatrix}$$

$$|10\rangle \langle 10| = (|01\rangle \langle 01|)^T = \begin{pmatrix} 0 & 0 & 0 & 0 \\ 0 & 0 & 1 & 0 \\ 0 & 0 & 0 & 0 \\ 0 & 0 & 0 & 0 \end{pmatrix}$$

Finally, the Exciton Hamiltonian matrix in this basis is

$$H = \begin{pmatrix} 0 & 0 & 0 & 0 \\ 0 & E^1 & J^{10} & 0 \\ 0 & J^{10} & E^2 & 0 \\ 0 & 0 & 0 & 0 \end{pmatrix}$$

The coupling with the electromagnetic field is, as it has been introduced,

$$H^I = g(b^\dagger \sigma^- + b\sigma^+)$$

where $b^\dagger$ and b are the creation and annihilation operators of the electromagnetic field and with the operators $S^+ = \sum_i \sigma_i^+$ and $S^- = \sum_i \sigma_i^-$, with σ_i^+ and σ_i^+ acting on the i-th molecule.

By using the Pauli matrices

$$\sigma_z = \begin{pmatrix} 1 & 0 \\ 0 & -1 \end{pmatrix}, \quad \sigma^+ = \begin{pmatrix} 0 & 1 \\ 0 & 0 \end{pmatrix}, \quad \sigma^- = \begin{pmatrix} 0 & 0 \\ 1 & 0 \end{pmatrix}$$

the following expressions are obtained

$$\sigma_1^+ = \sigma^+ \otimes \mathbb{1} = \begin{pmatrix} 0 & 1 \\ 0 & 0 \end{pmatrix} \otimes \begin{pmatrix} 1 & 0 \\ 0 & 1 \end{pmatrix} = \begin{pmatrix} 0 & 0 & 1 & 0 \\ 0 & 0 & 0 & 1 \\ 0 & 0 & 0 & 0 \\ 0 & 0 & 0 & 0 \end{pmatrix}$$

$$\sigma_2^+ = \mathbb{1} \otimes \sigma^+ = \begin{pmatrix} 1 & 0 \\ 0 & 1 \end{pmatrix} \otimes \begin{pmatrix} 0 & 1 \\ 0 & 0 \end{pmatrix} = \begin{pmatrix} 0 & 1 & 0 & 0 \\ 0 & 0 & 0 & 0 \\ 0 & 0 & 0 & 1 \\ 0 & 0 & 0 & 0 \end{pmatrix}$$

$$\sigma_1^- = (\sigma_1^+)^\dagger = \begin{pmatrix} 0 & 0 & 0 & 0 \\ 0 & 0 & 0 & 0 \\ 1 & 0 & 0 & 0 \\ 0 & 1 & 0 & 0 \end{pmatrix} \qquad \sigma_2^- = (\sigma_2^+)^\dagger = \begin{pmatrix} 0 & 0 & 0 & 0 \\ 1 & 0 & 0 & 0 \\ 0 & 0 & 0 & 0 \\ 0 & 0 & 1 & 0 \end{pmatrix}$$

and the collective raising and lowering operators S^+ and S^- are then

$$S^+ = \sigma_1^+ + \sigma_2^+ = \begin{pmatrix} 0 & 1 & 1 & 0 \\ 0 & 0 & 0 & 1 \\ 0 & 0 & 0 & 1 \\ 0 & 0 & 0 & 0 \end{pmatrix} \qquad S^- = \sigma_1^- + \sigma_2^- = \begin{pmatrix} 0 & 0 & 0 & 0 \\ 1 & 0 & 0 & 0 \\ 1 & 0 & 0 & 0 \\ 0 & 1 & 1 & 0 \end{pmatrix}$$

respectively, verifying the equality

$$S^- = (S^+)^\dagger$$

2. The N-molecule water ring

   The geometry of the system is captured through a graph and the dynamics of the water molecules modelled, using an exciton representation. It includes the interaction between the water molecules and the interaction with the electromagnetic field [16].

   By considering $N = 6$, the ground and generic excited states of each molecule are denoted by $|0\rangle_i$ and $|1\rangle_i$, respectively, with $i = 1, \ldots, 6$. They are associated with the eigenvalues $+1$ and -1 of the operator

$$\sigma_{3i} = |1\rangle_i \langle 1|_i - |0\rangle_i \langle 0|_i$$

The exciton Hamiltonian for the six-molecule water ring (6-ring) is obtained from (12) as

$$\begin{aligned} H = & \sum_{i=1}^{6} \left\{ E_i^0 |0\rangle_{ii} \langle 0| + E_i^1 |1\rangle_{ii} \langle 1| \right\} + \\ & \sum_{i=1}^{6} \sum_{\substack{j=1 \\ j \neq i}}^{6} \left\{ J_{ij}^{00} |0\rangle_{ij} \langle 0| + J_{ij}^{01} |0\rangle_{ij} \langle 1| + J_{ij}^{10} |1\rangle_{ij} \langle 0| + J_{ij}^{11} |1\rangle_{ij} \langle 1| \right\} \end{aligned} \tag{14}$$

The coefficient $J_{i,j}^{00}$ is the intermolecular coupling between molecules i and j in the ground state, $J_{i,j}^{01}$ and $J_{i,j}^{01}$ for both molecules in the case of having one in the excited state and one in the ground state, and $\mathrm{J}_{\mathrm{i,j}}^{00}$ for both molecules in the excited state. In this specific 6-ring case, the relative positions of the atoms are assumed fixed (water molecules forming an ice shield inside the nanotube) and the system is described by a network.

The network's adjacency matrix is then 15.

$$\mathbf{A} = \begin{pmatrix} 0 & 1 & 0 & 0 & 0 & 1 \\ 1 & 0 & 1 & 0 & 0 & 0 \\ 0 & 1 & 0 & 1 & 0 & 0 \\ 0 & 0 & 1 & 0 & 1 & 0 \\ 0 & 0 & 0 & 1 & 0 & 1 \\ 1 & 0 & 0 & 0 & 1 & 0 \end{pmatrix} \tag{15}$$

with the entries A_{ij} representing the configuration. The geometry of the system determines the interaction between the water molecules in the excitonic representation, determining which values of $J_{ij}^{\nu\mu}$ will be non-zero since

$$J_{ij}^{\nu\mu} = A_{ij} J^{\nu\mu}$$

Therefore, the Hamiltonian 14 becomes

$$\begin{aligned} H = & \sum_{i} \left\{ E^0 |0\rangle_{ii} \langle 0| + E^1 |1\rangle_{ii} \langle 1| \right\} + \\ & \sum_{i \neq j} A_{ij} \left\{ J^{00} |0\rangle_{ij} \langle 0| + J^{01} |0\rangle_{ij} \langle 1| + J^{10} |1\rangle_{ij} \langle 0| + J^{11} |1\rangle_{ij} \langle 1| \right\} \end{aligned}$$

where the interaction $J^{\nu\mu}$ only depends on the states of the molecules in interaction, with three possibilities, $J^{00}, J^{01} \equiv J^{10}$ and J^{11}, and the individual energies E_i^{ν} are identical for each molecule, only depending on the state ν

$$E_i^\nu = E^\nu$$

The interaction with the transverse electromagnetic potential is, as it has been presented, captured by the Hamiltonian

$$H^I = g(b^\dagger \sigma^- + b\sigma^+) \tag{16}$$

where $b^\dagger$ and b are the creation and annihilation operators of the electromagnetic field. The collective raising and lowering operators are, respectively, $\sigma^+ = \sum_i \sigma_i^+$ and $\sigma^- = \sum_i \sigma^-$, with $\sigma_i^+ = |1\rangle_{ii} \langle 0|$ and $\sigma_i^- = (\sigma_i^+)^\dagger$.

When dealing with Dicke superradiance, there are two key aspects relative to the system: the spatial size of the region occupied by the molecules, and the presence or absence of a cavity. If there is no cavity, the spontaneous emission requires to be close together, on a scale much shorter than the wavelength of the emitted photon. However, the dipole-dipole interaction between the molecules, when too close, act to break the symmetry of the Dicke model [57]. However, in this study, water in the nanotube is a symmetrical system, with water molecules in the ring having cylindrical symmetry with respect to the central water chain. Therefore, the water system can be decomposed into identical units, and then the dipole-dipole interaction can enter as a term of H^{IM}. This way, although molecules are pretty close together (3 Å approximately), and dipole-dipole interaction are strong, they do not break the symmetry needed for the Dicke dynamics to take place. A different argument but with similar conclusions is used in Chapter 4.3.6 to support that the water molecules are indeed in a synchronized state promoted by the symmetry of the system.

Let N^* be the number of molecules in each identical unit. The Hamiltonian is the usual Dicke or Dicke-Preparata one where the intermolecular interactions are instead of neglected, included in the dynamics as follows.

If $N^* = 1$, $S(N,i) = S(N,k)$ for each i,k and the intermolecular interaction term then reads

$$H^{IM} = J^{01} \cdot S(N,i) \cdot S(N,j) = J^{01} \cdot S(N,i) \cdot S(N,i)$$

The intermolecular interaction has $N(N-1)$ terms. As it has been introduced, the adjacency matrix $\mathbf{A}$, is used that reduces the number of Hamiltonian terms. It means that dipolar interaction is neglected for molecules that are at a distance $d > d_0$, let's say $d_0 > 3.5$ Å.

For the 6-ring case, the intermolecular interaction has 12 terms. By using the notation $S(6,i) := S(i)$ the following expression is obtained

$$\begin{aligned} H^{IM} = J^{01}(&S(0)\cdot S(1) + S(1)\cdot S(2) + S(2)\cdot S(3) \\ &+ S(3)\cdot S(4) + S(4)\cdot S(5) + S(5)\cdot S(0) \\ &+ \text{cc.cc.}) \end{aligned}$$

and, because $S(i) = S(j)$ due to symmetry, finally $H^{IM} = 12\, H^{IM}_{unit}$, where, in this case, the unit is the molecule.

For $N^* > 1$ it is equivalent, only in this case the number of terms and the system's unit will change depending on N^* value. Several cases are studied, based on the atomic positions from a Density Functional Theory simulation of water in the nanotube.

Note: $S(0) \cdot S(1)$ corresponds to the matrix product of column vector $S(0)$ by row vector $S(1)$, that is, $S(0) \cdot S^{\dagger}(1)$, where † has been omitted.

3. Nanotube water

   Let us consider the system formed by M stacked 6-rings ($N = 6$). The distance between the rings is approximately 3 Å, also between the molecules in the ring. The rings are assumed to be in the ground and first excited symmetrised states $|l\rangle$, with $l \in \{0, 1\}$, given by

$$|0\rangle = |000000\rangle = S(0)$$
$$|1\rangle = \frac{|100000\rangle + |010000\rangle + \ldots |000001\rangle}{\sqrt{6}} = \frac{S(1) + S(2) + \cdots + S(6)}{\sqrt{6}}$$

   The molecular Hamiltonian is then

$$H^M = E \cdot \sqrt{6}\, |1\rangle$$

   The transition dipole-dipole interaction between molecules in a ring is negligible due to symmetry.

   The coupling to the electromagnetic field is, as usual,

$$H^I = g\left(\sigma^+ a + \sigma^- a^\dagger\right)$$

   where the operators σ^+ and σ^- are, respectively, the raising and lowering operators for the symmetrised states $|l\rangle$, that here refers to the ring, and a and $a^\dagger$ are the photon creation and annihilation operators, respectively.

   The space of N rings is built, as usual, with the tensor product

$$S = S_1 \otimes S_2 \otimes \cdots \otimes S_M$$

   The interaction between two adjacent rings is

$$H^{IM} = J^{01}_{ring} \left(|0\rangle \langle 1| + |1\rangle \langle 0|\right)$$

   For M rings

$$H^{IM} = \sum_{i,j} J^{01} B_{ij} \left(|0\rangle_{ij} \langle 1| + |1\rangle_{ij} \langle 0|\right)$$

   where the adjacency matrix $\mathbf{B}$ with two possibilities is introduced, periodic boundary conditions (infinite chain) $\mathbf{B}_p$ and non-periodic $\mathbf{B}_{np}$. They are

$$\mathbf{B}_{np} = \begin{pmatrix} 0 & 1 & & \dots & 0 \\ 1 & 0 & 1 & & \vdots \\ & 1 & 0 & & \\ & & & \ddots & \\ \vdots & & \ddots & \ddots & 1 \\ 0 & \dots & & 1 & 0 \end{pmatrix}$$

$$\mathbf{B}_{p} = \begin{pmatrix} 0 & 1 & & \dots & 1 \\ 1 & 0 & 1 & & \vdots \\ & 1 & 0 & & \\ & & & \ddots & \\ \vdots & & \ddots & \ddots & 1 \\ 1 & \dots & & 1 & 0 \end{pmatrix}$$

As an initial state, initially random $|0\rangle$ and $|1\rangle$ states will be considered, for each ring, which is a symmetrised state. There is, however, variation along the length of the nanotube.

The space of states is no longer the Dicke space, as several rings are now stacked. Therefore, the dynamics are presumably different. For example, having $|2T, T, 9T, 5T\rangle$ would be corresponding to having a set of letters $|b, a, \dots\rangle$ and therefore an aperiodic (along the tube) crystal (periodic). Another possibility is to look at the ground and excited states for each ring $|10100\dots\rangle$ which is also a possible codification.

To understand what is possible and not, it could be useful to look at Ising model theoretical results, as there is a similarity with the water system, which is an extended Ising model. This is left for future work.

It seems reasonable to expect water to not have a structure by itself, as temperature and fluctuations induce disorder and then an average zero polarisation as usually considered. However, Del Giudice, Preparata and Vitiello show [35] that defects or some other structures can produce permanent polarisation in water. In the model of the origin of life, the external environment is included in the nanotube water system, which corresponds for example to a Halloysite clay nanotube setting, that could induce permanent polarisation in water and some spatio-temporal structure.

4. Bulk liquid water and temperature effects

   The dynamics can be extended and the variation of water's positions in space, introduced, through a time-dependent adjacency matrix $\mathbf{A}(t)$.

   To simulate the non-symmetric case, a random molecule is chosen to be excited by the photon. The states for the nodes are $|0\rangle$ and $|1\rangle$, this is, ground and excited states. The dynamics in the network are defined by the Hamiltonian [Dicke-Cabral]. In the case of bulk liquid water, the network of interaction can be captured, for example, through a random network structure. Then, the

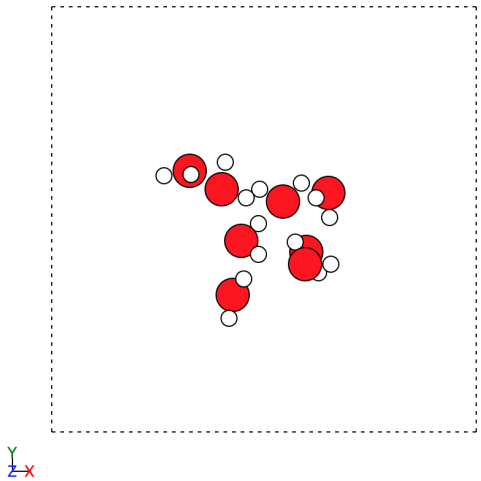

Figure 4: Disordered water cluster and cell in GPAW.

dynamics of the protons studied and compared with the case of fixed geometries that have been explored in sections **??** and **??**. The experimental data can be fitted to infer network structure in the bulk.

The Hamiltonian is

$$H = \sum_i \left\{ E^0 \left|0\right\rangle_{ii} \left\langle 0\right| + E^1 \left|1\right\rangle_{ii} \left\langle 1\right| \right\} + \sum_{i \neq j} A_{ij}(t) \left\{ J^{00} \left|0\right\rangle_{ij} \left\langle 0\right| + J^{01} \left|0\right\rangle_{ij} \left\langle 1\right| + J^{10} \left|1\right\rangle_{ij} \left\langle 0\right| + J^{11} \left|1\right\rangle_{ij} \left\langle 1\right| \right\}$$

where $A(t)$ is the time-dependent adjacency matrix.

The simulation setting has been prepared and the code presented. Results are in a preliminary state and thus are not presented here. This simulation setting would specifically allow exploring geometry effects, which has been an important aspect in this Chapter, and also temperature effects, through the use for example of Langevin dynamics combined with the ED simulation setting. Fig. 4 shows a disordered water cluster in GPAW.

4.3.3 Exciton Dynamics Analytical Treatment

[Here dynamics part of periodicity induced]

4.3.4 Synchronization of a Water Cluster

1. R Pearson Correlation Coefficient

   The following graphs show the R Pearson correlation coefficient for different initial states and environmental conditions, in the case of an ideal ring (Figs. 5–7) and random disposition (Fig. 8–10).

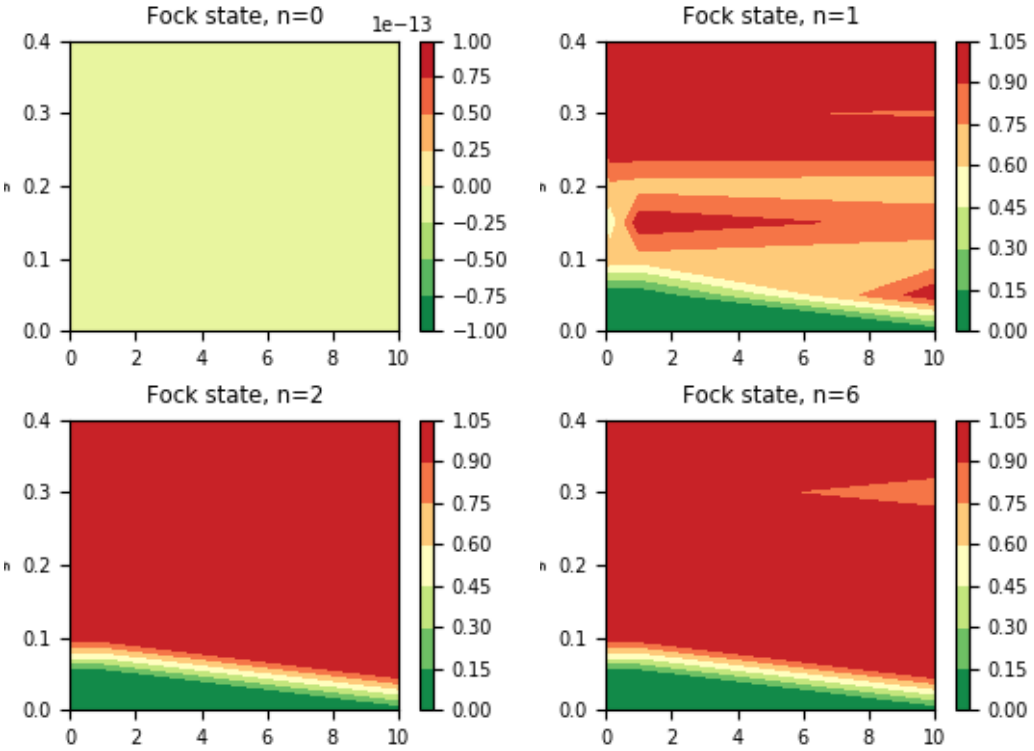

Figure 5: R Pearson correlation coefficient values of a ground initial state in a Fock electromagnetic environment with $n = 0, 1, 2, 6$ photons, for values of the coupling constant g (vertical axis) and intermolecular interaction J (horizontal axis), in the case of ideal ring disposition.

It can be observed (Fig. 5) that the R Pearson correlation coefficient is virtually zero for a ground state in an empty electromagnetic environment. For $n = 1, 2, 3$ there are similarities in the plots. We see, in the three cases, low values of the correlation coefficient for low values of g, which extends across J values. In the case a Fock electromagnetic environment with $n = 1$ and $n = 6$, there are regions of low values. We will see that the pattern of low and high values repeats, with some variations, for other initial states and environmental conditions. In the case of $n = 2$, there is a clear separation between a zone with almost perfect synchronization (0.8 to 0.9 correlation) and a zone with a very low correlation (between 0.0 and 0.1). This pattern repeats itself for $n = 1$ and $n = 6$, although the mentioned regions of intermediate values do differ in the case of $n = 1, 6$.

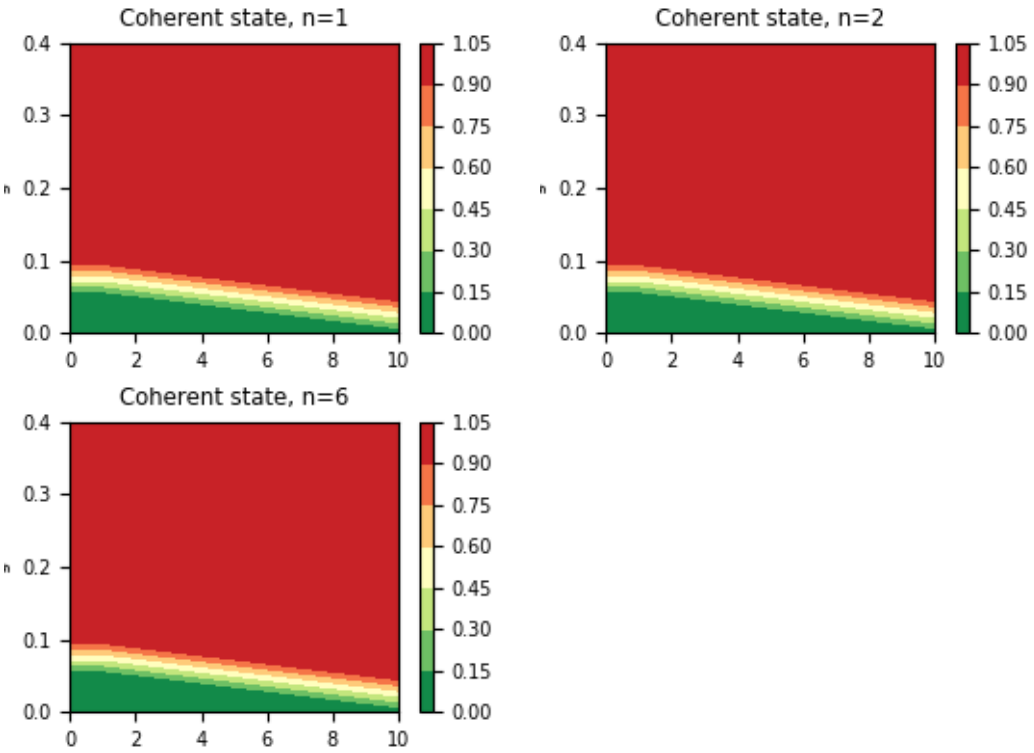

Figure 6: R Pearson correlation coefficient values of a ground initial state in an coherent electromagnetic environment with $n = 0, 1, 2, 6$ photons, for values of the coupling constant g and intermolecular interaction J, in the case of ideal ring disposition. For $n = 0$, R Pearson correlation coefficient is zero for all parameters values, as for a Fock state.

In the case of a ground initial state in a coherent electromagnetic environment (Fig. 6), we can observe the aforementioned pattern of separation of areas of almost perfect and almost zero synchronization. The area of zero synchronization corresponds to low g values, with a larger g interval for lower J values.

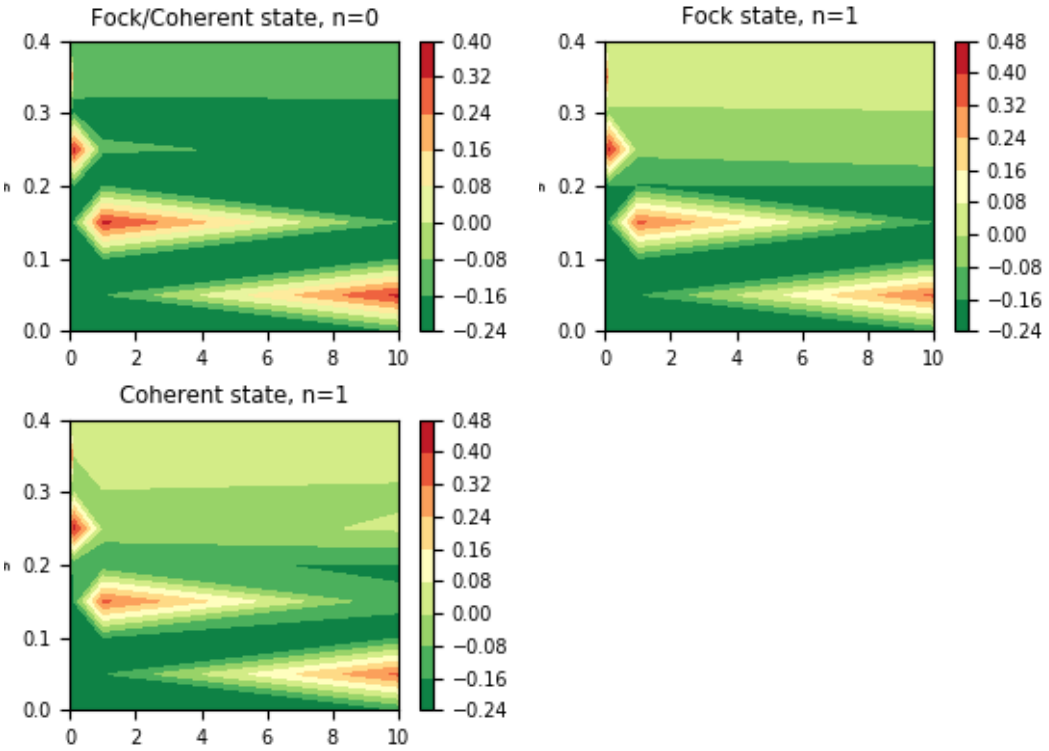

Figure 7: R Pearson correlation coefficient values in the case of a single excited initial state, for the coupling constant g and intermolecular interaction strength J, and an empty electromagnetic environment.

In the case of a single excited state (Fig. 7), there are some differences in the graphs for different n values, although we can observe a repeating pattern, with areas of the highest values concentrating in the same regions. We will see that this pattern repeats for other initial states and environmental conditions. It can be hypothesized then that there are certain relations of g to J that promote synchronization, and that these regions occur for combinations of g and J, across these parameters space. Therefore, high intermolecular coupling J values do promote synchronized behavior for low g values. High coupling constant g synchronization regions correspond to low J values. These g to J ratios are expected to have some physical relevance.

In Figure 8 and 9 we see a similar pattern, in this case for two random spatial configurations. It is then suggesting that synchronization in the case of a ground initial state, is not strongly affected by the molecular dispositions. Similar behavior of the water system is found in both cases.

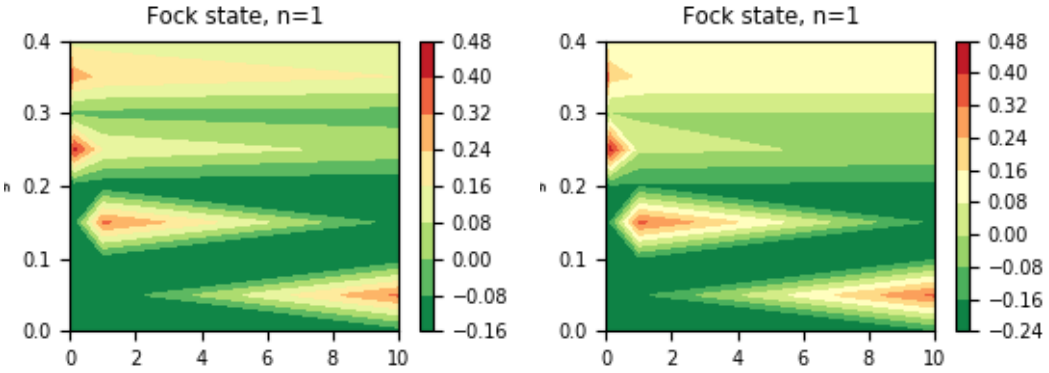

Figure 8: R Pearson correlation coefficient values in the case of an initial ground state for two random spatial configurations, for values of the coupling constant g and intermolecular interaction strength J. In both cases, the environment is initially in a Fock state with $n = 1$.

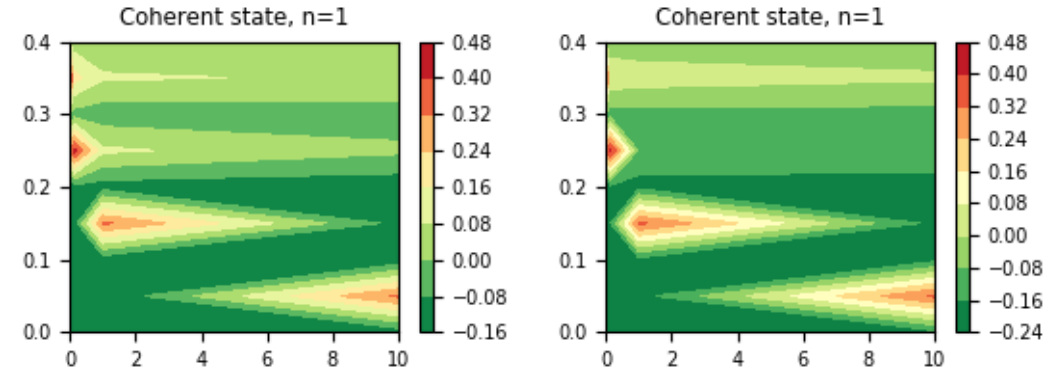

Figure 9: R Pearson correlation coefficient values in the case of an initial ground state for two random spatial configurations, for values of the coupling constant g and intermolecular interaction strength J. In both cases, the environment is initially in a coherent state with $n = 1$.

For the case of a single excited state (Fig. 10) the same pattern is found with slight variations.

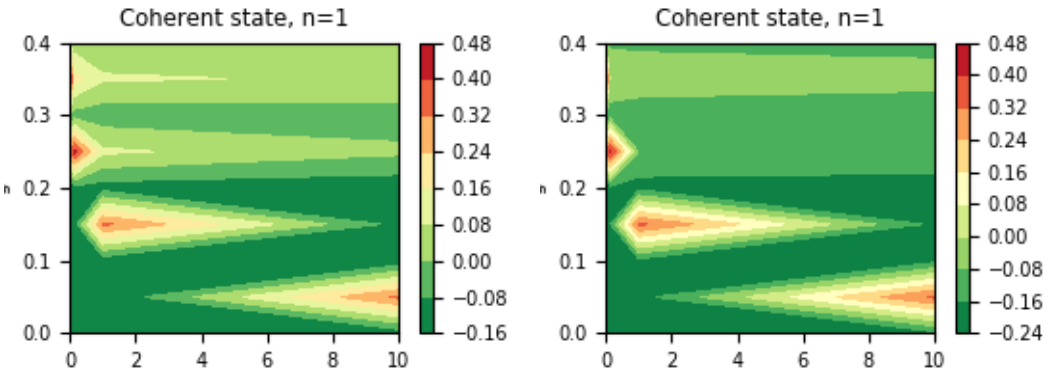

Figure 10: R Pearson correlation coefficient values in the case of a single excited initial state and coherent electromagnetic environment with $n = 1$ for two random spatial configurations, for values of the coupling constant g and intermolecular interaction strength J.

We can conclude that two main types of behavior are observed for R Pearson correlation coefficient in the studied cases. On one hand, a pattern of separated regions of very high and very low synchronization values, that occur in the cases where there is symmetry in the system, that is, in the case of an ideal ring with a ground initial state. On the other hand, a distributed high correlation coefficient values pattern occurs in the non-symmetric cases, that is, in the case of an ideal ring, with a single excited state that, thus, breaks the ring symmetry, and in the case of disordered clusters. In this last case, we see a sort of inverse relation between g and J, which can be interpreted physically as follows. A dispersed cluster of molecules needs high g values to be synchronized, while a tight or cluttered cluster synchronizes better with low g values. In other words, if we consider the ring as part of a larger group, we can say that the disperse cluster needs a large group to synchronize and that the tight cluster synchronizes better within a smaller group.

2. Mutual Information

   (a) Quantum Synchronization of an Ideal Ring

   The dynamics are simulated using ME solver from Qutip [67, 66], and MI is calculated and plotted.

   The study is restricted to ground state and single excited states.

   For a 6-ring ($N = 6$) the initial state is chosen to be

$$|\Psi\rangle_0 = |000000\rangle = \begin{pmatrix}0\\1\end{pmatrix} \otimes \begin{pmatrix}0\\1\end{pmatrix} \otimes \begin{pmatrix}0\\1\end{pmatrix} \otimes \begin{pmatrix}0\\1\end{pmatrix} \otimes \begin{pmatrix}0\\1\end{pmatrix} \otimes \begin{pmatrix}0\\1\end{pmatrix}$$

   The electromagnetic initial state is chosen to be the Fock state and coherent state, both with the number of photons from $n = 0$ to $n = 6$. The case for $n \in \{0, 1, 2, 6\}$ is presented.

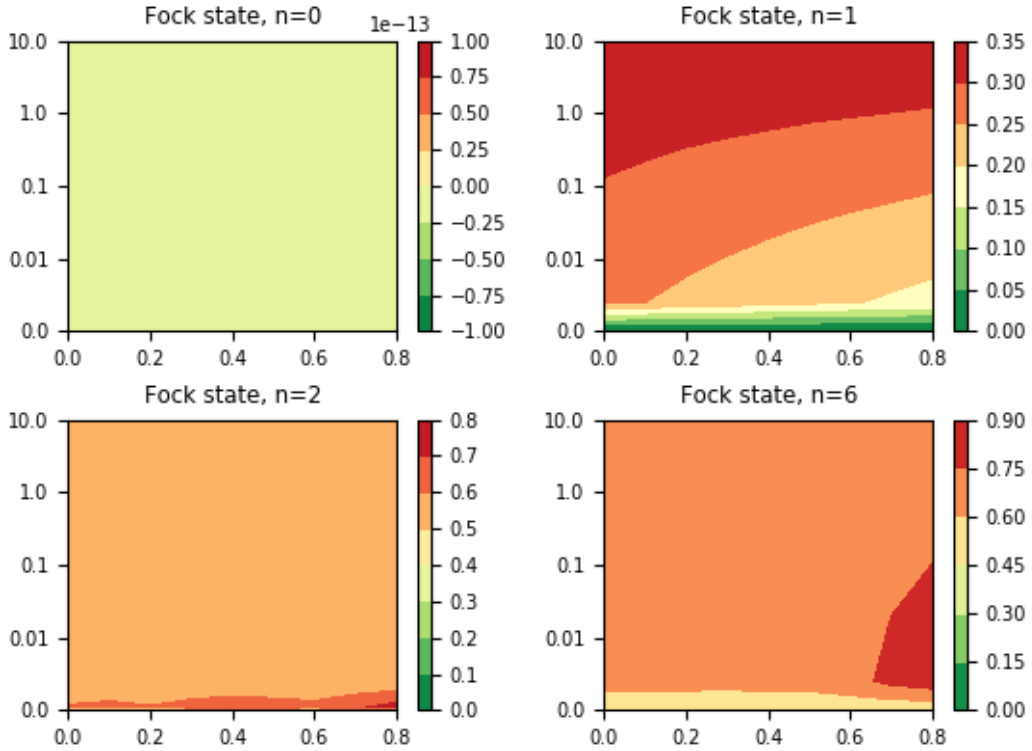

Figure 11: Mutual information values, in a Fock electromagnetic environment with $n = 0, 1, 2, 6$ photons, for values of the coupling constant g (vertical axis) and intermolecular interaction J (horizontal axis), in the case of ideal ring disposition. Note the different scale for each figure.

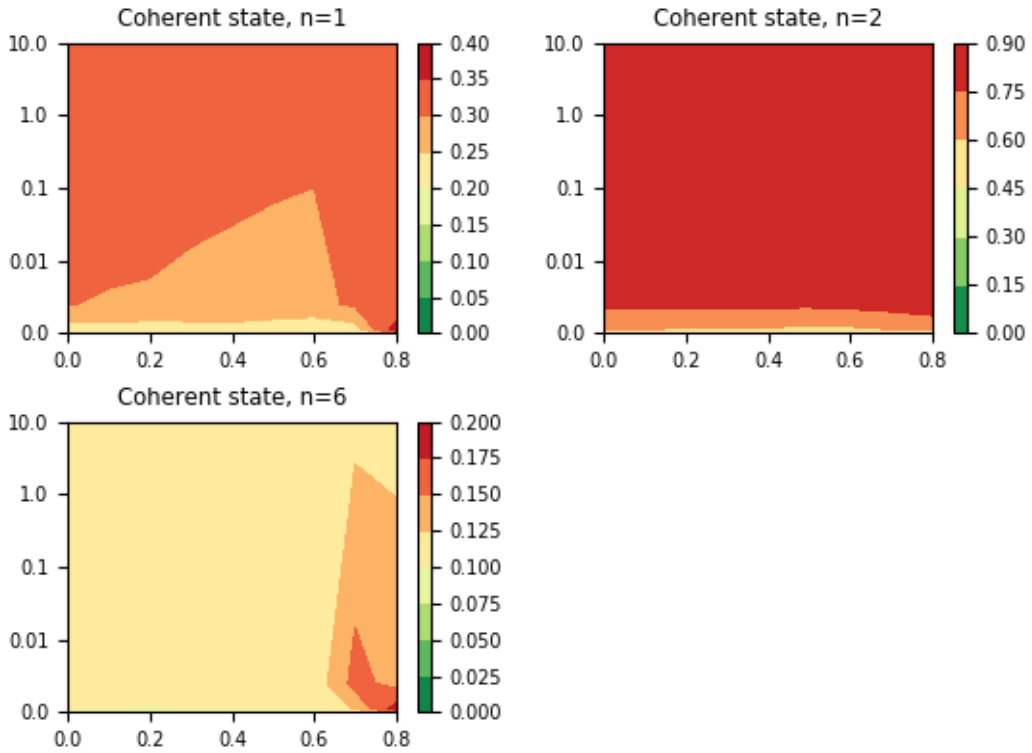

Figure 12: Mutual information values, in an coherent electromagnetic environment with $n = 0, 1, 2, 6$ photons, for values of the coupling constant g (vertical axis) and intermolecular interaction J (horizontal axis), in the case of ideal ring disposition. For $n = 0$, mutual information is zero for all parameters values g and J, as for a Fock state.

The dynamics, and the value of MI for the water system, is highly dependent on the electromagnetic environment. In the case of no photons, the ground state stays at the ground state and MI is zero. When there are photons, the dynamics is highly complex and depends strongly on the characteristics of the electromagnetic environment.

A single excited initial state is also considered and given by

$$|\Psi\rangle_0 = \begin{pmatrix}1\\0\end{pmatrix} \otimes \begin{pmatrix}1\\0\end{pmatrix} \otimes \begin{pmatrix}1\\0\end{pmatrix} \otimes \begin{pmatrix}1\\0\end{pmatrix} \otimes \begin{pmatrix}1\\0\end{pmatrix} \otimes \begin{pmatrix}0\\1\end{pmatrix}$$

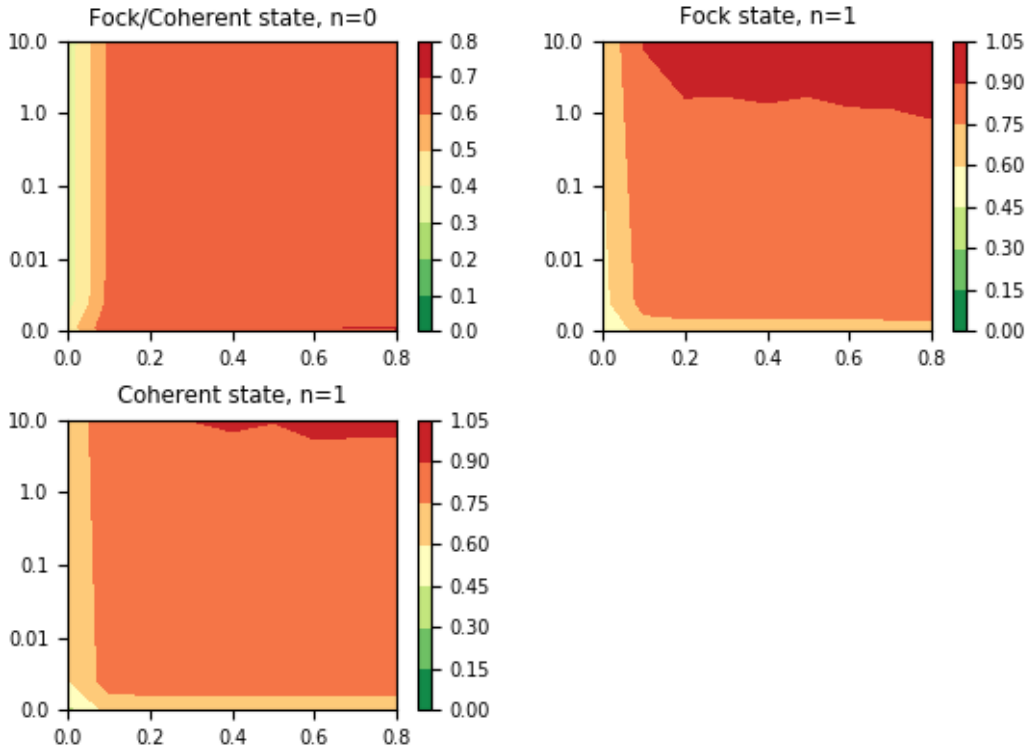

Figure 13: Mutual information values in the case of a single excited initial state, for the coupling constant g (vertical axis) and intermolecular interaction strength J (horizontal axis), and an empty electromagnetic environment.

A MI value of over 0.6 for J greater than 0.1, and for all values of g considered, supporting the idea that a random excitation of a molecule from vacuum oscillations can lead to a collective, synchronized state for the water system (Fig. 13).

There is a strong dependence of the dynamics on the initial conditions, that can be taken, a priori, as an indication of water dynamics being complex. An explicit study based on a distance between states measures, for example, the trace distance, is left for future work.

MI values are also calculated and presented in the case of disordered water clusters (Figs. 14-16), where the intermolecular coupling matrices J_1 and J_2, which were randomly generated, are the following

$$J_1 = \begin{pmatrix} 0 & 0.46 & 0.47 & 0.53 & 0.22 & 0.36 \\ 0.46 & 0 & 0.76 & 0.5 & 0.57 & 0.52 \\ 0.47 & 0.76 & 0 & 0.43 & 0.07 & 0.52 \\ 0.53 & 0.5 & 0.43 & 0 & 0.56 & 0.54 \\ 0.22 & 0.57 & 0.07 & 0.56 & 0 & 0.17 \\ 0.36 & 0.52 & 0.52 & 0.54 & 0.17 & 0 \end{pmatrix}$$

$$J_2 = \begin{pmatrix} 0 & 0.53 & 0.5 & 0.36 & 0.21 & 0.5 \\ 0.53 & 0 & 0.41 & 0.33 & 0.13 & 0.09 \\ 0.5 & 0.41 & 0 & 0.44 & 0.66 & 0.38 \\ 0.36 & 0.33 & 0.44 & 0 & 0.24 & 0.14 \\ 0.21 & 0.13 & 0.66 & 0.24 & 0 & 0.54 \\ 0.5 & 0.09 & 0.38 & 0.14 & 0.54 & 0. \end{pmatrix}$$

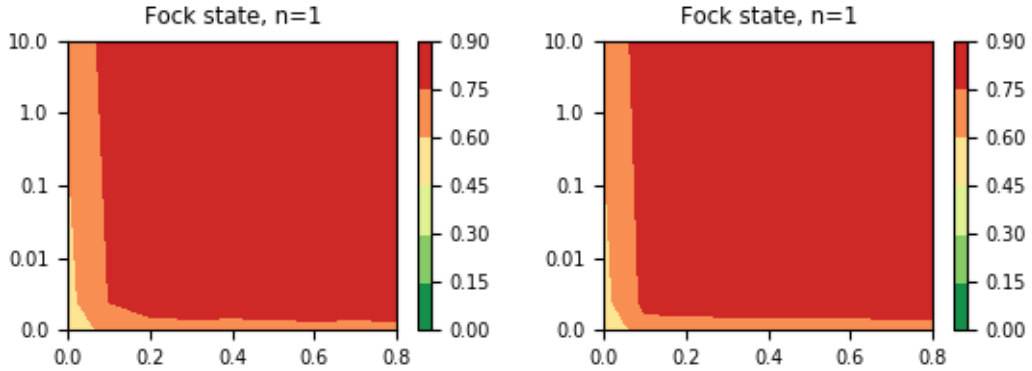

Figure 14: Mutual information values in the case of an initial ground state for two random spatial configurations, for values of the coupling constant g and intermolecular interaction J. In both cases, the environment is initially in a Fock state with $n = 1$.

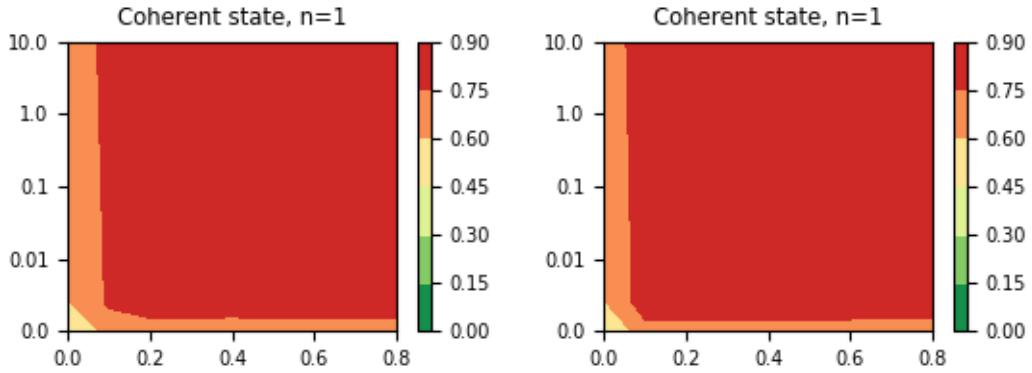

Figure 15: Mutual information values in the case of an initial ground state for two random spatial configurations, for values of the coupling constant g and intermolecular interaction strength J. In both cases, the environment is initially in a coherent state with $n = 1$.

It can be observed in Figures 14 and 15 that in the case of a ground initial state the behavior is almost identical for each of the two spatial configurations. However, in the case of a single excited initial state, the situation is radically different. We find that for the two spatial configurations high and low MI values seem to have inversed (Fig. 16).

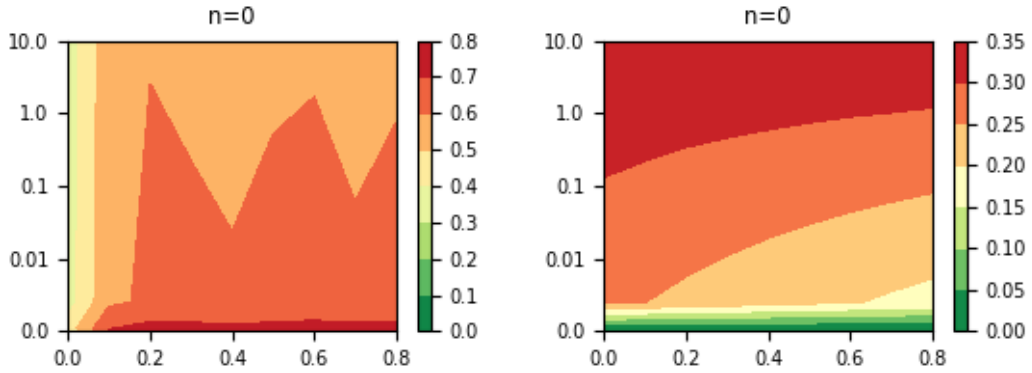

Figure 16: Mutual information values in the case of a single excited initial state for two random spatial configurations, for values of the coupling constant g and intermolecular interaction strength J. In both cases, the environment is initially empty, $n = 0$.

4.3.5 Synchronization Time Evolution

Figures 17 and 18 show the time evolution of MI values for several parameters g and J values, for ground initial states, in the case of a Fock and a coherent environment, with the number of photons $n = 6$ and $n = 2$, respectively. For parameters values $J = 0.7$ and $J = 0.8$ and $g = 1.0$, differences in the dynamic for rest parameter values can be observed, with a stabilization of the MI values, within a smaller variation interval, after an initial transient, indicating a peculiarity for the water system at these parameter values. Note that this is verified both for Fock and coherent environments, with different intensities for the different initial states and environmental conditions. The time evolution of MI for the rest of the initial and environmental conditions is presented in Appendix .1.

Quantitatively, we can anticipate the presence of a bifurcation point for these values of the parameters that, interestingly, is present in higher or lower degree across environmental conditions, despite the system's sensitivity to these. It seems to indicate that this behavior is characteristic of the system and robust to the different environmental conditions. A further investigation is, then, suggested. Due to time limitation, it is left for future work.

From a physical point of view, it is interesting to see that it implies the highest value of the dipole interaction, and therefore the common belief that dipole-dipole interaction acts to suppress collective behavior, can be challenged and in this case, it would be acting to promote it. It indeed supports the idea that H-bond could be acting to promote intertwined dynamics in the water system, which could have important implications for life, for example, the understanding of H-bond role in the origin of life.

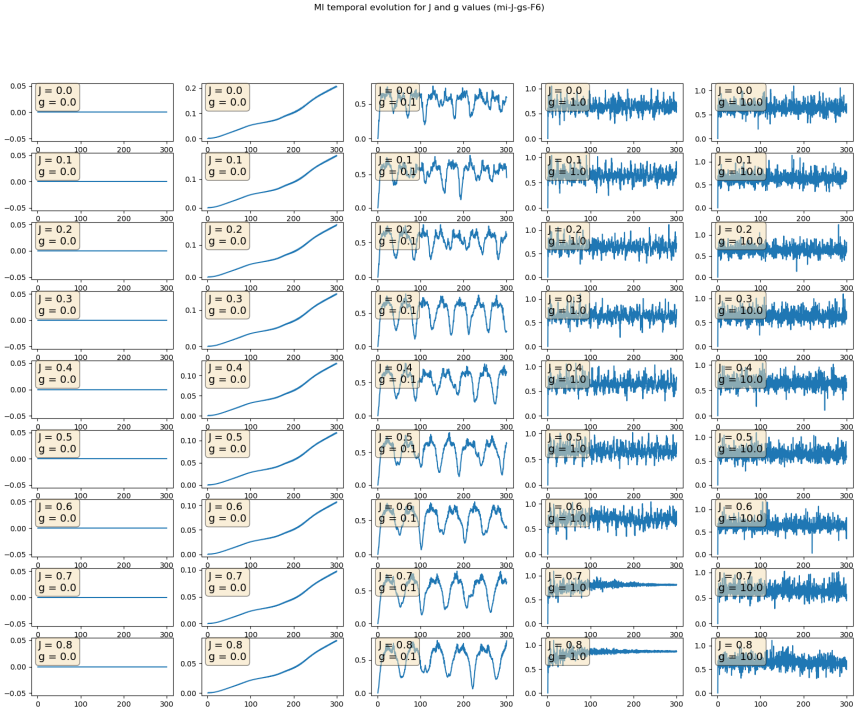

Figure 17: Mutual information synchronization measure time evolution for an ideal ring disposition, with ground initial state, and electromagnetic environment Fock state with $n = 6$. Note that the value of g in the second column is 0.05 (not visible).

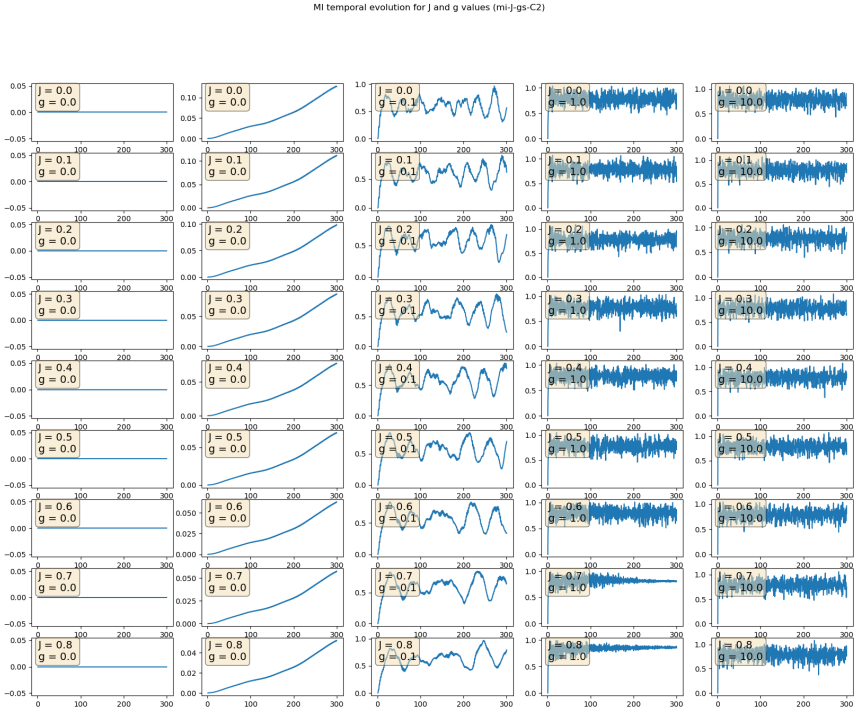

Figure 18: Mutual information synchronization measure time evolution for an ideal ring disposition, with ground initial state, and electromagnetic environment coherent state with $n = 2$.

4.3.6 Periodicity Induced Collective Order: Analytical Dynamics

1. Ring Periodic Wave Function

   The ordered, ice-like structure of water molecules is modelled inside the nanotube as an aggregate of (abstract, assumed identical) components, each characterised by the Schrdinger equation

   $$H_n\psi_n = E_n\psi_n.$$

   The wave function of the system is, then, the tensor product of the individual wave functions.

   The ground state of the system is noted as

   $$\Phi_G = |g\rangle_1 \otimes |g\rangle_2 \otimes \cdots \otimes |g\rangle_N := |g_1, g_2, \ldots g_N\rangle\,,$$

   and the single excited states a is noted as

   $$\Phi_a = |g_1, g_2, \ldots e_a \ldots g_N\rangle\,,$$

   where $|e\rangle_i$ represents the i-th component in the excited state.

   The k-th exciton stationary state wave function can be described by

   $$\Psi_k = \frac{1}{\sqrt{N}} \sum_{a=1}^{N} C_{ak}\Phi_a$$

   where $|C_{ak}|^2$ determines the probability that the a-th molecule is excited.

   For a periodic ring (with rotational invariance for some angle) it is assumed an ideal periodic distribution of the molecules, with one molecule per unit cell, and the corresponding periodic boundary conditions. The wave function can be written as

   $$\Psi_k = \frac{1}{\sqrt{N}} \sum_{a=1}^{N} e^{i\frac{2\pi}{N}ak}\Phi_a$$

   with $k = 0, +1, -1, +2, \ldots, \frac{N}{2}$ and for N even [5]. The exciton wave functions are assumed to be mutually orthogonal and normalized to unity.

   Only the dynamics restricted to the ground and first excited states will be considered, that is, the case of a two-level system.

2. Dynamics

   Each of the molecules interacting with a single mode field will now be considered [58],

   $$\hat{\boldsymbol{E}} = \boldsymbol{e}\sqrt{\frac{\hbar\omega}{\epsilon_0 V}}\left(\hat{a} + \hat{a}^\dagger\right) sin(kz).$$

In the rotating wave approximation, the terms in the Hamiltonian that oscillate rapidly are neglected. This is a valid approximation when the applied electromagnetic radiation is near resonance with an atomic transition, and the intensity is low. The Jaynes-Cummings Hamiltonian is then

$$\hat{H} = \frac{1}{2}\hbar\omega_0\hat{\sigma}_3 + \hbar\omega\hat{a}^\dagger\hat{a} + \hbar\lambda\left(\hat{\sigma}^+\hat{a} + \sigma^-\hat{a}^\dagger\right) \tag{17}$$

A two-level system interacting with the field is considered, with zero-detuning. The state vector is expressed as

$$|\psi(t)\rangle = C_i(t)\,|i\rangle + C_f(t)\,|f\rangle \tag{18}$$

where $|i\rangle = |e\rangle\,|n\rangle$ and $|f\rangle = |g\rangle\,|n+1\rangle$

The equation of motion for the coefficients is

$$\ddot{C}_i(t) + \lambda^2(n+1)C_i = 0 \tag{19}$$

The solution for the initial condition $C_i(t) = 1, C_f(t) = 0$ is $C_i(t) = cos(\lambda t\sqrt{n+1})$ and $C_f(t) = -isin(\lambda t\sqrt{n+1})$.

The Jaynes-Cummings Hamiltonian for N two-level systems is called the Tavis-Cummings Hamiltonian. It can be expanded in an ansatz analogous to 18. Restricting the study to the single excitation subspace,

$$|\Psi(t)\rangle = C_g(t)\,|g_1,\ldots,g_N\rangle + C_1(t)\,|e_1,g_2,\ldots,g_N\rangle + \cdots + C_n(t)\,|g_1,g_2,\ldots,g_N\rangle \tag{20}$$

The exciton states of a ring of N molecules are

$$\Phi_g = |g_1,g_2,\ldots,g_N\rangle$$

$$\Phi_e = \frac{1}{\sqrt{N}}\left(|e_1,g_2,\ldots,g_N\rangle + |g_1,e_2,g_3,\ldots,g_N\rangle + \cdots + |g_1,g_1,\ldots,e_N\rangle\right)$$

and a state of the system is given by

$$|\Psi(t)\rangle = C_g(t)\,\Phi_g + C_e(t)\,\Phi_e.$$

Therefore, for N molecules in this configuration it would be expected that $C_1(t) = C_2(t) = \cdots = C_N(t)$.

The ansatz (20) can then be expressed in terms of the exciton states, Φ_g and Φ_e, as

$$|\Psi(t)\rangle = C_g(t)\,\Phi_g + C_1(t)\,\sqrt{N}\,\Phi_e = C_g(t)\,\Phi_g + C_e(t)\,\Phi_e$$

with $C_g(t) = \sqrt{N}C_1(t)$.

Introducing the ansatz into the Shrdinger equation

$$i\frac{d}{dt}\,|\Psi(t)\rangle = i\left(\dot{C}_g(t)\Phi_g + \sqrt{N}\dot{C}_1(t)\Phi_e\right) = H_{II}\,|\Psi(t)\rangle$$

the following expression is obtained

$$\dot{C}_g(t) = -i\lambda\sqrt{N(n+1)}\,C_1(t)$$
$$\dot{C}_1(t) = -i\lambda\sqrt{\frac{n+1}{N}}C_1(t)$$

and eliminating C_1

$$\ddot{C}_g(t) + \lambda^2\,(n+1)\,C_g(t) = 0$$

which is identical to equation (22). Therefore, we can conclude that the dynamics of the ring is analogous to the case of the single-molecule, with the ground state of the molecule corresponding to the ground exciton state of the ring, and the excited state of the molecule corresponding to an excitation "distributed" across the elements of the ring. The oscillation happens with the same frequency in both cases, the Rabi frequency

$$\Omega(\bar{n}) = 2\lambda\sqrt{\bar{n}+1} \approx 2\lambda\sqrt{\bar{n}}$$

with $\bar{n}$ the initial number of photons in the cavity.

In the semiclassical case, where an external classical electromagnetic field is considered, the atomic inversion is also periodic. However, in the quantum case, there are Rabi oscillations even for the case of no initial photons present in the cavity, which are so-called *vacuum Rabi oscillations*. They are the result of the spontaneous emission and absorption of a photon, which is an example of reversible spontaneous emission, as no dissipation of the photons is being taken into account.

Having deduced that the dynamics of the N-molecule ring behaves as a single molecule, the same argument can be applied for a large number of stacked rings M to deduce that the water system would undergo collective dynamics, that is, the space of states would be that of a number of collective states for the whole system. The number of rings for a $10\,\mu m$ nanotube is $M \approx 3.6 \times 10^4$. These common electronic dynamics can provide the protons with a PES for synchronized motion, as suggested by Reiter [104] from their DINS measurement.

4.4 Conclusions

An Exciton Hamiltonian formulation of water for the simulation of electronic dynamics has been proposed. It has been used to study quantum synchronization in the nanotube water system. The dynamics in the case of water rings have been compared with those of a disordered cluster. Water dynamics dependency on the environmental conditions has been studied, through the simulation of ED for several environment states. It has been shown that quantum synchronization depends on the environmental conditions, as well as on the molecular dispositions. The dependency on the environmental conditions is more acute in the case of MI and less so in the case of R Pearson correlation coefficient. Within the studied conditions, we have observed that water molecular dispositions affect dramatically MI, while does not influence (apart from very small variations) in the case of R Pearson correlation coefficient. It can be deduced that water dynamics behave in a non-linear probably complex manner. Sensitivity to the environmental and initial conditions supports so. A formal study is proposed and is out of the scope of the presentation of this Chapter.

Reiter, in his article [104], claims that proton synchronization would explain the observed behavior of water in the nanotube, as reported in Section 1.1.5. In Section 4.3.6 we have applied the Bloch theorem to the water system and analytically deduced its dynamics, to show that the system's electrons are in a common collective state. These states are thus providing a common electromagnetic potential energy surface to the protons, which would allow for proton synchronization. An explicit electron density representation of these states is the subject of Chapter 6 in 1D, and Chapter 5 in 3D, for two complementary theoretical and simulation frameworks. Explicit analysis of the proton synchronization under the collective PES provided by the electrons in this setting is part of Preprint [21] and remains to be completed.

Part III
Microscopic Scale

In this Part, a microscopic description of the water system is used, so we are dealing with nuclear positions and electron density distributions in space. The nuclear wave function can also be calculated in the case of Chapter 6, for the Hydrogen involved in the H-bond.

In Chapter 5 we study the effects at the microscopic level of the emergent macroscopic electromagnetic potential, predicted by QED Coherence in Matter theory. It is done by imposing an external electric perturbation to the water system, using TDDFT to calculate the induced changes in the electron density, for the ground state electron density distribution, among other properties.

In Chapter 6, we are particularly interested in QED effects at the H-bond area, in order to compare with Reiter's observations. We use the Shin-Metiu model for the H-bonded dimer and study electron and proton dynamics, including interaction with the transverse electromagnetic potential. Because the effects are described as proton delocalisation in the bond direction, a one-dimensional model seems adequate. The explicit electronic wave functions are calculated in this context. They allow for the electron density distribution along the bond to be obtained and the proton dynamics to be studied.

5 Water Ring Excitation Analysis: Time-Dependent Density Functional Theory with Linear Combination of Atomic Orbitals Method

Density-Functional theory (DFT) is a computational QC method used to simulate atoms and molecules, composed of nuclei and electrons. Using this theory, the properties of a many-electron system can be determined based on the spatially dependent electron density, from which it can be derived, in theory, the information about the system. In practice, however, the dependence on the electron density of the system's properties has to be, in general, approximated, with the development of various functionals an important aspect of the method. Its computational advantage to other *ab-initio* methods has made it popular and widely used. TDDFT is an extension to time-dependent properties of the system, based in this case on the time-dependent electron density. Instead of the wave function, DFT and TDDFT use the electron density as the central quantum mechanical variable of the system.

In these simulations, the nuclei are considered classical objects and assumed to be fixed, and the electron density distribution calculated in the electromagnetic potential created by the positively charged nuclei (Born-Oppenheimer approximation). The difference in mass between nuclei and electrons allows this separation of time scales, with electrons considered to be fast and nuclei slow. The electron density distribution creates, then, a potential in which the motion of the nuclei would take place. [6]

In the case of TDDFT, the nuclei are also considered to be fixed, but it allows for the study of the effects on the system of time-dependent external potentials, through the use of the time-dependent electron density. CDs theory predicts that water, over a critical density, undergoes synchronized dipolar dynamics, with the emergence of a macroscopic electromagnetic field in phase with these dipolar dynamics. To contrast this prediction with observation, the following scheme is proposed. An external electromagnetic field is applied to the system, and the effect on the electron density, within linear response, studied. In linear response, the electron density is expanded in powers of the externally applied field, only keeping the linear term, and higher-order effects neglected. The details of the method are presented in the following sections.

Given the cylindrical symmetry of the system, it is argued that the electromagnetic potential described in CDs theory, in the case of water confined in the nanotube, would be along the nanotube axis, with the component perpendicular to the axis balancing and therefore zero. The external field is, therefore, applied to the system along the axis and assumed to be constant in space. The time dependency of the field is approximated by a δ-function E, with $E(t = 0) = E_{max}$ and $E(t > 0) = 0$. The effects of this field on the electron density distribution is presented in Results, as an "electron and hole" diagram, with "electron" representing negative induced density, and "holes" corresponding to positive electron density. Because within linear response, the response of the system is proportional to the applied field magnitude, and the

[6] This procedure, with the calculation of the electron density in 3D space, for a given nuclear configuration, followed by the classical evolution, using Newton's equation $m\ddot{x} = F$, is the basis of Molecular Dynamics (MD). This Chapter, however, will stop at the calculation of the electrostatic potential, in particular, the potential experienced by the protons at the H-bond.

sign is conserved with an identical distribution of electron and holes for any applied field strength, E_{max}. However, the field needs to be small for non-linear terms to be negligible, and the magnitude of the electron density redistribution proportional to the field.

The electron density redistribution induces a change in the potential energy surface for the nuclei, in particular, for the protons involved in Hydrogen-bonding. The ground state and induced potentials are calculated and presented in Results, to compare with Reiter observations. A top-down simulation approach is used, where the "emerged" field is imposed on the water system, and the effect of such a macroscopic field on the electron density obtained through TDDFT. It shows a possible mechanism for the softening of the potential observed and to date unexplained.

The time-dependent behaviour of the water system is studied in Chapter 7, where the abstract time-evolution of the system calculated in Chapter 4 is combined with the specific, 3D microscopic representation presented here, in a multi-scale treatment.

5.1 Elements of Theory

5.1.1 Time-dependent Density Functional Theory

The Kohn?Sham (KS) equation is the one-electron Schrdinger equation of a fictitious system (the "KS system") of non-interacting particles (typically electrons) that generate the same density as the system of interacting particles. Having a non-interacting particles system allows for easier calculations, and the KS wavefunction is a single Slater determinant constructed from a set of orbitals that are the lowest-energy solutions to the KS equation. The time-dependent version of the KS equations is

$$\left(-i\partial_t - \frac{1}{2}\nabla^2 + v_{KS}[n(\mathbf{r},t)](\mathbf{r},t)\right)\Psi_i(\mathbf{r},t) = 0 \tag{21}$$

where Ψ_i are the electronic orbitals, v_{KS} is the KS potential and $n(\mathbf{r},t)$ is the time-dependent density given by

$$n(\mathbf{r},t) = \sum_i f_i |\Psi_i(\mathbf{r},t)|^2$$

with f_i the occupation numbers of the orbitals. The electron density in space, allows, in theory, to calculate the same quantities as from the wave function. The KS equation in the time-independent case is identical, only removing any time t dependence in the equation.

In general, the exchange-correlation part of the KS potential, v_{xc}, depends on all previous densities. In the widely used adiabatic approximation, the potential depends only on the instantaneous density.

5.1.2 Linear Response of the Density Matrix in the Real-Time Propagation Method

The time-dependent KS equation (equation 21) can be rewritten as

$$i\frac{\partial}{\partial t}\Psi_n(\mathbf{r},t) = H_{KS}(t)\Psi_n(\mathbf{r},t)$$

where $H_{KS}(t)$ is the time-dependent Kohn-Sham Hamiltonian and $\Psi_n(\mathbf{r},t)$ is a Kohn-Sham wave function.

The density matrix operator is defined as

$$\rho(t) = \sum_n |\Psi_n(t)\rangle\, f_n\, \langle\Psi_n(t)|$$

with f_n are the occupation factor of the n-th state.

Expressing the density matrix in the Kohn-Sham basis, spanned by the ground state KS orbitals $\Psi_n^{(0)}(\mathbf{r})$, which satisfy the KS equation

$$H_{KS}^{(0)}\Psi_n^{(0)}(\mathbf{r}) = \epsilon_n\Psi_n^{(0)}(\mathbf{r})$$

where $H_{KS}^{(0)}$ is the ground-state KS Hamiltonian and ϵ_n the KS eigenvalue of the n-th state. The density matrix can be written in this basis as

$$\begin{aligned}\rho_{nn'}(t) &= \left\langle \Psi_n^{(0)} \right| \rho(t) \left| \Psi_{n'}^{(0)} \right\rangle \\ &= \sum_m \left\langle \Psi_n^{(0)} \middle| \Psi_m(t) \right\rangle f_m \left\langle \Psi_m(t) \middle| \Psi_{n'}^{(0)} \right\rangle\end{aligned}$$

In the real-time propagation method, it is usual to apply a δ-perturbation. It corresponds to the Hamiltonian

$$H_{KS}(t) = H_{KS}^{(0)} + zK_z\delta(t)$$

where the interaction with the external electromagnetic radiation is taken within the dipole approximation. The electric field is assumed to be aligned along the z direction, and the constant K_z is proportional to the external electric field strength, which is assumed to be small enough to induce only negligible non-linear effects.

It is sufficient to consider only $\rho_{ia}(t)$, where i represent occupied and a unoccupied KS states, that is, the electron-hole part. The linear response of the density matrix in the electron-hole space is

$$\delta\rho_{ia}^z(\omega) = \frac{1}{K_z}\int_0^\infty \left[\rho_{ia}^z(t) - \rho_{ia}(0^-)\right] e^{i\omega t}dt + O(K_z)$$

where $\rho_{ia}(0^-)$ is the initial density matrix before the δ-perturbation and the superscript z indicates the direction of the perturbation.

5.1.3 The Linear Combination of Atomic Orbitals Method

In the linear combination of atomic orbitals method (LCAO) the wave function $\Psi_n(\mathrm{r},t)$ is expanded in the localized basis functions $\phi_\mu(\mathbf{r})$ centered at atomic coordinates

$$\Psi_n(\mathrm{r},t) = \sum_\mu \phi_\mu(\mathbf{r})\, C_{\mu n}(t)$$

with expansion coefficients $C_{\mu n}(t)$. In the LCAO basis set, the density matrix reads (with implied summation over repeated indices)

$$\rho_{\mu\nu}(t) = \sum_n C_{\mu n}(t)\, f_n\, C^*_{\nu n}(t)$$

Equation (21) then can be expressed in the LCAO formalism as

$$\rho_{nn'}(t) = C^{(0)*}_{\mu n}(t)\, S_{\mu\mu'}\, \rho_{\mu'\nu'}(t)\, S_{\nu\nu'}\, C^{(0)}_{\nu n'}(t)$$

where $S_{\mu\mu'} = \int \phi^*_\mu(\mathbf{r})\phi_{\mu'}(\mathbf{r})d\mathbf{r}$ is the overlap integral of the basis functions.

5.1.4 Photoabsorption Kohn-Sham Decomposition

The dynamical polarizability is given by

$$\alpha_{xz}(\omega) = 2\sum_{ia}^{eh} \mu^{x*}_{ia}\delta\rho^z_{ia}(\omega)$$

and the photoabsorption is described by the dipole strength function

$$S_z(\omega) = \frac{2\omega}{\pi} Im[\alpha_{zx}(\omega)]$$

which is normalized to integrate to the number of electrons in the system N_e, that is,

$$\int_0^\infty S_z(\omega)d\omega = N_e$$

It is similar to the sum rule $\sum_I f^x_I = N_e$, where

$$f^x_i = 2\left|\sum_{ia} \mu^{z*}_{ia}\sqrt{f_{ia}\omega_{ia}F_{i,ia}}\right|^2$$

is the oscillator strength of the discrete excitation I. The KS decomposition of the absorption spectrum can then be defined as

$$S^z_{ia}(\omega) = \frac{4\omega}{\pi} Im[\mu^{z*}_{ia}\delta^z_{ia}(\omega)]$$

5.2 Simulation Scheme

Using GPAW Python Library [93, 42], the simulation is based on the projector-augmented wave (PAW) method and the atomic simulation environment (ASE) [74]. The PAW approach addresses issues related to having rapid oscillations of the valence wave functions near the ion cores, due to the requirement that they are orthogonal to core states, by transforming these rapidly oscillating wave functions into smooth wave functions which are more computationally convenient.

The water system is defined through the atoms' positions in 3D space (Fig. 19). Time-propagation TDDFT in LCAO mode is used in GPAW [107]. A δ-pulse is applied to the system to calculate its photoabsorption spectrum, presented in Section 5.3.1.

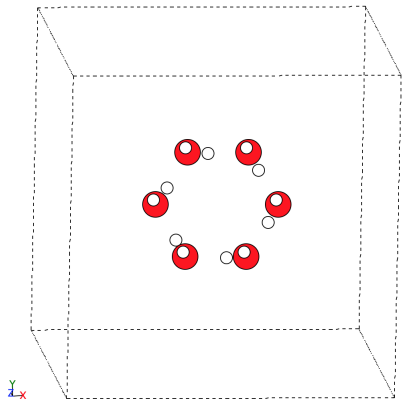

Figure 19: Water ring system, cell and axes in GPAW.

Once the photoabsorption spectrum is calculated, the main peaks are further analyzed, to obtain the response of the system's electron density distribution. Induced density plots are presented in Section 5.3.2.

5.3 Results and Discussion

5.3.1 Photoabsorption Spectrum

When an electromagnetic field is applied to the water system, it absorbs energy from the radiating field. The intensity of the absorption as a function of frequency is the absorption or photoabsorption spectrum. The absorption spectrum of a water ring is presented in Figure 21. The water ring system is represented in Figure 20.

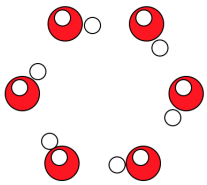

Figure 20: Water ring system.

5.3.2 Induced Densities

The induced density, that is, the density redistribution for the ground state density, due to the effects of the application of the external field, are presented in Figure 23, for frequencies corresponding to 13.85 eV, 15.80 eV and 16.75 eV, the main peaks in the lower energy region of the absorption spectrum. The ground state density is presented in Figure 22.

The case of 13.85 eV, which is close to the 12.06 eV estimated CDs frequency, is analyzed more in detail. Figure 24 shows the induced density values at several planes parallel to the ring plane (plane OXY in GPAW, Fig. 19), for distances to the reference values $z_0 = 7.14$ Å, corresponding to the plane in which the Oxygens

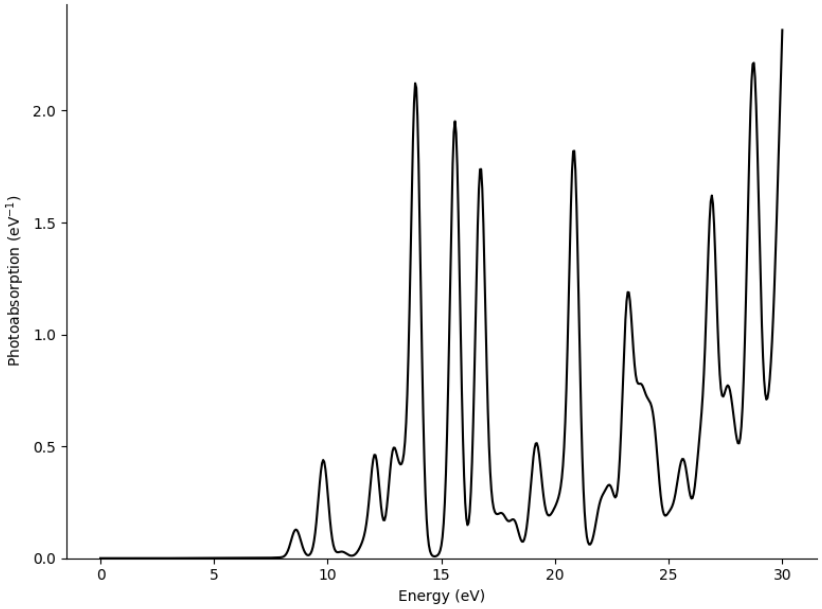

Figure 21: Water ring photoabsorption spectrum.

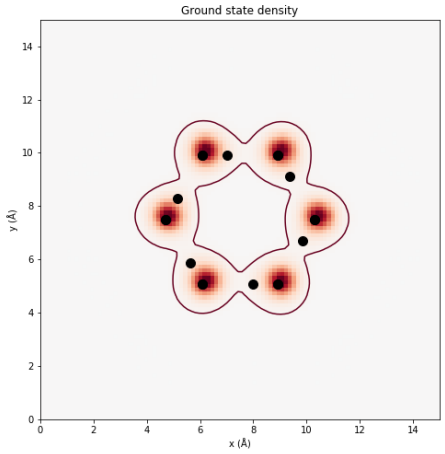

Figure 22: Ground state density for the ring.

in the ring are situated. As it would be expected, the density distribution respects the symmetry with respect to the central ring axis, in the z direction.

Also, the induced electron density for a plane perpendicular to the ring plane is presented in Figure 25, where it can be observed that the electric field induces a mainly positive part for values $z < z_0$ and mainly negative for $z > z_0$. There is a diminution of electron density around the proton, which would contribute to a softening of the potential over the proton, as observed by Reiter. These induced changes in the electron density could account for some of the observed features of nanoconfined water. Here, the proton is considered a classical entity, however, non-adiabatic effects could be important, as for the proton the mass difference is not as high. These non-adiabatic effects could magnify the impact, over the H-bond area,

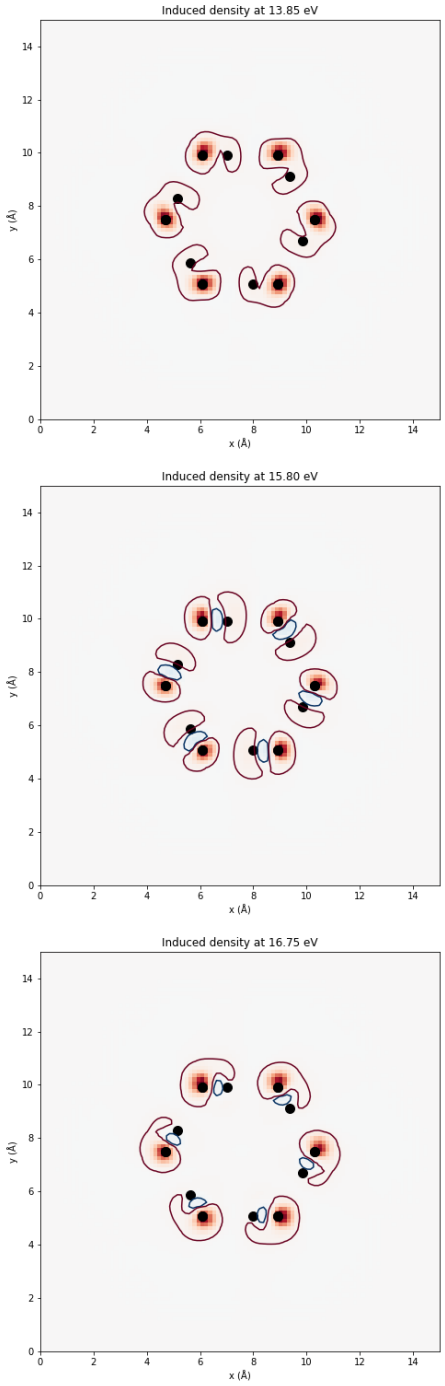

Figure 23: Induced density for the water ring. The red areas are areas of positive induced density values (hole) and the blue areas are negative induced density (electron).

of having electronic excitations as predicted by CDs theory. The study of the proton as a quantum system is presented in Chapter 6.

I hypothesize that the electronic oscillations that are expressed in the ED with

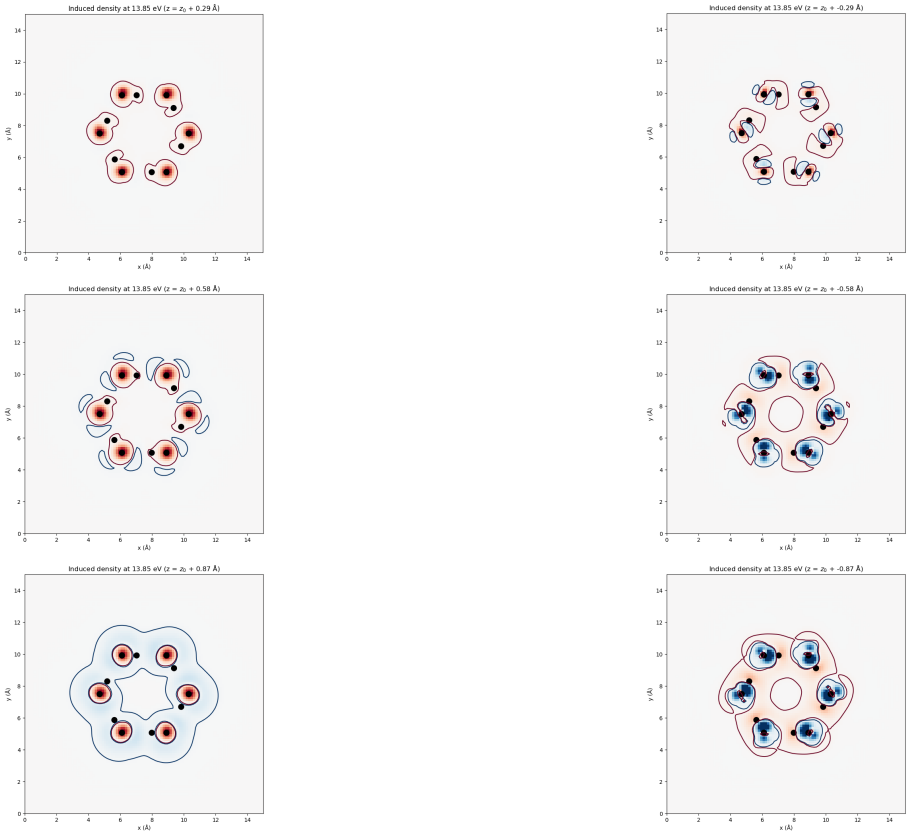

Figure 24: Induced density for the water ring for planes parallel to the ring plane.

the ground and excited states could involve some excited configuration such as these. The predicted CDs oscillations, and the emergent property of the system which is the electromagnetic field, translate into changes in the electron density and therefore of the potential over the central H-bond proton. The time-averaged potential over the fast electronic excitation and deexcitations would involve a softer potential. The periodic variation of the potential over the proton, which is identical, both in space and time, for each of the elements (eg. sides) of the ring due to periodicity and as observed in the plots, can then lead to the hypothesized proton synchronization, to explain Reiter's observations.

For comparison, induced density plots of water rings are presented (Figs. 27), for a perturbation in the x direction, contained in the plane of the ring, and not perpendicular as in the previous case. This situation could correspond to the interaction of water rings with the emergent macroscopic fields in bulk water, as it has been reported that there is a predominance of the ring, as well as the chain structures [48]. The spectrum for x-perturbation is presented in Figure 26.

5.3.3 Electrostatic Potential in the H-bond Region

The electron density redistribution in space, due to the applied "external" electromagnetic field, would then imply a variation of the electrostatic potential for that at the ground state. It is hypothesized that the softening of the proton potential

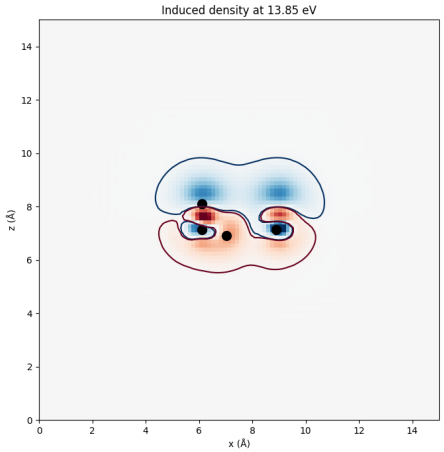

Figure 25: Induced density for a plane perpendicular to the ring plane and that contains the uppermost water dimer (parallel to plane Oxz).

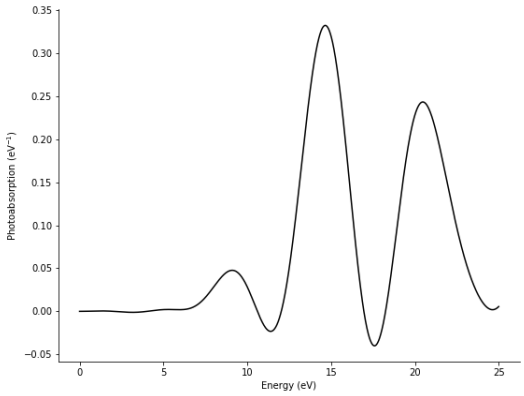

Figure 26: Photoabsorption spectrum for an electric perturbation in the x direction.

presented by Reiter (Section 1.1.5) for water in the nanotube could be an indirect observation of the coherent dynamics predicted by CDs theory. The variation on the electrostatic potential is presented here, in particular, in the proton area, due to the applied electromagnetic field. The following figures show the ground state (Fig. 28) and induced (Fig. 29) electrostatic potentials in the H-bond area.

The induced field is proportional to the strength of the applied external field, as we probing the water system within linear response. For a kick strength of 0.1 Hartree/Bohr or 5.14 eV/Å, the induced electrostatic potential is 5-15 eV around the H-bond proton area. A softening of the potential of 30% is obtained. The lowest dimer is the one that has been studied and for which the variation on the potential in the H-bond area has been represented. Because of the symmetry of the water system, the induced potential is the same for the rest of the dimers.

5.4 Conclusions

The softening of the potential observed by Reiter could be justified by the electron density redistribution and corresponding induced electrostatic potential caused by

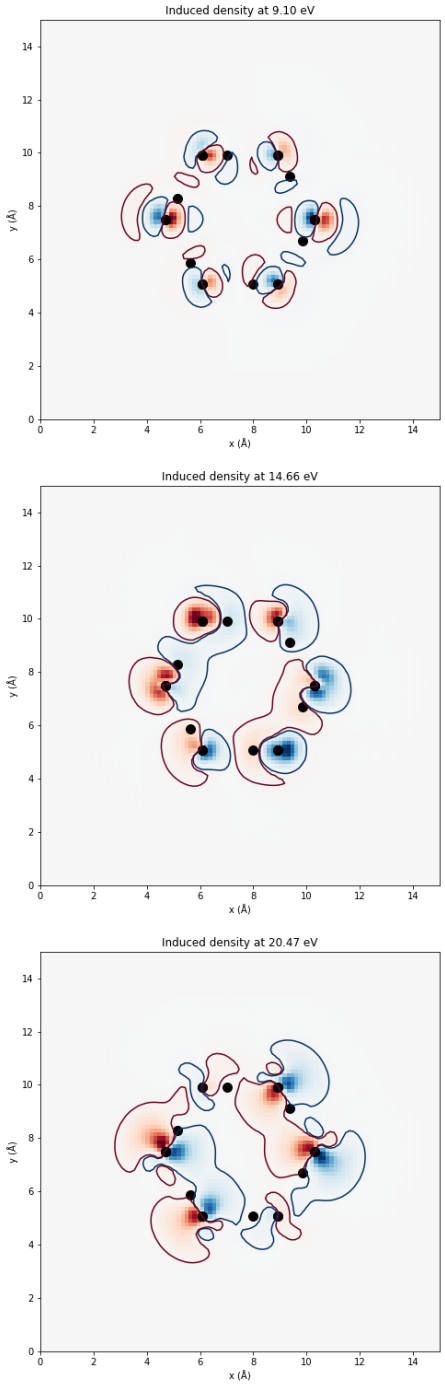

Figure 27: Induced density plots for an excitation along x for the first three resonant frequencies.

the emergent macroscopic electromagnetic potential predicted by CDs theory. In this Chapter, this possibility has been analyzed using linear response TDDFT, imposing an external perturbation to the water system, that would correspond to the effect of the emergent electromagnetic potential. In linear response, the softening of the

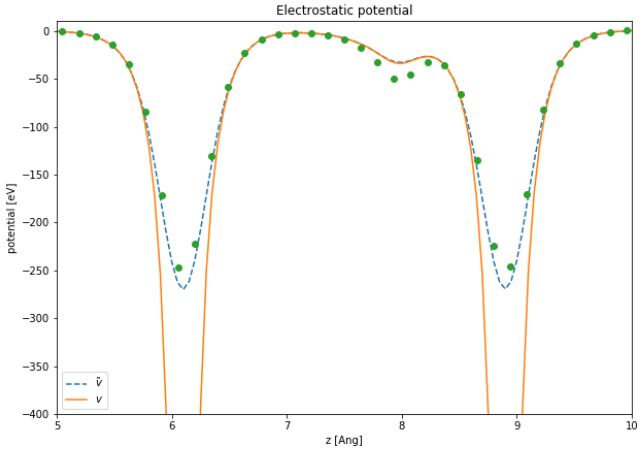

Figure 28: Ground state electrostatic potential at the H-bond area for the uppermost water dimer in the ring.

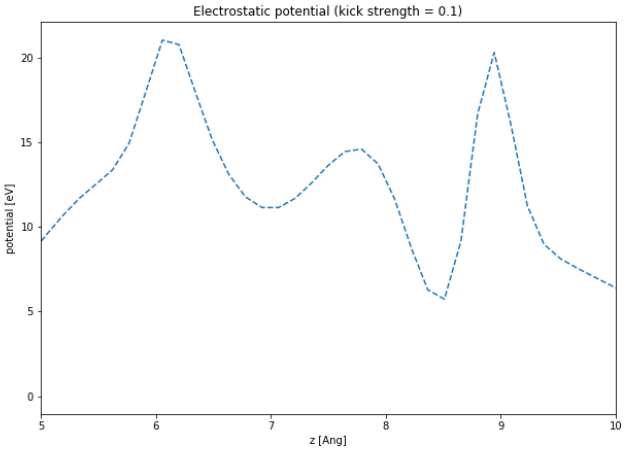

Figure 29: Induced electrostatic potential at the H-bond area for the uppermost water dimer in the ring for a kick of 5.14 eV/Å at 13.85 eV.

potential is proportional to the applied external field. For a kick strength of 0.1 Hartree/Bohr or 5.14 eV/Å, a softening of the potential of 30% is obtained, assuming fixed atom positions. An equivalent setting, for moving atoms in 3D, is presented in Section 7.6. Other effects beyond linear response are treated within the SAE approximation in Chapter 6.

6 Single-Active Electron Model of the H-bonded Dimer

In this Chapter, the Shin and Metiu Model [54] is used and applied to the case of an H-bonded dimer. The SAE approximation is used, in which all but one electron are frozen around the nuclei. Additionally, the motion of the active electron is restricted to one dimension. Furthermore, we treat only one nuclear degree of freedom.

A fixed distance between the Oxygen atoms of the two molecules is considered. The nuclei and all the electrons but one are included in a pseudo-potential. The free (active) electron –in the model, one of the electrons of the lone pair of one of the molecules– is considered to move only in the direction of the bond, considered the axis between both Oxygens. The nuclear degree of freedom considered is the distance between the acceptor's Oxygen and Hydrogen also along this axis. Figure 30 shows the location of the dimer in the coordinate system.

6.1 Elements of Theory

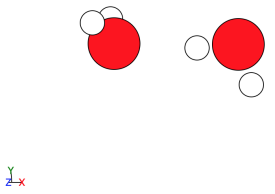

Figure 30: Dimer and Axes

6.1.1 Born-Oppeinheimer Approximation for a Single Active Electron

The electronic Hamiltonian of QC [122] is

$$H_{elec} = K_e + U_{e-ion} + U_{e-e}$$

and the electronic Shrdinger Equation in the BOA is

$$H_{elec}\,\phi_{elec} = E_{elec}\,\phi_{elec}$$

The variable dependence is

$$E_{elec} = E_{elec}(\{\mathbf{r}_i\}, \{\mathbf{R}_A\})$$

and the total energy is

$$E_{total} = E_{elec} + U_{ion-ion}$$

Separating the active electron from the rest of the electrons

$$H_{elec} = \underbrace{K_e + U_{e-ion} + U_{e-e'}}_{H_e} + \underbrace{K_{e'} + U_{e'-ion} + U_{e'-e'}}_{H_{e'}}$$

In the SAE approximation, the Hamiltonian part H'_e is constant. The electronic problem can be written as

$$(H_e + H'_e)\,\phi = (E_e + H'_e)\,\phi$$

and write

$$H_e\,\phi = E_e\,\phi$$

Then E can be obtained by adding H'_e, $E = E_e + H'_e$. This will be used to parametrise the SAE model, section 6.2.2. Finally, the following approximation is made

$$U_{e-ion} + U_{e-e'} \approx U_{e-\tilde{Z}}$$

where $\tilde{Z}$ are the reduced charges in the TIP3P model. The following problem is solved

$$\left(K_e + U_{e-\tilde{Z}}\right)\,\phi = \tilde{E}_e\,\phi$$

using the Discrete Value Representation (DVR) numerical method. The electronic energy is calculated using DFT and the value of H'_e, obtained by substracting $\tilde{E}_e$ to $[E_{elec}]_{DFT}$. Also, $\Delta E = E^0 - E^1$ is independent of H'_e.

6.1.2 Localised Charges Approximation Potentials

The potential function used for the model consists of two contributions. Firstly, V_{en} captures the interaction of the active electron with each nucleus and the electronic frozen core, so feels an effective charge of z and avoid the singularity at the nucleus. We use a soft Coulomb potential, with charges located in the atomic positions, and calculate interaction with the free electron. The parameters used are α=0.1 and q=3.0 for the soft Coulomb potential denominator $(x^q + \alpha^q)^q$. Secondly, V_{nn} is a Morse potential that captures the interaction between the nuclei and $2Z - 1$ frozen electrons, that is, it is the ground-state potential energy for the molecular ion.

$$V_{nn}(R) = D_e(1 - e^{A(R-R_0)})^2$$

where D_e is the dissociation energy, A is the width of the potential well, and R_0 is the equilibrium position. The potentials are represented in Figure 31. The location and value of the charges, based on the s22 water dimer and the TIP3P water model, respectively, are presented in Table 8. The active electron is subtracted from the leftmost oxygen and included in an additional row.

6.1.3 Photon Part

We add a photonic mode and its coupling to the molecule within the dipole approximation to the molecular Hamiltonian

$$H = H_m + H_{ph} + H_{int} \tag{22}$$

with the molecular part

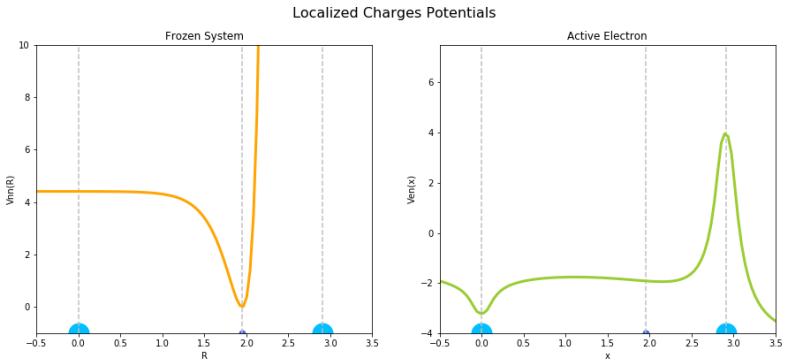

Figure 31: Single active electron model of the H-bonded dimer potentials.

Table 8: Charges and positions in the SAE model of the H-bonded dimer.

Atom	Position	Charge	Active Electron (initial)
O1	(0.00, 0.00, 0.00)	0.152	-1
H11	(-0.55, 0.96, -1.44)	0.424	0
H12	(-0.54, 0.96, 1.43)	0.424	0
O2	(5.50, 0.00, 0.00)	-0.848	0
H21	(6.09, -1.70, 0.00)	0.424	0
H22	(3.69, -0.15, 0.00)	0.424	0

$$H_{mol} = T_{nuc} + T_{el} + V_{el-el} + V_{el-nuc} + V_{nuc-nuc}$$

the photonic part

$$H_{ph} = \omega_a a^\dagger a$$

and the interaction part

$$H_{int} = g\mu(a^\dagger + a)$$

For a static treatment, analogous to the previous section, we can separate the nuclear part from the electronic and photonic part, and obtain the potential energy surface (PES) for the protons.

6.1.4 Dynamics

The Hamiltonian **??** can be written, explicitly, as [54]

$$H = H_m + \omega_c a^\dagger a + g\mu(a^\dagger + a) \tag{23}$$

where μ is the dipole operator of the molecule, $a^\dagger$ and a are the creation and annihilation operators for the bosonic electromagnetic field mode, ω_c is its frequency and g is the coupling strength constant. The dipole operator is taken to be $\mu = x$, with x the position operator of the electron. The photon energy ω_c is set to achieve

zero detuning, that is, $\omega_c = E_e(R_e) - E_g(R_e)$, the difference between the energies of the ground and excited state. R_e is the equilibrium position at which $E_g(R)$ has its minimum.

In order to deal with the continuous part, we use the Discrete Value Representation (DVR) method with a Fourier sine-basis [88] to solve the eigenvalue problem $H\Psi = E\Psi$, to obtain the system's eigenstates and eigenenergies.

The Hamiltonian **??** consists of a molecular part, that is based on continuous variables x and R, and the coupling to the photon, where the photon is represented by a Fock state. R is treated as a parameter and the Schrdinger Equation solved for x. To do so, a matrix representation for H_m is constructed write the total Hamiltonian **??**, specifying tensor products, as

$$H = H_m \otimes \mathbb{1} + \mathbb{1} \otimes \omega_c a^\dagger a + gX \otimes (a^\dagger + a)$$

where H_m is the Hamiltonian matrix for the molecular part, $a^\dagger$ and a are the creation and annihilation operators, respectively, for the photonic field, and X is the position operator matrix.

6.2 Simulation Scheme and Parameters

6.2.1 Simulation

The molecular Hamiltonian is first discretised using DVR with a Fourier sine-basis in Python (see Appendix **??**, for details).

PySCF Quantum Chemistry Library [120] is used for the Quantum Chemistry calculations, in particular Hartree-Fock and Density Functional Theory.

The dynamical part is simulated using QuTip Python Library [67, 66] for Open Quantum Systems, once the molecular Hamiltonian has been discretized, to obtain eigenstates and eigenenergies.

6.2.2 Parametrisation

The values of the parameters used in the simulation are summarized in Table 9.

Table 9: Model parameters values and source.

Parameter	Value	Source
k_e	10.369 eV/Å^2,	Fitted the DFT potential from GPAW with an harmonic function
D_e	5.15 eV	Source: `https://en.wikipedia.org/wiki/Bond-dissociation_energy`
A	30.31 $^{-1}$	$A = \sqrt{k_e/(2\,De)}$ where k_e is the force constant at the bottom of the well
R_0	2.91 - 1.95 = 0.96	Dimer in s22 dataset

6.3 Results and Discussion

6.3.1 Quantum Chemical Calculations

Simulations for the water dimer have been run using PySCF and the energy for a water molecule and a dimer, calculated. The results are presented in Table 10.

Table 10: Water molecule and water dimer energies.

Method	Energy H_2O	Energy $(H_2O)_2$
HF	-75.869	-151.980
DFT (LDA)	-75.049	-150.327

Also, Mulliken analysis is used to estimate partial atomic charges. Results are presented in Table 11, along with the chosen charge values in the model, based on the TIP3P water model charge values.

Table 11: Water molecule and water dimer energies.

Atom	HF	DFT (LDA)	TIP3P	Loc. ch.	SAE (initial)
O1	-0.629	-0.590	-0.834	0.152	-1
H11	0.332	0.326	0.417	0.424	0
H12	0.332	0.326	0.417	0.424	0
O2	-0.677	-0.659	idem	-0.848	0
H21	0.311	0.300	idem	0.424	0
H22	0.331	0.297	idem	0.424	0

6.3.2 Comparison with Mulliken Charges for the Dimer and Ion-Dimer

Mulliken atomic charges are calculated for comparison with the values of the charges used. In particular, the DFT method in PySCF is applied and the electronic configuration obtained. Then Mulliken atomic charges analysis is used to obtain the electron density contribution for each of the atoms. The Mulliken atomic charges are presented in Table 12 for the H-bonded dimer and in Table 13 for the dimer, once subtracted one electron to the system.

Table 12: Mulliken atomic charges for the water dimer.

Atom	Charge
0O	-0.65609
1H	0.33069
2H	0.33069
3O	-0.88218
4H	0.41656
5H	0.46034

Table 13: Mulliken atomic charges for the water dimer ion.

Atom	Charge
0O	0.28960
1H	0.53132
2H	0.53160
3O	-0.41045
4H	0.46092
5H	0.59701

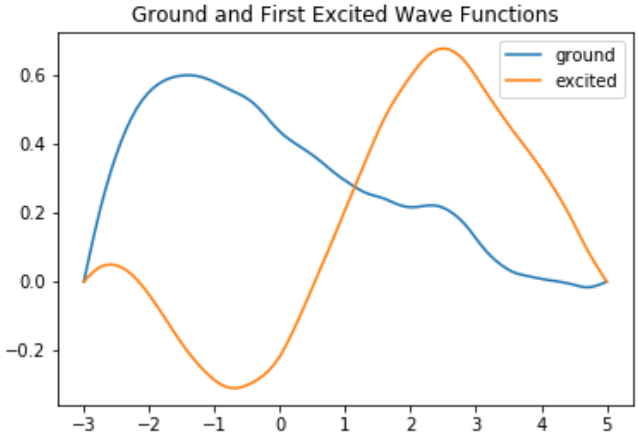

Figure 32: Ground and first excited wave function for the single active electron model of the water dimer.

6.3.3 Solution to the Shrdinger Equation and Induced Potential

Solving the system with DVR, the excitation energy of 6.34 eV is obtained. This corresponds to a coupling constant of $328\,ps^{-1}$. That is, an effective coupling constant for 5×10^4 molecules of approximately $15\,as^{-1}$.

The ground and first excited state wave functions are presented in Figure 32. Effect over the proton potential can be seen in Figure 33 for $g = 10^{10}$.

We observe the strengthening of the potential, with a more negative value, and larger absolute value, for the proton. The effect is opposite to softening of the potential observed by Reiter in the nanotube, and it could be that the 1D model is not enough to capture the effects of electron density redistribution in the water system. A 3D system able to capture a softening of the potential has been presented in Chapter 5. A dynamical simulation analogous to the one presented in this Chapter, based on the results of Chapter 5 is presented in Chapter 7.

6.3.4 Proton Decoherence and Classical Synchronization

As we have presented in Chapter 4, at the quantum level, due to the symmetry of the water system, the protons would be in a synchronized state. However, due to decoherence and the protons becoming classical objects [68], this condition of perfect synchronization could be violated. However, still, in that case, there would be an

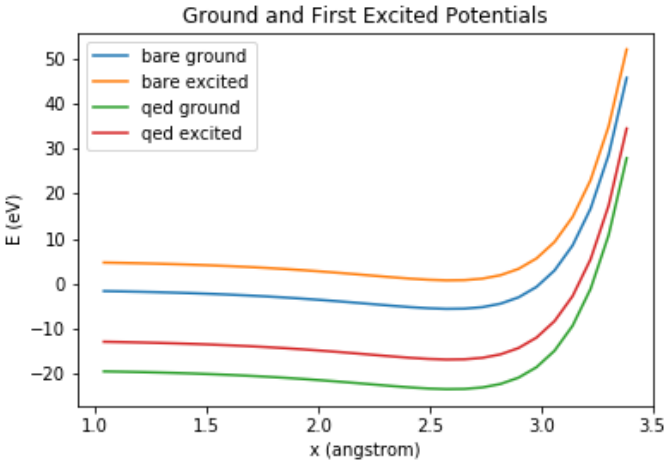

Figure 33: Potential in the single active electron model of the water dimer.

electronic oscillating potential acting over the protons that could lead to proton classical synchronization. This study was drafted as part of Article [21] and left to be completed. Note that in that case, the study is again a multi-scale one, as BOA is.

6.4 Conclusions

As it has been presented, the general tendency for different values of g is to make the potential over the proton more negative, so opposite of the observed behavior by Reiter of the softening of the potential in the nanotube. The reason for it to not be present in this model could be that it is only considering 1D, the axis along the bond. In Chapter 5 we see that electron density is redistribution due to an external macroscopic electromagnetic field, predicted in water CDs theory, perpendicular to the bond axis, translate in that case to the softening of the potential. The direction along the nanotube axis of the field is, as presented, justified by the cylindrical symmetry of the water system. The model and method used in this Chapter can be extended to 3D and is left for future work. A different method has been used to explore the electron density redistribution and its effects over the proton in 3D in the mentioned Chapter 5.

Part IV
Multiple Scale

In this Part, a multi-scale approach is proposed, where the study of the mesoscopic dynamics at the dipole level (such as ED) is integrated with a lower scale microscopic representation.

In Chapter 7, an approach to combine ED results with a microscopic representation based on TDDFT is delineated, and the calculation of the KE and its variation explored. It is proposed a way to combine both methods into a single simulation framework, and the explicit formulation within QED-QC is suggested to be further developed. Some preliminary results are obtained. In the case of water in the nanotube, the constraint due to water molecular disposition would be promoting collective behavior and "force" a collective state. The oscillatory dynamics could then be observed as, for example, synchronized protons (Preprint [21]). In particular, a self-generated electromagnetic field, that would be along the nanotube axis due to symmetry, produces an electron density redistribution and a variation over the proton potential. Other effects, such as interaction with the nanotube phonons could also be influencing nanoconfined water behavior.

The origin of the allegedly "forming and breaking" of H-bonds in water is not well understood, and Preparata has suggested that CDs theory could help explain the origin of these [101]. An algorithm to extend TIP3P simulation is proposed in Appendix .1. Electron redistribution due to ED could impact the H-bond characteristics providing a temporal variation of H-bond strength, that superposed to the MD could be observed as such forming and breaking dynamics. Molecular Dynamics simulations have been conducted in some preliminary settings to study the implication of collective electronic effects in the movement of the molecules in space, although this aspect needs further study. The incorporation of ED into semi-empirical water models, as the TIP3P, may provide a route to integrate QED-QC into routinary water simulations.

7 QED-QC Model of Water Confined in the Nanotube

7.1 The Light-Matter System: a Water Ring

The coupled light-matter Hamiltonian of the water system can be written as

$$H = H_e + H_n + H_{en} + H_p + H_{ep} + H_{pn} + H_{pen} \tag{24}$$

where H_e, H_n, and H_p refer to the electronic, nuclear and photonic parts, respectively, and H_{en}, H_{ep}, H_{pn} and H_{pen} refer to the electron-nucleus, electron-photon, photon-nucleus and photon-electron-nucleus interaction parts, respectively.

It is customary to neglect the photon part in QC treatments, and only consider

$$H = H_e + H_n + H_{en}.$$

Furthermore, due to the mass difference between electrons and nuclei, further simplification is achieved applying the Born-Oppenheimer Approximation (BOA), where the nuclei are assumed to move very slow in comparison with the electron dynamics. In this article, this assumption will be made. However, the protons will be assumed to move in polaritonic potential energy surfaces (PES), that is, combined electron-photon PES for the nuclei, where the effects of the interaction with the photons are included beyond merely Coulomb interaction. The photon energy is considered in the range of the energy of the electrons, and thus the interaction between the nuclei and the photons is neglected. The Hamiltonian (**??**) then becomes

$$H = H_e + H_n + H_{en} + H_p + H_{ep} = H_m + H_p + H_{ep}$$

where H_m stands for molecular Hamiltonian. The molecular Hamiltonian part is modelled using an exciton representation [30, 84, 83], where each molecule is considered as a site or *hole* where an electron is bound. The single exciton approximation is used, and then the system Hilbert space is $\mathcal{H} = \mathbb{C}^N$, spanned by a basis $\mathcal{B} = |n\rangle_{n=1}^{N}$, where N is the total number of molecules and $|n\rangle$ denotes the state in which the n-th molecule is excited. The ground state of the system, with all molecules in the ground state, is represented as $|0\rangle$. The Hamiltonian is then

$$H_m = \sum_i E_i \left|i\right\rangle \left\langle i\right| + \sum_{i \neq j} J_{ij} \left|i\right\rangle \left\langle j\right| \tag{25}$$

where E_i is assumed to be equal for all molecules $E_i = E = E_e - E_g$ and J_{ij} is the intermolecular interaction matrix.

Because of the ring periodic geometry, the states of the ring are restricted to the fully symmetrized states

$$|l\rangle = \frac{1}{\sqrt{N}} = \sum_{\pi \in \mathcal{S}_n} |\pi(00\ldots011\ldots1)\rangle$$

with l the number of excitations and π a permutation in the symmetric group over N elements, $\mathcal{S}_n$. Furthermore, in this article the number of excitations is limited to $n \leq 1$, and thus

$$|\Phi_g\rangle := |l=0\rangle = |0\ldots0\rangle = |0\rangle$$
$$|\Phi_e\rangle := |l=1\rangle = \frac{1}{\sqrt{N}}\sum_{n=1}^{N}|n\rangle$$

where $|\Phi_g\rangle$ and $|\Phi_e\rangle$ denote the ring symmetrized ground ($l=0$) and excited states ($l=1$), respectively.

Expressed in terms of $|\Phi_g\rangle$ and $|\Phi_e\rangle$ the Hamiltonian (**??**) is

$$H_m = (E+J)\,|\Phi_e\rangle\,\langle\Phi_e|$$

with

$$J = \sum_{i\neq j}\frac{J_{ij}}{N}$$

(calculation in Supplementary Information).

Finally, the interaction between the photons and the electrons is modelled as

$$H_{pe}(=H_i) = g(\sigma^+ a + \sigma^- a^\dagger)$$

where $\sigma^+ = \sum_i \sigma_i^+$ and $\sigma^- = \sum_i \sigma_i^-$ are the collective creation and annihilation operators, respectively, for the ring.

On the other hand, we would like to have space-resolved information, so we link both treatments using a δ-pulse excitation in TDDFT, to obtain the excited state (linear response, neglect non-linearities), characterized by its electron density in space, which then corresponds to the excited state $|e\rangle$ in a master equation treatment:

$$|g\rangle + ph \rightarrow |e\rangle\ (Master\ Equation) \Leftrightarrow \delta - pulse\,excitation\,(TDDFT)$$

Then we have two "static" states in 3D and the time-evolution between them is obtained at an aggregated level of representation, using ME simulation. This way we avoid difficulties and limitation of TDDFT such as linearity, and we are able to deal with the non-linear complex dynamics in a computationally cheap way. The following diagram points out the relationship between the ground $|g\rangle$ and excited $|e\rangle$ states, in ED and the ground n_g and excited n_e densities within TDDFT.

$$\begin{array}{rcl} (Master Equation) & & (TDDFT) \\ |g\rangle & \Leftrightarrow & n_g(\mathbf{r}) \\ |e\rangle & \Leftrightarrow & n_e(\mathbf{r}) \end{array}$$

7.2 Electronic Dynamics

In Section 4.3.6, we obtained the equation of motion for the coefficients is

$$\ddot{C}_g(t) + \lambda^2\,(n+1)\,C_g(t) = 0$$

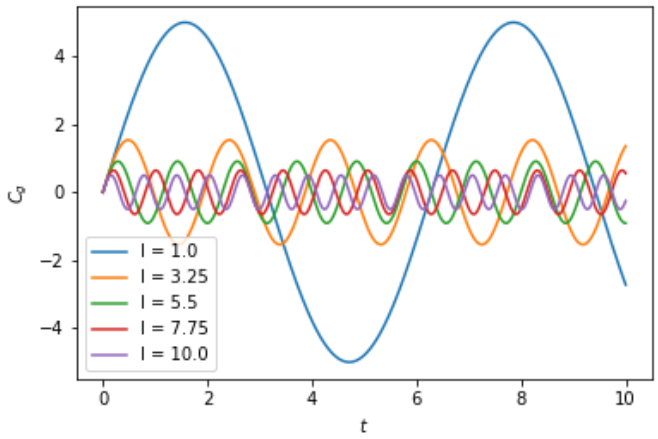

Figure 34: Ground state coefficient as a function of time, for various coupling strength λ values.

We can solved the differential equation. We had done so in Chapter 4.3.6 and obtained the expression $C_e(t) = cosg\sqrt{n+1}t$ where g is the coupling constant, n the number of photons present in the environment, and initially the system is in the excited state. Assuming initially $n = 0$, we have $C_e(t) = cos(gt)$.

Previously, we have estimation the value for the coupling constant. For the resonant frequency $\omega = 13.85eV$ eV, calculated using TDDFT, we obtain a coupling constant enhanced by the factor $\sqrt{NM}$ of $g \approx 33\,\mathrm{fs}^{-1}$ for the CD and of $g \approx 333\,\mathrm{as}^{-1}$ for the nanotube water. In the case of a 6-molecule ring ($N = 6$), the values is $g \approx 1.75\,\mathrm{fs}^{-1}$ and $g \approx 1.75\sqrt{M}\,\mathrm{fs}^{-1}$ for M rings. The value of the Rabi frequency is, then, $\Omega \approx 3.5\,\mathrm{fs}^{-1}$ for a ring, $\Omega \approx 67\,\mathrm{fs}^{-1}$ for a CD and $\Omega \approx 667\,\mathrm{fs}^{-1}$ for the nanotube.

7.3 Effects over the Proton

We calculate the ground state potential U_g over the proton using DFT, and the induced potential δU for the δ-kick using TDDFT. The excited-state potential is then

$$U_e = U_g + \delta U.$$

The induced force over the proton is

$$\delta F = \frac{d(\delta U)}{dx}.$$

Writing the potential time-dependency as

$$\begin{aligned} U(t) &= C_g^2(t)U_g + C_e^2(t)U_e = C_g^2(t)U_g + C_e^2(t)(U_g + \delta U) \\ &= (C_g^2(t) + C_e^2(t))U_g + C_e^2(t)\delta U = U_g + C_e^2(t)\delta U \end{aligned}$$

The proton would be experiencing then an oscillating force

$$f(t) = C_e^2(t)\frac{d(\delta U)}{dx} = cos^2(gt)(\delta F)$$

considering the 1D movement.

We use the expression $cos^2(x) = (1 + cos(2x))/2$ and write the force as

$$f(t) = \frac{\delta F}{2} + cos(2gt)\frac{\delta F}{2}$$

which will be useful in the next section.

7.4 Dynamics for a Fast Oscillating Force

We begin by introducing a general result for a particle subject to a fast oscillating field. Consider the motion of a particle subject to a time-independent field U and to a force

$$f(t) = f_1 cos(\omega t) + f_2 sin(\omega t)$$

varying in time with a high frequency $\omega \gg T$, where T is the order of magnitude of the period of the motion of the particle in the field U, and f_1 and f_2 are only functions of the coordinates. The value of the force f does not need to be small, only the oscillation to be fast.

Considering 1D motion, with U dependent on the space coordinate x only, the equation of motion for the particle is

$$m\ddot{x} = -\frac{dU}{dx} + f \tag{26}$$

From the nature of the field, we will expect the particle to follow a smooth path and at the same time execute small oscillations of frequency w about this path. Then, we represent the function $x(t)$ as

$$x(t) = X(t) + \xi(t),$$

where $\xi(t)$ are small oscillations and X(t) is the smooth motion, averaged over the small oscillations. The mean value of the function $\xi(t)$ over its period $2\pi/\omega$ is zero, and $X(t)$ changes only slightly in time, with respect to the time-scale of the oscillations.

It can be shown [73] that the motion for smooth trajectory $X(t)$ is determined by the differential equation

$$m\ddot{X} = -\frac{dU_{eff}}{dX}$$

with the effective potential energy defined as

$$U_{eff} = U + \frac{\overline{f^2}}{2m\omega^2} = U + \frac{f_1^2 + f_2^2}{4m\omega^2},$$

where $\overline{f^2}$ is the average over the oscillation period of f^2. The term added to U is the mean kinetic energy of the oscillatory motion $m\overline{\dot{\xi}^2}/2$.

We now apply this result to the case of the proton subjected to the fast oscillating field due to the electronic oscillations.

The trajectory is restricted to the H-bond axis, to study the effects of the force on the proton vibration motion.

We have calculated the time orders of magnitude of the electronic oscillations and we know the orders of magnitude of the O-H vibration frequency.

The equation of motion (22) is, then,

$$\begin{aligned} m\ddot{x} &= -\frac{dU}{dx} + \frac{\delta F}{2} + \frac{\delta F}{2} cos(2gt) \\ &= -\frac{d}{dx}\left(U + \frac{\delta U}{2}\right) + \frac{\delta F}{2} cos(2gt) \end{aligned}$$

and therefore the oscillating term is, in this case, $cos(2gt)\delta F/2$. Finally, the effective potential is equal to

$$U_{eff} = U + \frac{\delta U}{2} + \frac{(\delta F)^2}{32mg^2}$$

We adjust the kick strength to match the kinetic energy difference due to the oscillating force that compares with the 35 meV kinetic energy difference in confined water at 5K to ice at the same temperature, measured by Reiter [103].

7.5 Proton Kinetic Energy

A theoretical framework for proton kinetic energy is presented in [92]. The variation in the kinetic energy of the proton is the case of water confined in the nanotube, which can not be successfully explained within it. It is thus proposed to explore the modification that considering collective dynamics would imply. This has not been fully completed and is presented here to point out where the study of QED-QC may be providing improvements needed to explain water has this observed behaviour when confined.

7.6 Ehrenfest Dynamics and Synchronization

It is possible to apply Ehrenfest dynamics formalism to simulate the MD of water molecules in the presence of an external electromagnetic field. Some preliminary results of proton synchronization were obtained, which need to be further explored. It is suggested to explore this method to study the kinetic energy differences observed by Reiter in the nanotube. We have studied the emergence of synchronized electronic dynamics in Chapters 4 and 4.3.6. The effects of the emergent macroscopic electromagnetic field can then be studied using a top-down simulation setting. It corresponds to type (1), that is, ontological according to the classification presented in Section 1.2.3, as the emergence of the macroscopic field is not within the theoretical framework but the emergent property, the macroscopic field, is imposed as an external macroscopic field to the system.

7.7 Discussion and Conclusion

The predicted CDs oscillations, and the emergent property of the system, the electromagnetic field, translate into a softening of the potential over the central H-bond proton. That periodic variation of the potential over the proton, which is identical, both in space and time, for each of the elements (eg. sides) of the ring due to periodicity and as observed in the plots, can then lead to the suggested proton synchronization, to explain Reiter's observations.

Part V
Water and the Living State

The sensitivity of water dynamics to the environment characteristics supports the hypothesis that life depends on the electromagnetic environment in which it takes places, beyond the most central dependency of Sunlight for life as a whole. Also, it suggests the study of life within this electromagnetic context (Earth electromagnetic field and Earth's received radiations) with water as a mediator, *and the lack of study of water collective dynamics.*

8 Water-filled Halloysite Nanotube Model for the Origin of Life

8.1 A Model for the Origin of Life and Evolution

For a halloysite nanotube of length $10\,\mu m$ filled with water, there would be about 100 CDs of size $0.1\,\mu m$. For some given conditions, as predicted by CDs theory and shown in the ED model, the system will evolve to a synchronized state. Assuming that the water CD evolves to synchronized dynamics and that the specific dynamics depends on the environmental conditions (as seen in Chapter 4). For simplicity, we assume that the i-th CD will evolve to a synchronized state of a certain frequency pattern that for simplicity note ν_i, which will be synchronized to an extent s_i. Imagining a setting where the halloysite nanotube is surrounded by different molecules, they will then provide a particular spectral density, to add to the common halloysite density. The following diagram summarizes the situation

$z_1 =$	$z_2 =$
ABNOQ	AWTM
$CD_1(\nu_1)$	$CD_2(\nu_2)$

To add to this situation, there will be an external environmental state to the system, that is noted E. The system CD_i, whose dynamics will be strongly influenced by z_i will be mildly influenced by the state E. Each CD water dynamics will then stay more or less synchronized depending on how affected it is by the external state E. The following table shows an example with some synchronization values s_i for four molecular pattern and four environmental states.

	z_1	z_2	z_3	z_4
E_1	1	3	4	5
E_2	2	2	1	3
E_3	2	4	5	3
E_4	3	2	2	1

The synchronization values s_i can be thought of as an indicator of the robustness of the dynamics to the particular environment. The more chaotic dynamics will have a weaker overall electromagnetic field, as the different dipole contributions will tend to cancel, than in the case of the synchronized case. Therefore, the synchronized

dynamics will tend to override the desynchronized ones. The different CDs of the system will acquire the dynamics of the "strongest" or "fittest" subsystem. Thinking of the overall fitness, as the sum of the individual states, this situation will show an advantage to just keeping the individual states. In particular, $5{\cdot}4{+}3{\cdot}4{+}5{\cdot}4{+}3{\cdot}4 = 64$ versus $1 + 3 + 4 + 5 + 2 + \cdots = 41$.

Water dynamics and the molecular patterns together could start to have some reaction pathways, promoted by water and themselves inducing changes in water dynamics. The pathways of a certain section or CD would then be promoted whenever the dynamics of that CD is "running" the system, that is, when the dynamics of the rest of CDs have been overruled by its dynamics, as they are optimal for the environmental conditions.

Now let us imagine a process of mixing the water-filled clay and molecular patterns, for environmental conditions randomly changing in time. The mentioned process would then promote for the synchronized pieces to stay more intact than the desynchronized pieces, as they would be slightly more stable due to being undergoing common electromagnetic dynamics, and then more likely to survive as such. This way we would end up with clusters of molecules and water that have the highest optimal behavior for the most common environmental conditions. Not only are the different sections more likely to survive, but the system will be promoted to stay as a whole, as the different sections provide the optimal dynamics for certain environmental conditions. We can see here an early mechanism for the combination of molecular species into ordered systems that behave dynamically adapting their reactions to certain environmental conditions. It also provides a mechanism for the improvement of the response to the environment and the increase of the fitness of the system. There would be an increase of complexity in the system, in the coordination of the reaction and water dynamics, paralleled with improved function, that over time could lead to what we call a living system. The system is undergoing a type of computation where the internal and external conditions are the inputs and the system dynamics are the output. It can be seen as a precursor of behavior and decision making.

The system presented can be seen as a prototypical DNA system, with the activation of the different sections inducing the expression of certain genes, providing an orchestrated behavior with certain variation, the different section expressing themselves at different times, within some constant behavior, that is the dynamics for each of the sections including water. The combination of novelty and steadiness, and the capacity to adapt to the environment are characteristic of living systems. Also, there would be a pulse that would be animating the behavior, in this case, the basic water oscillations, that then become more complex as an expression of the singularity and richness of the system and conditions.

The electromagnetic efficient molecular and water dynamics of an area in the clay would over time promote similar systems to survive over time. Because these dynamics would themselves be part of the environmental conditions for adjacent systems, it could then be expected that copies of the initial system would be replicated over a long period. Although slow, this could provide a prototypical mechanism for replication. Some electromagnetic dynamics would promote some particular structures as may be the case in growth and development.

It has been postulated in CDs theory that water can store energy, as the noisy

environmental electromagnetic dynamics would be transformed into lower entropy synchronized dynamics and the stored energy then be released to activate certain pathways. Photosynthetic systems are an example, which uses electromagnetic energy, in particular, the radiated light from the sun, that is stored in the system and then released.

These are some important characteristics of life, that in this model are suggested to be met by considering water and molecular dynamics in halloysite nanotubes and adjacent molecular clusters. The model may be implemented extending ED simulation to include an external environment, and some evolution and selection algorithm, for example, simulated annealing type of optimization algorithms.

8.1.1 On Metabolism

The system is in an out-of-equilibrium state with respect to the varying electromagnetic environment. This means that it can act as a dissipative system (links from introduction coherence and life) and the energy gradient be exploited. The spontaneous evolution from desynchronized state to synchronized state in the nanotube water system, due to interaction with the electromagnetic vacuum (case paragraph single excited state empty environment ED), is a kind of "negentropy" tendency, where the desynchronized messy state becomes ordered, with the decrease in entropy. This characteristic in water could be a source of the resourced "negentropy" observed in living systems. The system could be pumped energy from the background electromagnetic fields such as the sun and the rest of environmental radiation that provides high entropy electromagnetic fields (as this was commented by Del Giudice, link to intro) and turn into low entropy states and store the energy.

So, in other words, life's commented "negentropy" is already present in water where there is the spontaneous synchronization that moves the system from high entropy to a low entropy state. The understanding of this phenomena in nanotube water from the point of view of quantum electrodynamics is only in its first stages of evolution.

The type of model we have presented shows then, that a proto-metabolism process was prior to the evolution of chemical complexity and the assortment of molecules and gain of structure. The basis of this energy source comes from the interaction with water with the varying electromagnetic and periodic environmental conditions, from the out-of-equilibrium state where the system shows a sort of inertia, and the tendency of the system to evolve towards equilibrium pumps the complex water dynamics that eventually are expressed as growing biochemical complexity and optimization of function, including optimization of the mechanism of energy production and storage. There is observed evidence of the interaction between ATP and ultraweak electromagnetic fields, that support this hypothesis that energy production was at some early stage linked to the electromagnetic variations of the environment. ATP is activated through the oscillating field, so in a sense, it is storing electromagnetic energy, with the difference in the energy magnitudes between ATP and the weak field to be addressed, maybe in terms of a better understanding of water quantum electro and thermodynamics. As we have introduced, water is then mediating between the electromagnetic environment and the reaction pathways dynamics, including metabolism.

8.1.2 On Complexity and Water

So water dynamics are highly chaotic (presumably) ordered in the CDs, but overall macroscopically, at the scale of many CDs, structureless (available dynamical potential). When there is the presence of other structured media around it, such as clay nanotubes and adsorbed molecules, this dynamical potential becomes actualized, in the sense that some of the possible dynamical regimes are realized. The complexity of water in the nanotube water system is already huge, with the observed sensitivity of water dynamics on the environmental conditions (Ch. 4). Water dynamics could be therefore promoting self-organization in matter, as the preferred dynamics due to the environmental (robust, due to molecular dispositions in the nanotube and other molecules) themselves promote certain organization to be expressed in the type of molecules that are preferably adhered to the surface. In other words, clay templates with molecules limit the dynamics of water providing structure. Water, on its side, promotes the structure to evolve and grow, as we have presented, maybe in terms of first energetically favourable dispositions that eventually, when a critical complexity is achieved, imply just a better overall functioning for the range of environmental conditions in which it is most likely situated.

8.1.3 About Halloysite

Halloysite is an aluminosilicate clay mineral. Its chemical formula, along with related clay minerals, is presented in Table 14. It is mainly composed of oxygen (55.78%), silicon (21.76%), aluminium (20.90%), and hydrogen (1.56%). Halloysite is formed by hydrothermal alteration of aluminosilicate minerals and can occur mixed with dickite, kaolinite, montmorillonite and other clay minerals.

Halloysite naturally occurs as nanotubes with a wall thickness of 10?15 atomic alumosilicate sheets, an outer diameter of 50?60 nm, an inner diameter of 12?15 nm, and a length of 0.5?10 μm. The outer surface is mainly composed of SiO2 and the inner surface of Al2O3. For this reason, these surfaces are oppositely charged. Two common forms are found. Hydrated, where it exhibits a 1 nm spacing between the layers, and dehydrated (meta-halloysite), where the spacing is 0.7 nm. Because of its layered structure, halloysite has a large specific surface area, up to 117 m^2/g.

Table 14: Clay minerals

Name of mineral and group	Structural formula
Kaolinite	$(OH)_4$ Al_4 Si_4 O_{10}
Halloysite	$(OH)_4$ Al_4 Si_4 O_{10} 4H2O
Montmorillonite	$(OH)_4$ Al_4 Si_4 O_{20} nH2O
Illite	$(OH)_4$ K_y $(Si_{g\ y}$ $Al_y)(Al_4$ Mg_6 Fe_4 $Fc_6)$ O_{20}

Table 15 shows the main reported absorption bands for Halloysite [102]. These frequencies form the spectrum which would act as a boson environment in ED.

Table 15: Band Component Analysis of the Region Below 1200 cm^{-1} of Halloysite (10 Å) and Comparison with Dehydrated Halloysite

Hydrated halloysite Raman [123]	Dehydrated halloysite Raman [51]	Ward?s halloysite No. 12 IR [20]	Slovak halloysites IR [81]	Assignment
?	?	1630 cm^{-1}	?	OH bend H2O
?	1100 cm^{-1}	1100 cm^{-1}	1090 cm^{-1}	Si?O stretch
?	?	1020 cm^{-1}	1036 cm^{-1}	?
?	?	?	1013 cm^{-1}	?
944 cm^{-1}	?	?	?	?
910 cm^{-1}	?	910 cm^{-1}	912?914 cm^{-1}	Al?O libration
826 cm^{-1}	844 cm^{-1}	?	?	Si?O?Al deformation
794 cm^{-1}	779 cm^{-1}	?	795 cm^{-1}	OH translation
748 cm^{-1}	728 cm^{-1}	740 cm^{-1}	750 cm^{-1}	OH translation
710 cm^{-1}	693 cm^{-1}	700 cm^{-1}	690 cm^{-1}	OH translation
548 cm^{-1}	540 cm^{-1}	535 cm^{-1}	540 cm^{-1}	Si?O bend
503 cm^{-1}	510 cm^{-1}	?	?	Si?O bend
465 cm^{-1}	?	465 cm^{-1}	471 cm^{-1}	Si?O bend
430 cm^{-1}	442 cm^{-1}	435 cm^{-1}	434 cm^{-1}	Al?O stretch
?	396 cm^{-1}	?	?	Si?O deformation
359 cm^{-1}	?	?	?	H-bonded H2O
332 cm^{-1}	?	?	?	H-bonded H2O
275 cm^{-1}	?	?	?	O?H?O antisym. stretch
245 cm^{-1}	?	?	?	O?H?O sym. stretch

Halloysite and kaolinite are part of the kaolin group. Both halloysite and kaolinite have predominantly tubular hollow inner structures in the submicron range. They are similar chemically, both consisting of two-layered aluminosilicates. Interlayer water in Halloysite is it's the main difference with kaolinite [41].

8.2 Discussion and conclusions

The emergence of life from no-life, of course, depends on how we define life. But I would go to say that the characteristics of the processes that conform to life could have been present before life as we have considered it. I would hypothesize that life has important characteristics that are scale-free, and that approaching life from this point of view could help understand the processes that animate life in a wider more profound way. Water would need to be considered a very active ingredient of life itself, influencing the dynamics across scales. In particular, water dynamics would be animating and being animated by the reaction pathways given a tapestry of frequencies that would be the fingerprint of the system. Living systems would not be isolated from the environment, but would be open quantum systems deeply engrained within the rest of the earth and beyond. We could say that experiencing ourselves as separated units, the sense of I, promotes granting a special privilege or

importance to a certain scale. However, when we observing ourselves, we can see that we are formed of cell that were once separate entities and that at some point started to function together. The process of ecosystem maturation has implied, indeed, the emergence of new levels of organisation, where the equilibrium of the ecosystem moved from a competitive state to a cooperative state [76]. Electromagnetism could provide for an integration of the different scales, expressed in us through the nervous system, but whose importance at closer scales needs to be explored.

The study of life has focused on matter, such as the molecules and reaction pathways, and the role of the electromagnetic fields for life has not been fully understood, probably also due to the difficulty of characterizing their structure, and the fact that life is usually studied in vitro, where the electromagnetic environment of the rest of the organism, local to the subsystem studied, is not included. Moreover, the influence of non-local environments is also possible through entanglement. Water could be providing a temporal structure, based on electromagnetism, to the enzymatic reactions in early life to be coordinated in time among themselves, allowing for a critical complexity and the emergence of life. Having a study focused on matter and not the electromagnetic environment and conditions seem natural while Chemistry itself stays based on QC methods, which deal with atoms, and bit by bit starts including light beyond the simplified models that are accessible to being tested and confirmed, for example, in cavity electrodynamics experiments, where quantum effects can be controlled and isolated. The study of matter and light, in a more vast and spatially resolved way, could promote a better understanding of life. The development in the field of QED-QC provides a framework in which to do so, to be able to apply simulation tools to complex biological settings. This could help alleviate the lack of environmental conditions that in vitro studies have. This cut from the environment, in contrast to considering life as an expression and as a continuation of the environmental dynamics at some physical level, could therefore be making the emergence of the property of life foreign to the theoretical framework used. It is thus proposed in this Thesis, the complex open quantum dynamics of water and its electromagnetic environment be considered to understand better what life is. From there, evolution could just be an extension to the original process of gaining function through complexity and creativity and maybe not that different to the origin of life. System's biology may provide the approach to understanding life's different scales of agency, and distributing action and direction across these scales may help understand better life.

A model of the origin would be granting the system with some computation capacity. Through the computation capacities and just by the laws of QP, the system can read itself, a sort of self-reference. It also, through this property, grant the system with unity, in contrast with an environment. It gives the system the possibility of improving the way the system responds to the environment and therefore to evolve. Evolution is understood as learning, in a wider sense, which is usually described concerning the nervous system and memory, to include the possibilities of matter, its space of states and configurations. This understanding would also stem from the suggested consideration of the electromagnetic field and structure as importantly influencing matter and biology. The placebo effect, or the proliferation of the use of alternative healing techniques such as Reiki, could be examples of how biology can be affected, in a top-down way, by the nervous system functioning and arguably through

electromagnetic fields. I would say, that it is just that we are studying the systems and agency in the system, and the emergence of organisation, at a level which needs to be expanded into including also electromagnetic fields, its relations and information. It would represent the exploration and inclusion of subtle effects, which are dealt with and explained in the domain of alternative medicine, into mainstream medicine. The study of water's interaction with light (including the electromagnetic vacuum), and the development of techniques to simulate the molecular interaction and water in a spatially resolved and heterogeneous setting, could provide a route for doing so.

9 Conclusions

A novel study of water as a complex system is proposed and advanced, that combines quantum electrodynamics and quantum chemistry approaches and simulation methods. Several water scales and representations have been explored, aiming at the development of a QED-QC multi-scale simulation framework potentially well-adapted to be extended to water simulation in a biological environment. Water confined in carbon nanotubes has been used as a paradigmatic example of water perplexing behavior, which in the case of the observations by Reiter et al., challenge the standard water electrostatic picture, then proposing water quantum oscillatory dynamics and synchronization as a plausible explanation of such behavior.

In particular, at the macroscopic scale, a rough picture of water in the nanotube has been drafted, based on the polaron classical picture by Landau, to conclude that the proton kinetic energy difference of 35 meV observed by Reiter could be accounted considering a polaron, either in the vicinity of each proton or in the space between 4 protons, on the sides of the hexagonal prism formed by the Oxygens in two stacked rings. The polaron size for each case is obtained.

At the mesoscopic scale, then, an Exciton Hamiltonian formulation of water for the simulation of electronic dynamics is proposed. It has been used to study quantum synchronization in the nanotube water system. The dynamics in the case of water rings have been compared with those of a disordered cluster. Water dynamics dependency on the environmental conditions has been studied, through the simulation of ED for a number of environment states. It has been shown that quantum synchronization depends on the environmental conditions, as well as on the molecular dispositions. The dependency on the environmental conditions is more acute in the case of MI and less so in the case of R Pearson correlation coefficient. Within the studied conditions, we have observed that water molecular dispositions affects dramatically MI, while does not influence (apart from very small variations) in the case of R Pearson correlation coefficient.

Also at the mesoscopic scale, and using the water exciton model, we have applied Bloch theorem to the water system and analytically deduced its dynamics, to show that the system's electrons are in a common collective state. These states are thus providing a common electromagnetic potential energy surface to the protons, what would allow for proton synchronization.

Furthermore, at the microscopic scale, the possibility of the softening of the potential observed by Reiter et al. provided by the electron density redistribution and corresponding induced electrostatic potential caused by the emergent macroscopic electromagnetic potential predicted by CDs theory has been analyzed using linear response TDDFT. An external perturbation to the water system, that would correspond to the effect of the emergent electromagnetic potential.

Using a different approach, still at the microscopic scale, the H-bonded water dimer is represented by the Shin and Metiu model in 1D and the solution obtained using Discrete Variable Representation. Electron density redistribution due to the electronic oscillations translate into a change of the potential over the central H-bond proton. That periodic variation of the potential over the proton, which is identical, both in space and time, for each of the sides of the water ring system due to periodicity, can then lead to the suggested proton synchronization, to explain

Reiter's observations.

Finally, some implications of water dynamics and synchronization have been explored in the context of the origin of life. We suggest that water dynamics in a Halloysite nanotube could have promoted self-organization in matter towards a critical complexity for the emergence of life. A model of a prototypical DNA system is proposed based on CDs, and a possible mechanism for evolution outlined. It is proposed that water could serve as a mediator between the environmental electromagnetic conditions and function in biological systems, as well as helping integration in the organism. This could help better understand mind-body techniques, an exploration that needs further consideration.

The methodology used has, of course, some advantages and disadvantages. The variety of approaches leads to a rich simulation eco-system that allows for cross-validation and fertilization and contributes towards a non-reductionist characterization of water behavior, with multiple co-existing representations. It is, however, in detriment in the detailed exploration and exploitation of each of the different proposals. It contributes, and motivates further development, an exciting QED-QC water study and simulation, and into the integration of water QED-QC effects into the complex heterogeneous environment of biological systems, with potentially important applications for biology and medicine.

10 Bibliography

References

[1] R. Alicki and K. Lendi. *Quantum dynamical semigroups and applications*, volume 717. Springer, 2007.

[2] A. Altland and B. D. Simons. *Condensed matter field theory*. Cambridge university press, 2010.

[3] C. Andreani, D. Colognesi, J. Mayers, G. F. Reiter, and R. Senesi. Measurement of momentum distribution of lightatoms and molecules in condensed matter systems using inelastic neutron scattering. *Advances in Physics*, 54(5):377–469, 2005.

[4] R. Arani, I. Bono, E. Del Giudice, and G. Preparata. QED Coherence and the Thermodynamics of Water. *International Journal of Modern Physics B*, 9:1813–1841, 1995.

[5] L. G. Augenstein et al. Physical processes in radiation biology. In *International Symposium on Physical Processes in Radiation Biology (1963: East Lansing, Mich.)*. Academic Press, 1964.

[6] P. Ball. Water—an enduring mystery. *Nature*, 452(7185):291–292, 2008.

[7] A. Barati Farimani and N. R. Aluru. Existence of multiple phases of water at nanotube interfaces. *The Journal of Physical Chemistry C*, 120(41):23763–23771, 2016.

[8] M. Barbieri. *The Organic Codes*. Cambridge University Press, 2004.

[9] R. O. Becker. the significance of bioeiectic potentials. *Bioelectrochetnistry and Bioenergetics*, 1:187–199, 1974.

[10] M. Bischof and E. Del Giudice. Communication and the emergence of collective behavior in living organisms: A quantum approach. *Molecular Biology International, Hindawi Publishing Corporation*, 2013.

[11] I. Bono, E. Del Giudice, L. Gamberale, and M. Henry. Emergence of the coherent structure of liquid water. *Water*, 4:510–532, 2012.

[12] M. Born and J. R. Oppenheimer. On the quantum theory of molecules. - *« »/. . ; ,* , 1927.

[13] G. Briganti, G. Rogati, A. Parmentier, M. Maccarini, and F. De Luca. Neutron scattering observation of quasi-free rotations of water confined in carbon nanotubes. *Scientific reports*, 7(1):1–10, 2017.

[14] L. Brizhik, E. Del Giudice, S. E. Jørgensen, N. Marchettini, and E. Tiezzie. The role of electromagnetic potentials in the evolutionary dynamics of ecosystems. *Ecological Modelling, Elsevier*, 220:1865–1869, 2009.

[15] M. Buiatti and M. Buiatti. The living state of matter. In *Rivista di biologia biology forum*, volume 94, pages 59–82. ANICIA SRL, 2001.

[16] M. Buiatti and M. Buiatti. Towards a statistical characterisation of the living state of matter. *Chaos, Solitons & Fractals*, 20(1):55–61, 2004.

[17] C. Burnham, T. Hayashi, R. Napoleon, T. Keyes, S. Mukamel, and G. Reiter. The proton momentum distribution in strongly h-bonded phases of water: A critical test of electrostatic models. *The Journal of chemical physics*, 135(14):144502, 2011.

[18] H. S. Burr. *The fields of life. Our links with the universe.* Ballantine Books, 1972.

[19] H. S. Burr and F. S. C. Northrop. The electro-dynamic theory of life. *The Quarterly Review of Biology*, 10(3):322–333, 1935.

[20] F. Calhoun, V. Carlisle, Z. Luna, et al. Properties and genesis of selected colombian andosols 1. *Soil Science Society of America Journal*, 36(3):480–485, 1972.

[21] F. Cano Marchal, R. Laureano, and E. Preoteasa. Proton synchronisation in a water cluster: geometry effects. *(Preprint)*, 2020.

[22] F. Cano Marchal, R. Laureano, and E. Preoteasa. Quantum synchronization of water exciton dynamics. *(Preprint)*, 2020.

[23] F. Cano Marchal, E. Preoteasa, and R. Laureano. Water under cylindrical confinement: a multi-scale model. *(Preprint)*, 2020.

[24] H. Carmichael, C. Gardiner, and a. . T. D.F. Walls". Higher order corrections to the dicke superradiant phase transition. *Physics Letters A*, 46(1):47 – 48, 1973.

[25] A. Chatterjee and S. Mukhopadhyay. *Polarons and Bipolarons: An Introduction.* Chapman & Hall Pure and Applied Mathematics. CRC Press, 2017.

[26] M. Combescot and W. Pogosov. Microscopic derivation of frenkel excitons in second quantization. *Physical Review B*, 77(8):085206, 2008.

[27] I. Cosic. Resonant recognition model of protein-protein and protein-dna interaction. *Bioinstrumentation and Biosensors, ed Wise D., Marcel Dekker, inc, New York*, pages 475–510, 1990.

[28] I. Cosic. Macromolecular bioactivity: is it resonant interaction between macromolecules?-theory and applications. *IEEE Transactions on Biomedical Engineering*, 41(12):1101–1114, 1994.

[29] I. Ćosić, E. Pirogova, V. Vojisavljević, and Q. Fang. Electromagnetic properties of biomolecules. *FME Transactions*, 34(2):71–80, 2006.

[30] A. Davydov. *Theory of Molecular Excitons.* Springer US, 1971.

[31] P. M. M. de Melo and A. Marini. Unified theory of quantized electrons, phonons, and photons out of equilibrium: A simplified ab initio approach based on the generalized baym-kadanoff ansatz. *Physical Review B*, 93(15):155102, 2016.

[32] A. De Ninno, A. Congiu Castellano, and E. Del Giudice. The supramolecular structure of liquid water and quantum coherent processes in biology. *Journal of Physics: Conference Series*, 442, 2013.

[33] A. De Ninno, E. Del Giudice, L. Gamberale, and A. Congiu Castellano. The structure of liquid water emerging from the vibrational spectroscopy: Interpretation with qed theory.

[34] E. Del Giudice and L. Giuliani. Coherence in water and the kt problem in living matter. *European Journal of Oncology*, 5, 2010.

[35] E. Del Giudice, G. Preparata, and G. Vitiello. Water as a free electric dipole laser. *Physical review letters*, 61(9):1085, 1988.

[36] E. Del Giudice, R. M. Pulsellic, and E. Tiezzi. Thermodynamics of irreversible processes and quantum field theory: An interplay for the understanding of ecosystem dynamics. *Ecological Modelling, Elsevier*, 220:1874–1879, 2009.

[37] E. Del Giudice and G. Vitiello. The Role of the electromagnetic field in the formation of domains in the process of symmetry breaking phase transitions. *Phys. Rev.*, A74:022105, 2006.

[38] E. Del Giudice, V. Voiekov, A. Tedeschi, and G. Vitiello. *The Origin and the Special Role of Coherent Water in Living System*, chapter 5, pages 95–111. Research Signpost, 2015.

[39] R. H. Dicke. Coherence in spontaneous radiation processes. *Phys. Rev.*, 93:99–110, Jan 1954.

[40] P. A. M. Dirac. The quantum theory of the emission and absorption of radiation. *Proceedings of the Royal Society of London. Series A, Containing Papers of a Mathematical and Physical Character*, 114(767):243–265, 1927.

[41] J. Du, G. Morris, R. A. Pushkarova, and R. St. C. Smart. Effect of surface structure of kaolinite on aggregation, settling rate, and bed density. *Langmuir*, 26(16):13227–13235, 2010.

[42] J. e. Enkovaara, C. Rostgaard, J. J. Mortensen, J. Chen, M. Dułak, L. Ferrighi, J. Gavnholt, C. Glinsvad, V. Haikola, H. Hansen, et al. Electronic structure calculations with gpaw: a real-space implementation of the projector augmented-wave method. *Journal of Physics: Condensed Matter*, 22(25):253202, 2010.

[43] F. H. Faisal. *Theory of multiphoton processes*. Springer Science & Business Media, 2013.

[44] E. Fermi. Quantum theory of radiation. *Reviews of modern physics*, 4(1):87, 1932.

[45] J. Flick, H. Appel, M. Ruggenthaler, and A. Rubio. Cavity born–oppenheimer approximation for correlated electron–nuclear-photon systems. *Journal of Chemical Theory and Computation*, 13(4):1616–1625, 2017. PMID: 28277664.

[46] J. Flick, M. Ruggenthaler, H. Appel, and A. Rubio. Kohn–sham approach to quantum electrodynamical density-functional theory: Exact time-dependent effective potentials in real space. *Proceedings of the National Academy of Sciences*, 112(50):15285–15290, 2015.

[47] J. Flick, M. Ruggenthaler, H. Appel, and A. Rubio. Atoms and molecules in cavities, from weak to strong coupling in quantum-electrodynamics (qed) chemistry. *Proceedings of the National Academy of Sciences*, 114(12):3026–3034, 2017.

[48] F. Franks. *Water a comprehensive treatise: volume 4: aqueous solutions of amphiphiles and macromolecules*. Springer Science & Business Media, 2013.

[49] H. Fröhlich. Long-range coherence and energy storage in biological systems. *International Journal of Quantum Chemistry*, 2(5):641–649, 1968.

[50] H. Fröhlich. Long range coherence and the action of enzymes. *Nature*, 1093, 228.

[51] R. Frost. The structure of the kaolinite minerals- a ft-raman study. *Clay Minerals*, 32(1):65–77, 1997.

[52] H. J. Gabius. Biological information transfer beyond the genetic code: The sugar code. *Naturwissenschaften*, 87(3):108–121, 2000.

[53] H.-J. Gabius, S. Andre, J. Jimenez-Barbero, A. Romero, and D. Solis. From lectin structure to functional glycomics: principles of the sugar code. *Trends Biochem Sci*, 36(6):298–313, Jun 2011.

[54] J. Galego, F. J. Garcia-Vidal, and J. Feist. Cavity-induced modifications of molecular structure in the strong-coupling regime. *Phys. Rev. X*, 5:041022, Nov 2015.

[55] F. Galve, G. L. Giorgi, and R. Zambrini. Quantum correlations and synchronization measures. In *Lectures on General Quantum Correlations and their Applications*, pages 393–420. Springer, 2017.

[56] V. Garbuio, C. Andreani, S. Imberti, A. Pietropaolo, G. Reiter, R. Senesi, and M. Ricci. Proton quantum coherence observed in water confined in silica nanopores. *The Journal of chemical physics*, 127(15):154501, 2007.

[57] B. M. Garraway. The dicke model in quantum optics: Dicke model revisited. *Philosophical Transactions of the Royal Society A: Mathematical, Physical and Engineering Sciences*, 369(1939):1137–1155, 2011.

[58] C. Gerry, P. Knight, and P. L. Knight. *Introductory quantum optics*. Cambridge university press, 2005.

[59] E. D. Giudice and A. Tedeschi. Water and autocatalysis in living matter. *Electromagnetic Biology and Medicine*, 28(1):46–52, 2009.

[60] E. D. Giudice, A. Tedeschi, G. Vitiello, and V. Voeikov. Coherent structures in liquid water close to hydrophilic surfaces. *Journal of Physics: Conference Series*, 442(1):012028, 2013.

[61] E. D. Giudice and G. Vitiello. Quantum fluctuations, gauge freedom and mesoscopic/macroscopic stability. *Journal of Physics: Conference Series*, 87:012009, nov 2007.

[62] W. Heitler. The quantum theory of radiation, new york, 1954.

[63] M.-W. Ho. Towards a theory of the organism. *Integrative Physiological and Behavioral Science*, 32(4):343–363, 1997.

[64] J. D. Jackson. *Classical electrodynamics*. John Wiley & Sons, 2007.

[65] L. Jaeken and V. Vasilievich Matveev. Coherent behavior and the bound state of water and k+ imply another model of bioenergetics: Negative entropy instead of high-energy bonds. *The open biochemistry journal*, 6(1), 2012.

[66] J. R. Johansson, P. Nation, and F. Nori. Qutip: An open-source python framework for the dynamics of open quantum systems. *Computer Physics Communications*, 183(8):1760–1772, 2012.

[67] J. R. Johansson, P. D. Nation, and F. Nori. Qutip 2: A python framework for the dynamics of open quantum systems. *Computer Physics Communications*, 184(4):1234–1240, 2013.

[68] E. Joos, H. D. Zeh, C. Kiefer, D. J. Giulini, J. Kupsch, and I.-O. Stamatescu. *Decoherence and the appearance of a classical world in quantum theory*. Springer Science & Business Media, 2013.

[69] P. Kirton, M. M. Roses, J. Keeling, and E. G. Dalla Torre. Introduction to the dicke model: From equilibrium to nonequilibrium, and vice versa. *Advanced Quantum Technologies*, 2(1-2):1800043, 2019.

[70] K. Koga, G. Gao, H. Tanaka, and X. C. Zeng. Formation of ordered ice nanotubes inside carbon nanotubes. *Nature*, 412(6849):802–805, 2001.

[71] A. I. Kolesnikov, J.-M. Zanotti, C.-K. Loong, P. Thiyagarajan, A. P. Moravsky, R. O. Loutfy, and C. J. Burnham. Anomalously soft dynamics of water in a nanotube: a revelation of nanoscale confinement. *Physical review letters*, 93(3):035503, 2004.

[72] A. I. Kolesnikov, J.-M. Zanotti, C.-K. Loong, P. Thiyagarajan, A. P. Moravsky, R. O. Loutfy, and C. J. Burnham. Anomalously soft dynamics of water in a nanotube: A revelation of nanoscale confinement. *Phys. Rev. Lett.*, 93:035503, Jul 2004.

[73] L. Landau and E. Lifschitz. Mechanics: Vol. 1 of course of theoretical physics, the third edition in 1976, 1960.

[74] A. H. Larsen, J. J. Mortensen, J. Blomqvist, I. E. Castelli, R. Christensen, M. Dułak, J. Friis, M. N. Groves, B. Hammer, C. Hargus, et al. The atomic simulation environment—a python library for working with atoms. *Journal of Physics: Condensed Matter*, 29(27):273002, 2017.

[75] A. R. Liboff. Toward an electromagnetic paradigm for biology and medicine. *The Journal of Alternative and Complementary Medicine*, 10(1):41–47, 2016/12/07 2004.

[76] S. Liebes, E. Sahtouris, and B. Swimme. *A walk through time: From stardust to us: The evolution of life on earth.* John Wiley and Sons, 1998.

[77] J. Liu, X. He, J. Z. H. Zhang, and L.-W. Qi. Hydrogen-bond structure dynamics in bulk water: insights from ab initio simulations with coupled cluster theory. *Chem. Sci.*, 9:2065–2073, 2018.

[78] S. Lovesey. *Theory of neutron scattering from condensed matter, Volume II.* Clarendon Press, 1984.

[79] P. L. Luisi. *The emergence of life: from chemical origins to synthetic biology.* Cambridge University Press, 2006.

[80] E. J. Lund. Bioelectric fields and growth. *Soil Science*, 64(3):253, 1947.

[81] J. Madejova, I. Kraus, D. Tunega, and E. Samajova. Fourier transform infrared spectroscopic characterization of kaolin group minerals from the main slovak deposits. *Geologica Carpathica Clays*, 6(1):3–10, 1997.

[82] N. Marchettinia, E. Del Giudice, V. Voeikov, and E. Tiezzi. Water: A medium where dissipative structures are produced by a coherent dynamics. *Journal of Theoretical Biology, Elsevier*, 265(4):511, 2010.

[83] H. F. M. C. Martiniano, N. Galamba, and B. J. C. Cabral. Ab initio calculation of the electronic absorption spectrum of liquid water. *The Journal of Chemical Physics*, 140(16):164511, 2014.

[84] R. A. Mata, H. Stoll, and B. J. C. Cabral. A simple one-body approach to the calculation of the first electronic absorption band of water. *Journal of Chemical Theory and Computation*, 5(7):1829–1837, 2009. PMID: 26610007.

[85] J. C. Maxwell. *A dynamical theory of the electromagnetic field.* Wipf and Stock Publishers, 1996.

[86] V. May and O. Kühn. *Charge and energy transfer dynamics in molecular systems*, volume 2. Wiley Online Library, 2011.

[87] C. P. McKay. What is life—and how do we search for it in other worlds? *PLOS Biology*, 2(9), 09 2004.

[88] H.-D. Meyer. Numerical methods of quantum dynamics. discrete variable representation (dvr) integrators lecture notes. 2017.

[89] G. Michal and D. Schomburg. *Biochemical pathways: an atlas of biochemistry and molecular biology*. John Wiley & Sons, 2012.

[90] F. Mikami, K. Matsuda, H. Kataura, and Y. Maniwa. Dielectric properties of water inside single-walled carbon nanotubes. *ACS nano*, 3(5):1279–1287, 2009.

[91] R. K. Mishra. *Molecular and biological physics of living systems*. Springer, 1990.

[92] R. Moreh and D. Nemirovsky. On the proton kinetic energy in h 2 o and in nanotube water. *The Journal of chemical physics*, 133(8):084506, 2010.

[93] J. J. Mortensen, L. B. Hansen, and K. W. Jacobsen. Real-space grid implementation of the projector augmented wave method. *Physical Review B*, 71(3):035109, 2005.

[94] P. V. Murphy, S. Andre, and H. J. Gabius. The third dimension of reading the sugar code by lectins: design of glycoclusters with cyclic scaffolds as tools with the aim to define correlations between spatial presentation and activity. *Molecules*, 18(4):4026–4053, Apr 2013.

[95] W. H. Noon, K. D. Ausman, R. E. Smalley, and J. Ma. Helical ice-sheets inside carbon nanotubes in the physiological condition. *Chemical Physics Letters*, 355(5-6):445–448, 2002.

[96] A. Paciaroni, L. Comez, M. Longo, F. Sebastiani, F. Bianchi, A. Orecchini, M. Zanatta, R. Verbeni, A. Bosak, F. Sacchetti, et al. Terahertz collective dynamics of dna as affected by hydration and counterions. *Journal of Molecular Liquids*, 318:113956, 2020.

[97] C. Pantalei, A. Pietropaolo, R. Senesi, S. Imberti, C. Andreani, J. Mayers, C. Burnham, and G. Reiter. Proton momentum distribution of liquid water from room temperature to the supercritical phase. *Phys. Rev. Lett.*, 100:177801, May 2008.

[98] C. Pellegrini, J. Flick, I. V. Tokatly, H. Appel, and A. Rubio. Optimized effective potential for quantum electrodynamical time-dependent density functional theory. *Physical review letters*, 115(9):093001, 2015.

[99] F.-A. Popp, J. Chang, A. Herzog, Z. Yan, and Y. Yan. Evidence of non-classical (squeezed) light in biological systems. *Physics letters A*, 293(1):98–102, 2002.

[100] E. A. Preoteasa and M. V. Apostol. Collective dynamics of water in the living cell and in bulk liquid. New physical models and biological inferences. *ArXiv e-prints*, Dec. 2008.

[101] G. Preparata. *QED Coherence in Matter*. World Scientific, Singapore-London-New Jersey, 1995.

[102] G. Ranjan and A. Rao. *Basic and applied soil mechanics*. New Age International, 2007.

[103] G. Reiter, C. Burnham, D. Homouz, P. Platzman, J. Mayers, T. Abdul-Redah, A. Moravsky, J. Li, C.-K. Loong, and A. Kolesnikov. Anomalous behavior of proton zero point motion in water confined in carbon nanotubes. *Physical review letters*, 97(24):247801, 2006.

[104] G. F. Reiter, A. Deb, Y. Sakurai, M. Itou, and A. I. Kolesnikov. Quantum coherence and temperature dependence of the anomalous state of nanoconfined water in carbon nanotubes. *The journal of physical chemistry letters*, 7(22):4433–4437, 2016.

[105] G. F. Reiter, A. Deb, Y. Sakurai, M. Itou, V. G. Krishnan, and S. J. Paddison. Anomalous ground state of the electrons in nanoconfined water. *Phys. Rev. Lett.*, 111:036803, Jul 2013.

[106] G. F. Reiter, A. I. Kolesnikov, S. J. Paddison, P. M. Platzman, A. P. Moravsky, M. A. Adams, and J. Mayers. Evidence for an anomalous quantum state of protons in nanoconfined water. *Phys. Rev. B*, 85:045403, Jan 2012.

[107] T. P. Rossi, M. Kuisma, M. J. Puska, R. M. Nieminen, and P. Erhart. Kohn–sham decomposition in real-time time-dependent density-functional theory: an efficient tool for analyzing plasmonic excitations. *Journal of Chemical Theory and Computation*, 13(10):4779–4790, 2017.

[108] M. Ruggenthaler, J. Flick, C. Pellegrini, H. Appel, I. V. Tokatly, and A. Rubio. Quantum-electrodynamical density-functional theory: Bridging quantum optics and electronic-structure theory. *Physical Review A*, 90(1):012508, 2014.

[109] M. Ruggenthaler, F. Mackenroth, and D. Bauer. Time-dependent kohn-sham approach to quantum electrodynamics. *Physical Review A*, 84(4):042107, 2011.

[110] M. Ruggenthaler, N. Tancogne-Dejean, J. Flick, H. Appel, and A. Rubio. From a quantum-electrodynamical light–matter description to novel spectroscopies. *Nature Reviews Chemistry*, 2(3):1–16, 2018.

[111] C. Schäfer, M. Ruggenthaler, and A. Rubio. Ab initio nonrelativistic quantum electrodynamics: Bridging quantum chemistry and quantum optics from weak to strong coupling. *Phys. Rev. A*, 98:043801, Oct 2018.

[112] C. Schäfer, M. Ruggenthaler, and A. Rubio. Ab initio nonrelativistic quantum electrodynamics: Bridging quantum chemistry and quantum optics from weak to strong coupling. *Physical Review A*, 98(4):043801, 2018.

[113] E. Schödinger. *What is Life?* Cambridge University Press, 1944.

[114] M. O. Scully and M. S. Zubairy. Quantum optics, 1999.

[115] S. Sivasubramanian, A. Widom, and Y. Srivastava. Gauge invariant formulations of dicke–preparata super-radiant models. *Physica A: Statistical Mechanics and its Applications*, 301(1):241 – 254, 2001.

[116] D. Solís, N. Bovin, D. A.P., J. Jiménez-Barbero, A. Romero, R. Roy, K. J. Smetana, and H. J. Gabius. A guide into glycosciences: How chemistry, biochemistry and biology cooperate to crack the sugar code. *Biochimica et Biophysica Acta*, 1850(1):186–235, 2015.

[117] J. Spitzer, G. J. Pielak, and B. Poolman. Emergence of life: Physical chemistry changes the paradigm. *Biology Direct*, 10(1):33, 2015.

[118] H. Spohn. *Dynamics of charged particles and their radiation field*. Cambridge university press, 2004.

[119] B. D. Strahl and C. D. Allis. The language of covalent histone modifications. *Nature*, 403(6765):41–45, 2000.

[120] Q. Sun, T. C. Berkelbach, N. S. Blunt, G. H. Booth, S. Guo, Z. Li, J. Liu, J. D. McClain, E. R. Sayfutyarova, S. Sharma, et al. Pyscf: the python-based simulations of chemistry framework. *Wiley Interdisciplinary Reviews: Computational Molecular Science*, 8(1):e1340, 2018.

[121] L. Susskind and A. Friedman. *Quantum mechanics: the theoretical minimum*. Basic Books, 2014.

[122] A. Szabo and N. S. Ostlund. *Modern Quantum Chemistry: Introduction to Advanced Electronic Structure Theory*. Dover Publications, Inc., Mineola, first edition, 1996.

[123] J. Theo Kloprogge and R. L. Frost. Raman microprobe spectroscopy of hydrated halloysite from a neogene cryptokarst from southern belgium. *Journal of Raman spectroscopy*, 30(12):1079–1085, 1999.

[124] I. V. Tokatly. Time-dependent density functional theory for many-electron systems interacting with cavity photons. *Physical review letters*, 110(23):233001, 2013.

[125] J. Tuszyński, R. Paul, R. Chatterjee, and S. Sreenivasan. Relationship between fröhlich and davydov models of biological order. *Physical Review A*, 30(5):2666, 1984.

[126] G. Vitiello. Coherent states, fractals and brain waves. *New Mathematics and Natural Computation*, 05(01):245–264, 2009.

[127] G. Vitiello. Fractals, coherent states and self-similarity induced noncommutative geometry. *Physics Letters A*, 376(37):2527 – 2532, 2012.

[128] G. Vitiello. On the isomorphism between dissipative systems, fractal self-similarity and electrodynamics. toward an integrated vision of nature. *Systems*, 2(2):203, 2014.

[129] F. Westall and A. Brack. The importance of water for life. *Space Science Reviews*, 214(2):50, 2018.

[130] J. M. Zheng, W. C. Chin, E. Khijniak, E. J. Khijniak, and G. H. Pollack. Surfaces and interfacial water: evidence that hydrophilic surfaces have long-range impact. *Advances in Colloid and Interface Science*, (19-27), 23.

[131] J. M. Zheng and G. H. Pollack. Long range forces extending from polymer surfaces. *Physical Review E*, 68, 2003.

Appendices to Chapter 4

.1 Mutual Information Time Evolution in Exciton Dynamics

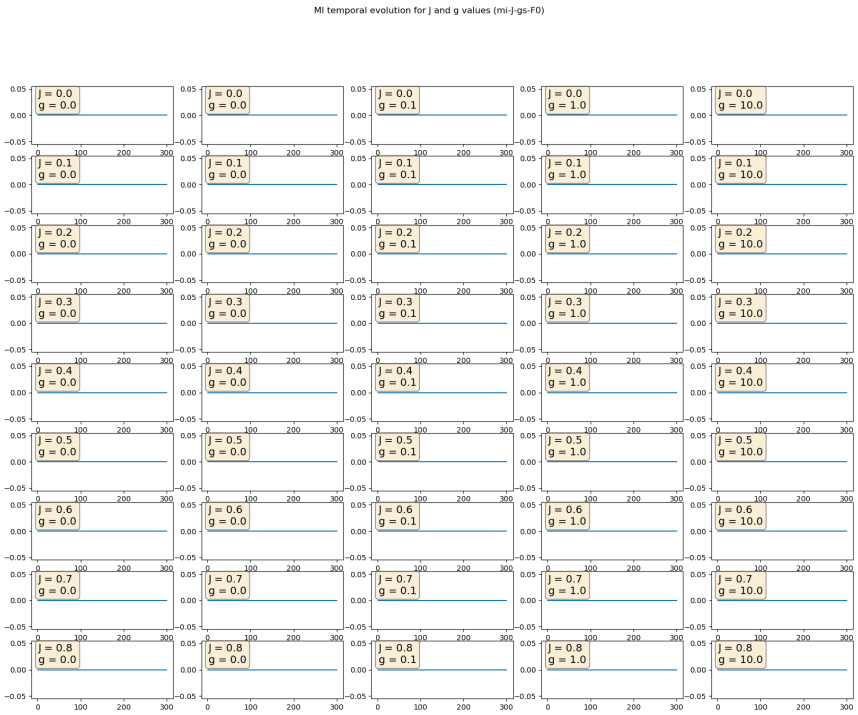

Figure 35: Mutual information time evolution. Ideal ring disposition, ground initial state, electromagnetic environment Fock state with $n = 0$.

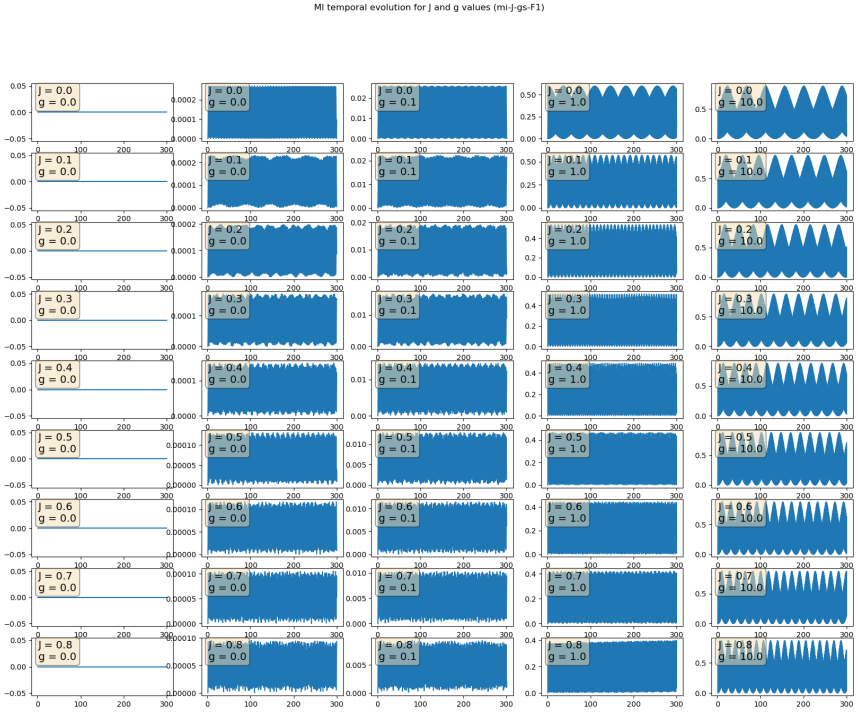

Figure 36: Mutual information time evolution. Ideal ring disposition, ground initial state, electromagnetic environment Fock state with $n = 1$.

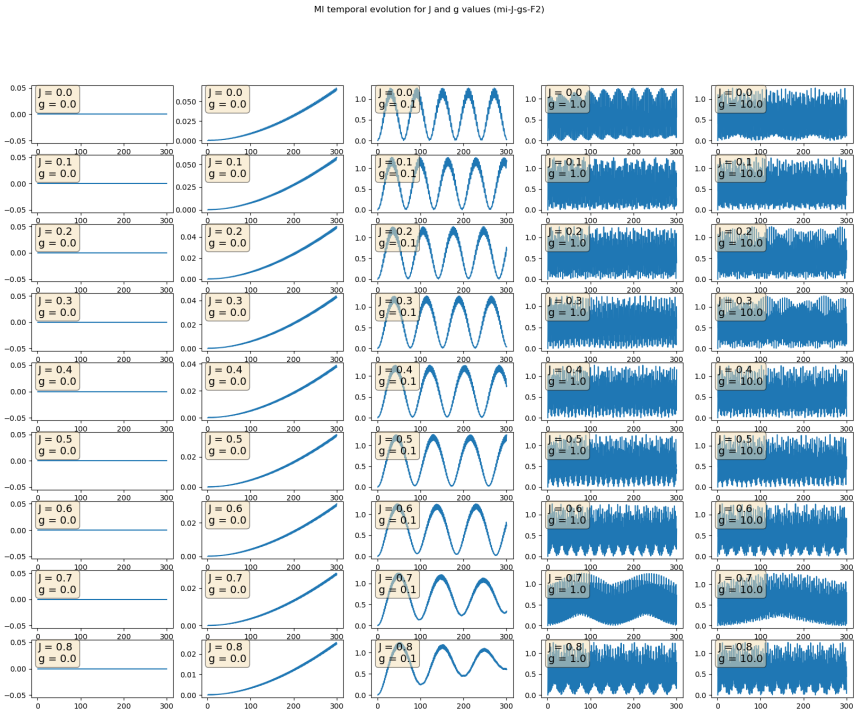

Figure 37: Mutual information time evolution. Ideal ring disposition, ground initial state, electromagnetic environment Fock state with $n = 2$.

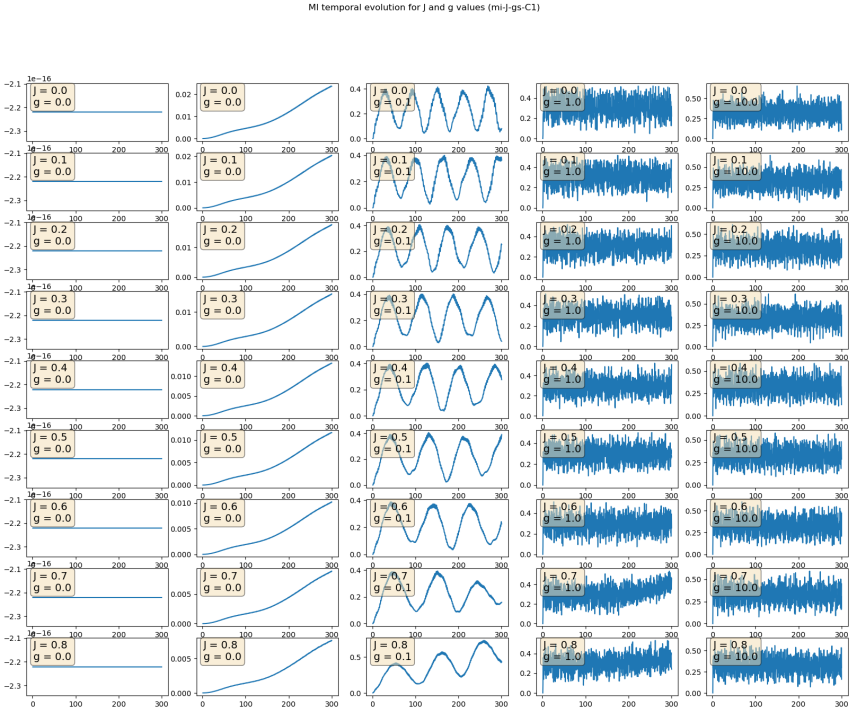

Figure 38: Mutual information synchronization measure time evolution. Ideal ring disposition, ground initial state, electromagnetic environment coherent state with $n = 1$.

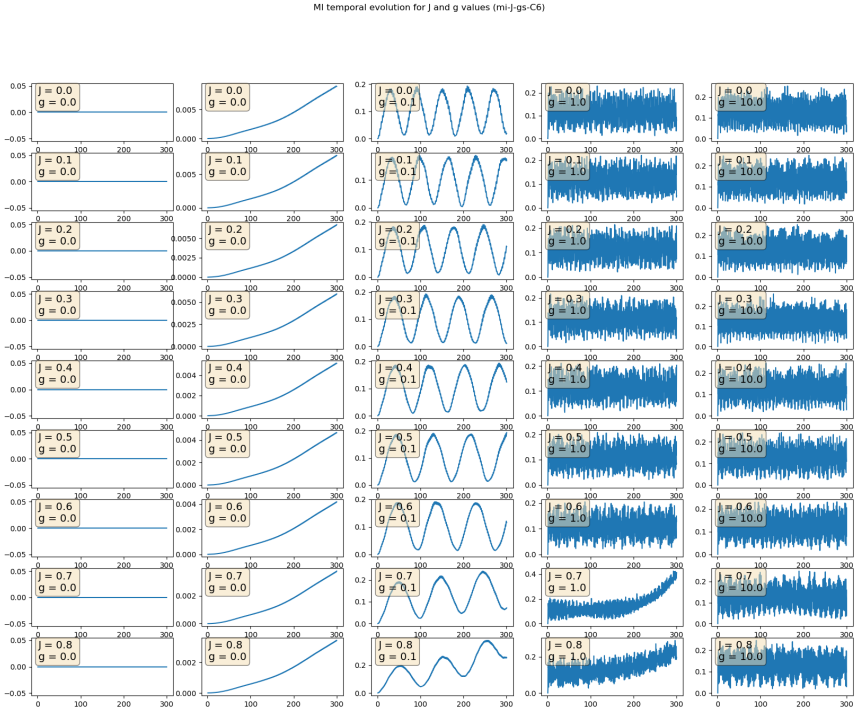

Figure 39: Mutual information synchronization measure time evolution. Ideal ring disposition, ground initial state, electromagnetic environment coherent state with $n = 6$.

Figure 40: Mutual information synchronization measure time evolution. Disordered ring disposition, electromagnetic environment Fock state with $n = 1$.

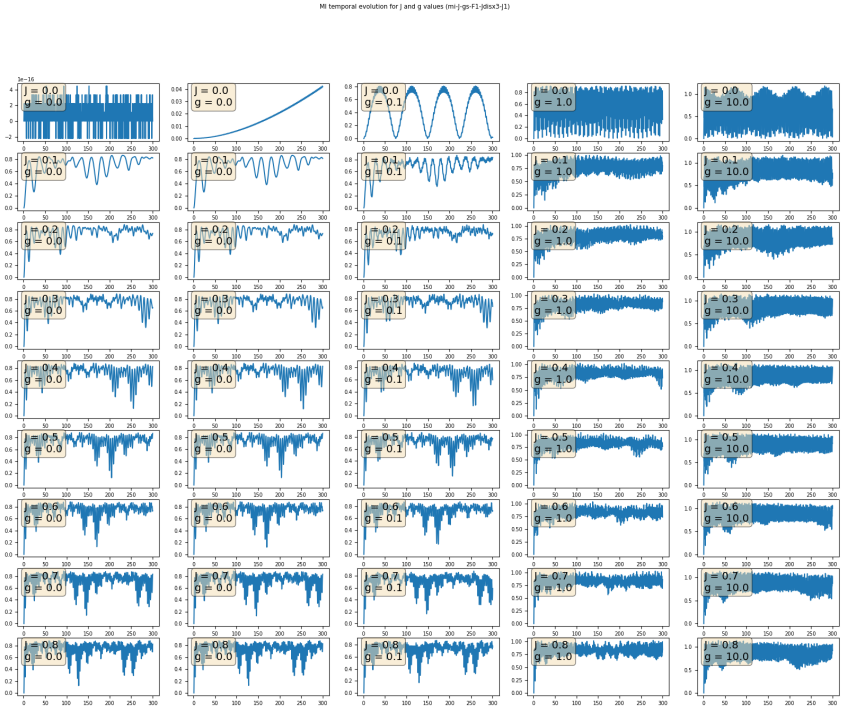

Figure 41: Mutual information synchronization measure time evolution. Disordered cluster disposition, ground initial state, electromagnetic environment Fock state with $n = 1$, interaction matrix J_1.

Figure 42: Mutual information synchronization measure time evolution. Disordered cluster disposition, ground initial state, electromagnetic environment Fock state with $n = 1$, interaction matrix J_2.

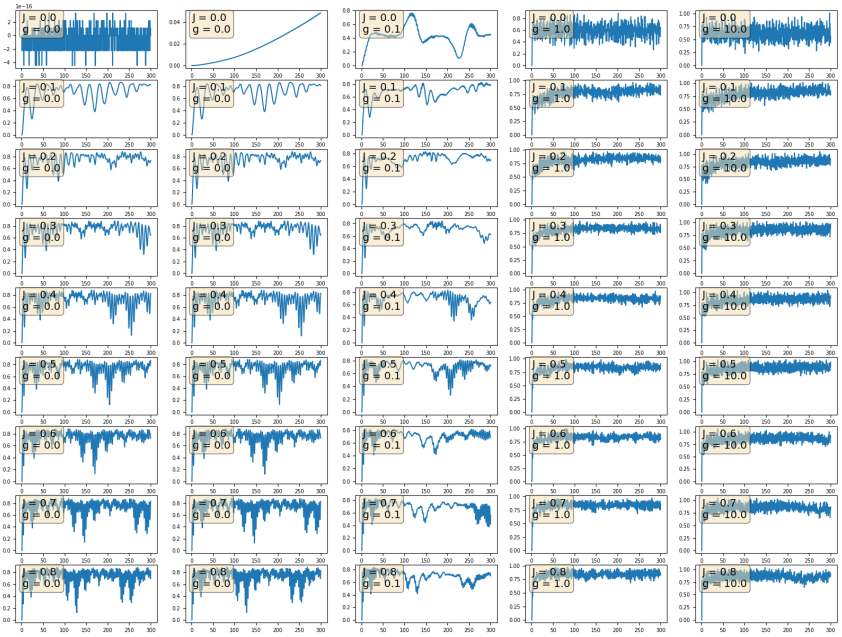

Figure 43: Mutual information synchronization measure time evolution. Disordered cluster disposition, ground initial state, electromagnetic environment coherent state with $n = 1$, interaction matrix J_1.

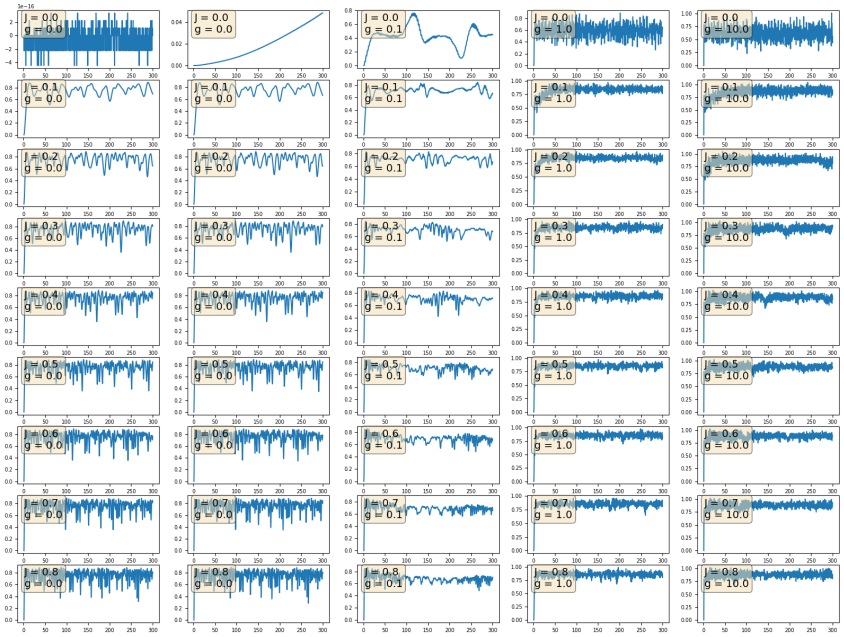

Figure 44: Mutual information synchronization measure time evolution. Disordered cluster disposition, ground initial state, electromagnetic environment coherent state with $n = 1$, interaction matrix J_2.

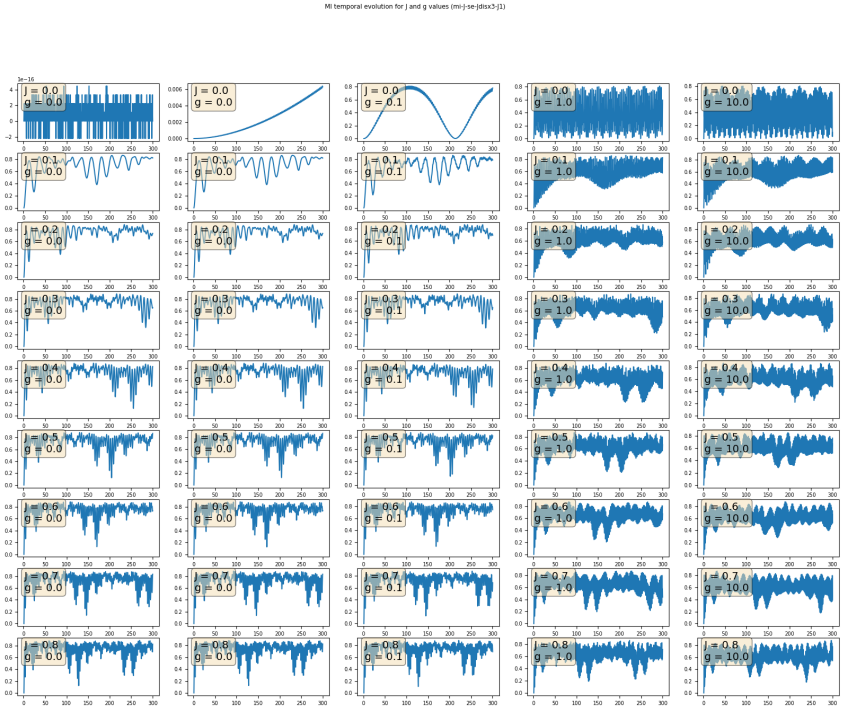

Figure 45: Mutual information synchronization measure time evolution. Disordered cluster disposition, single excited initial state, environment with $n = 0$, interaction matrix J_1.

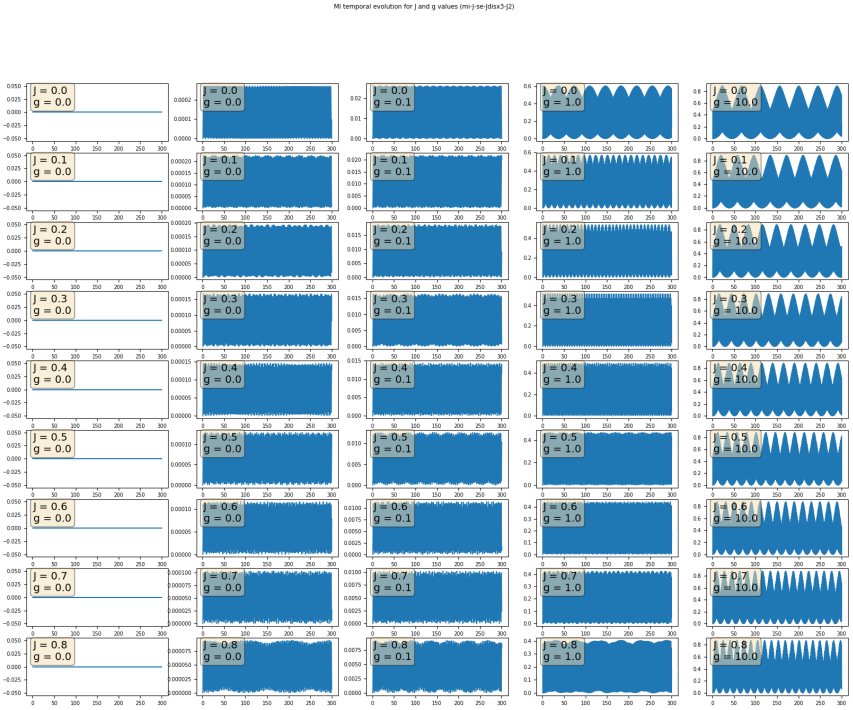

Figure 46: Mutual information synchronization measure time evolution. Disordered cluster disposition, single excited initial state, environment with $n = 0$, interaction matrix J_2.

Appendices to Part IV

.2 QED-TIP3P Water Molecular Dynamics

A simulation scheme for QED-TIP3P Molecular Dynamics is proposed, in order to compare with common water measurements such as H-bond correlation functions and radial distributions, in order to test if water ED can translate into the observed "forming and breaking" of H-bonds.

1. Time-scales

   QED Coherence in Matter Theory, predicts coherent oscillation dynamics with timescale of the order of 15 fs.

   We then consider two time-scales

   - $\tau_1 = 1$ ps is the time-step for the MD simulation, that is, for the evolution of the atom positions
   - $\tau_2 = 1/n$ is the time-step for the excitonic dynamics, that capture the fast dynamics of interaction of the electrons with the transverse electromagnetic potential

2. Simulation Algorythm

   For a given τ_1 time-interval, the atoms positions remain fixed, and the excitonic dinamics are simulated. The values $\tau_2 = 1/n$, with $n = \{10, 15, 20\}$ are used for the simulation.

   Let us consider t to correspond to a discrete time variable of time-step length τ_2. The algorithm is the following:

   (a) Given an initial atomic configuration, we can obtain A_{ij} adjacency matrix, that indicates there is a H-bond between molecules i and j. A state variable $s_k(t)$ is assigned to the H-bond.

   (b) The variable $s_k(t)$ is evolved using Master Equation dynamics and Hamiltonian, a number n of time-steps, which corresponds to a time-interval of length $\tau_1 = n\tau_2$

   (c) Depending on the s_k state, molecules i and j will have a variation in the LJ potential between Oxygens, therefore U_{O-O} is updated

   (d) Molecular positions are evolved, using standard MD algorithm (eg. Velocity Verlet) for a τ_1 time-lapse

   (e) The adjacency matrix A_{ij} is re-calculated based on the atomic positions and the definition

   (f) Variables s_k corresponding to broken H-bonds are erased; when the bond is still existent, s_k is considered to stay in the same state it was in before evolving the molecular positions

3. Inter-step exciton evolution

   MD considers inter-step evolution of the H-bond states. For a given time t, the state of the system is given by 23.

(27) $$(s_1 \otimes s_2 \otimes \cdots \otimes s_m)(t) := S(t)$$

where m is the number of H-bonds at time t.

Let now t denote a discrete time variable with time-step equal to τ_2.

We can, then, evolve the system using Master Equation dynamics, with Hamiltonian

$$H = \omega a a^\dagger + g(a^\dagger \sigma^- + a\sigma^+)$$

4. Variation on Leonard Jones potential between Oxygens

   We consider an increase to LJ potential U_{OO} of 10, 20 and 50%, due to electron delocalisation effects. We may also expect an effect on the stability of the H-bond to rotation, given the differences in electron density distribution for ground and excited state. Could we say that the excited state is more fragile or viceversa? If this is the case, the forming and breaking of H-bonds could be explained in relation to the change of the electron density in the H-bond area due to electrodynamics effects.

5. Interaction parameter g

   Collective dipolar behavior has the effect of increasing g [39] [61].

6. Increase in the Leonard-Jones potential U_{O-O}

   We consider a percentual increase of the LJ-potential due to the electronic delocalisation in the bond area.

   The LJ-potential in the excited state is

   $$U^1_{O-O} = U_{O-O}(1+\alpha)$$

   with $\alpha \in \{0.1, 0.2, 0.5\}$.

   The LJ-potential for the ground-state case remains constant

   $$U^0_{O-O}(\theta) = U_{O-O}$$

7. Decrease in stability under rotations $U_{O-O}(\theta)$

   We add a decay factor in the case of the excited state H-bond. The exponential factor $e^{-41\theta/\pi}$ behaves as follows:

   - in the case of $\theta = 0$ the potential remains intact
   - in the case of $\theta = \pi/6$ has the approximate value 0.001

   The LJ-potential in the excited state is

   $$U^1_{O-O}(\theta) = U_{O-O}\, e^{-\frac{41\theta}{\pi}}$$

The LJ-potential for the ground-state case remains constant

$$U^0_{O-O}(\theta) = U_{O-O}$$

8. H-bond Life-Time and Correlation Function

   The H-bond lifetime distributions can be obtained from the simulation.

   Forming and breaking of Hydrogen-bonds can be characterised by the correlation function ([24]) [77].

(28)
$$C(t) = \frac{\langle h(0)h(t)\rangle}{\langle h\rangle}$$

   where $h(t)$ is a H-bond population descriptor, which is unity when a pair of molecules is H-bonded at time t and is zero otherwise. Two molecules are considered to be H-bonded if the distance between their respective oxygen atoms is $r_{OO} < 3.5$ and the angle $\theta_{OA...OD-HD} < 30$.

9. Radial distribution

   The parameter g can be adjusted to study its effects on the d_{OO} Oxygen-Oxygen radial (distance) distribution to compare with data.